Numerical Weather Prediction

Boscastle and North Cornwall Post Flood Event Study - Meteorological Analysis of the Conditions Leading to Flooding on 16 August 2004

Forecasting Research Technical Report No. 459

Edited by Brian Golding
Head of Forecasting Research

email: nwp_publications@metoffice.gov.uk

Revision History

Date of this revision:
Date of Next revision:

Revision date	Version number	Summary of Changes	Changes marked
21-09-04	0.1	First Issue. Version 0.1	No
18-11-04	0.2	Addition of observational evidence	No
30-11-04	0.3	Evidence complete. First draft of analysis	No
10-12-04	0.4	First draft of complete paper	No
22-12-04	0.5	Amended in light of internal reviewers comments. Draft submitted for internal approval.	No
17-01-05	1.0	Amended in light of Keith Groves' and other comments	No
8-03-05	1.1	Additional photograph credits added	No
22-03-05	1.2	Additional information from model reruns	No

Approvals

This document has been approved as follows:

Name	Signature	Comments	Date of Issue	Version
Keith Groves	See e-mail dated 22-12-04	Subject to minor amendments marked on paper copy	22-12-04	0.5

Contributors and acknowledgements

Met Office
Brian Golding: Synoptic analysis, radar & satellite analysis, editing
Murray Dale: Return period analysis
Ross Melville: Rain gauge quality control
Roderick Smith & Andrew Bennett: Soil moisture information
Andy Cooper: Radar images and diagnostics
Bryony May: Initial radar analysis and GIS maps
Malcolm Kitchen: Radar quality analysis
Mark Beswick: Antecedent weather and MORECS data
Will Hand: Convection diagnostics
Peter Clark: Model analysis
Humphrey Lean: High resolution model runs
Nigel Roberts: Global NWP model diagnostics
Sarah Watkin, Michael Saunby & Joanne Crawford: Meteosat satellite imagery
Mark Smees: EA Technology lightning data
Environment Agency
Tim Wood: historical data
Roger Quinn: preliminary analysis of rain gauge data
HR Wallingford
Steven Wade: coordination with hydrological work
Others
Rod McInnes-Slegg : eye-witness description of storm
John Rowlands: photograph
Mr Wallace: photograph

This report was commissioned by the Environment Agency

Contents

Figures

Page

1. Introduction

During the afternoon of Monday 16 August 2004, heavy rainfall brought flash flooding to the village of Boscastle on the north Cornish coast. Around 60 properties were flooded, over 100 people were rescued by helicopter and thirty vehicles were washed into the harbour.

This report looks at the meteorological conditions that generated the heavy rainfall, the temporal and spatial characteristics of the rain, and the likelihood of its recurrence.

The first section looks at the spring and summer period prior to the storm, focussing on the precipitation amounts relative to normal. This provides the history which determined the capacity of the soil to absorb storm rainfall.

The second section deals with the meteorological conditions that led to the extreme rainfall event. It is approached through looking first at the larger scale setting, then progressively focussing in on the details of the storms themselves. A large variety of observation sources is used to carry out the analysis.

The third section turns to the detailed observations of rainfall from radar and rain gauges, analysing the quality of the available data.

The fourth section looks at the distribution of rainfall in time and space, as shown by these data.

The fifth section addresses the probability of occurrence of the observed rainfall totals, approaching from two directions; the first looking at indirect indicators, and the second using the standard FEH approach.

A final summary draws together the main conclusions.

In putting together this report, a large amount of material generated for other purposes has been drawn on. The additional material that could be produced specifically for this report was very limited. This has resulted in some of the diagrams being less suited to their context that would ideally have been the case.

In this report all times are stated in the internationally agreed Universal Time Coordinate (UTC). This is numerically identical to Greenwich Mean Time (GMT), and one hour behind British Summer Time (i.e. 1500UTC is 4pm BST).

2. Antecedent conditions: the summer of 2004 in SW England

The ability of the soil to absorb rainfall depends on the amount of rain that has fallen over the period preceding an event and the loss of moisture by evaporation. In this section we look at statistics of the weather of spring and summer 2004 to gain an overview of the degree to which the moisture absorbing capability may have been abnormal. We look first at a crude overview using preliminary statistics computed prior to quality control for Cornwall as a whole. Then we focus in on precipitation in the Boscastle area using maps of anomalies computed using the full set of quality controlled rainfall data.

Table 1 summarises the key statistics for spring and summer 2004 for Cornwall as a whole, relative to the period 1971-2000. It was produced quickly using only data from Met Office observing sites, and without full quality control. In summary, the spring period (March, April and May) was dry, sunny and warm relative to normal. These statistics would indicate above average evapotranspiration which, taken with below average rainfall, would produce a modestly enhanced soil moisture deficit at the start of summer. June was also dry, sunny and warm relative to normal, further enhancing the drying of the ground. However, July was wet, cool and lacking in sun relative to normal. This will have reversed some of the effect of the previous months. We will not comment on August here since it includes the precipitation occurring after the 15th.

Table 1 Climate statistics for Cornwall, Spring & Summer 2004 relative to 1971-2000 averages

Month (units)	Max Temp (°C)	Diff	Min Temp (°C)	Diff	Mean Temp (°C)	Diff	Sun (hrs)	%	Rain (mm)	%
Spring	12.8	0.7	5.9	0.6	9.4	0.6	571.1	115	200.3	84
June	18.6	1.5	11.1	1.2	14.9	1.4	230.7	120	67.1	94
July	18.2	-1.2	11.8	-0.3	15.0	-0.7	162.1	80	82.3	126

Turning to the summer period in more detail, we look first at the distribution of the June rainfall anomaly in Figure 1. Whereas the preliminary values were expressed relative to the more recent averaging period, 1971-2000, the official anomalies are portrayed relative to the standard comparison period of 1961-90. They have been computed using all available daily gauges as well as the real-time hourly data included in Table 1. This confirms that the north coast region of Cornwall is consistent with the preliminary indication for Cornwall as a whole, having total accumulations below normal, the deficit in the Valency catchment being about 10%.

Figure 2 shows the distribution of precipitation anomaly for July, again expressed relative to the 1961-90 averages. Here we see a much more complex picture, with areas of above and below average precipitation accumulation distributed across the county. In north Cornwall, there is an area of above average precipitation in the Bude area, but the Valency and neighbouring catchments are close to normal, indicating that the pre-existing dry anomaly in soil conditions may have continued throughout July. These conclusions should, however, be used with the caveat that with such a small scale of variation in the structure of the anomaly, the results may be limited by the density of the available raingauges.

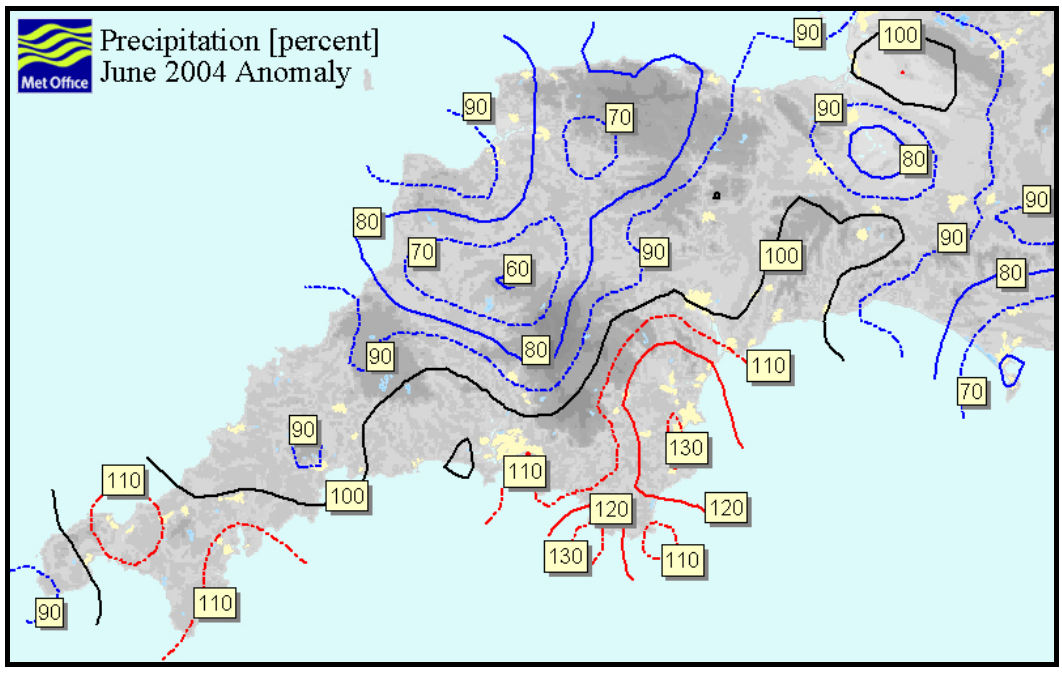

Figure 1 Precipitation anomaly map for southwest England, June 2004, relative to 1961-90 averages

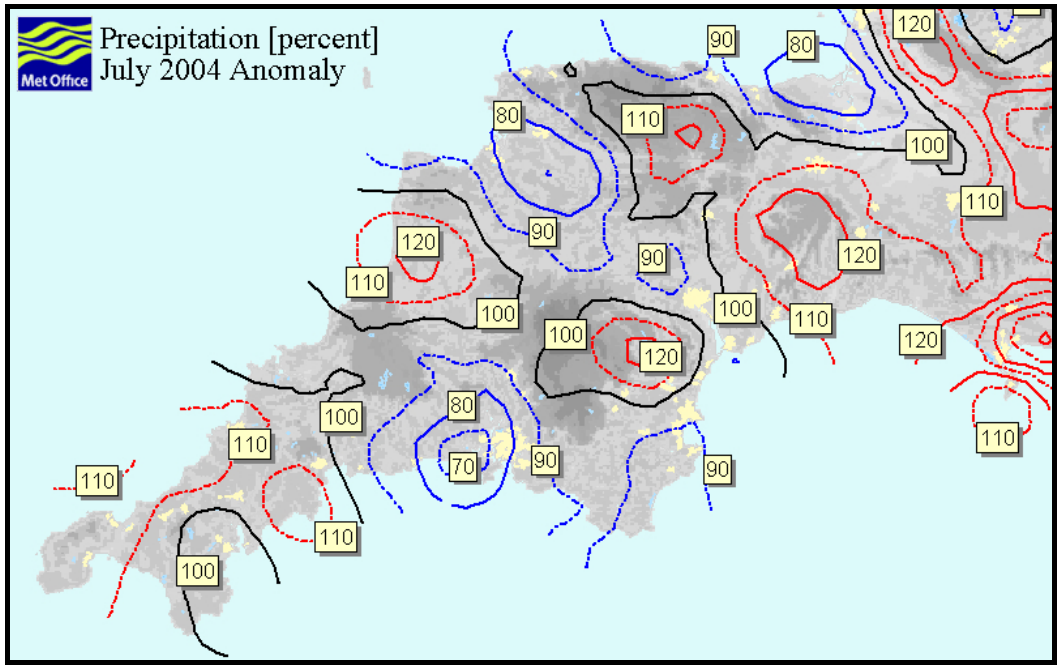

Figure 2 Precipitation anomaly map for southwest England, July 2004, relative to 1961-90 averages

Before looking at the anomaly for the first half of August, it is useful to look at the actual climatological precipitation distribution, shown in Figure 3. This map emphasises the large natural variability of the August precipitation accumulation across the region. Coastal areas as close as Padstow and Bude have monthly normals in the driest range (38-63mm), while the Valency catchment itself falls into a local maximum extending to the coast from the larger area of high accumulation (>100mm) associated with Bodmin moor. As will be shown later in section 6.1, the distribution of convective storms, which generate most summer precipitation, is strongly modulated by the interaction between wind direction and topography. Returning to August 2004, Figure 4 shows the distribution of anomalies for the first

half of the month, based on the assumption that the average is evenly split between the two halves of the month. It shows that this period, prior to the storm on 16th, was already substantially wetter than normal, with anomalies of 25-50% in the north Cornwall area, the Valency being at the lower end of this range. Note the very large anomalies at locations in south Cornwall associated with specific convective storms early in the month. As with July, the caveat must be stated that high variability indicates the possibility that the available gauges were insufficient to capture all of the relevant detail.

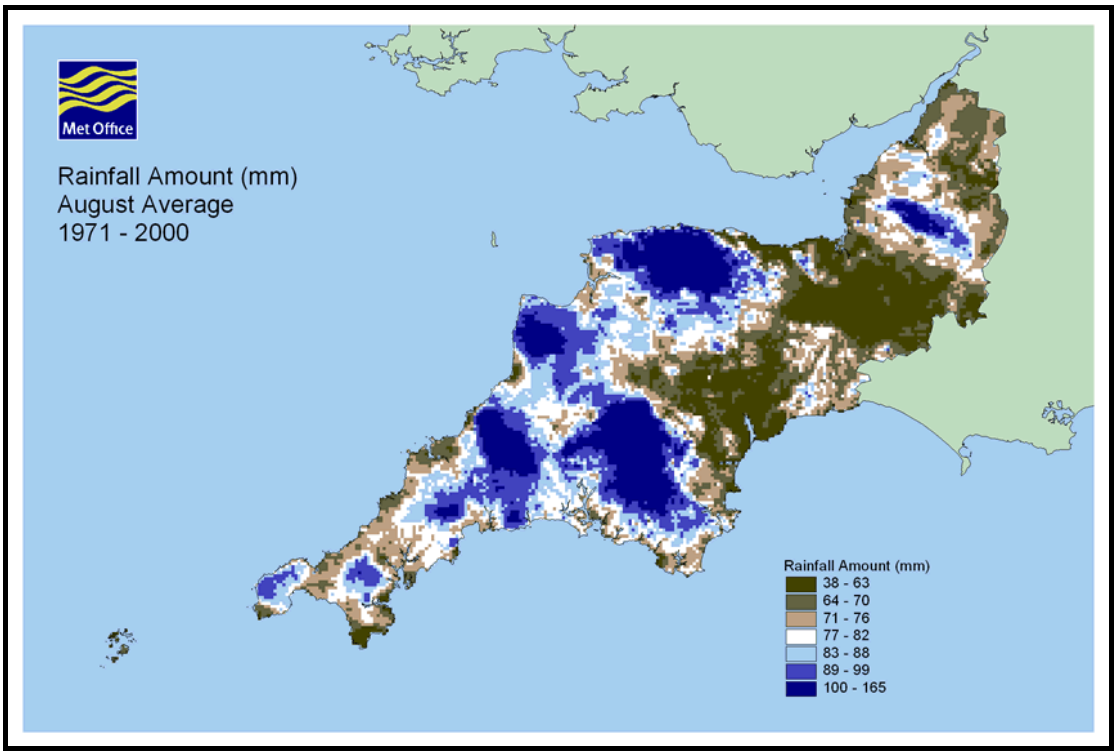

Figure 3 South West England 1971-2000 rainfall averages for August

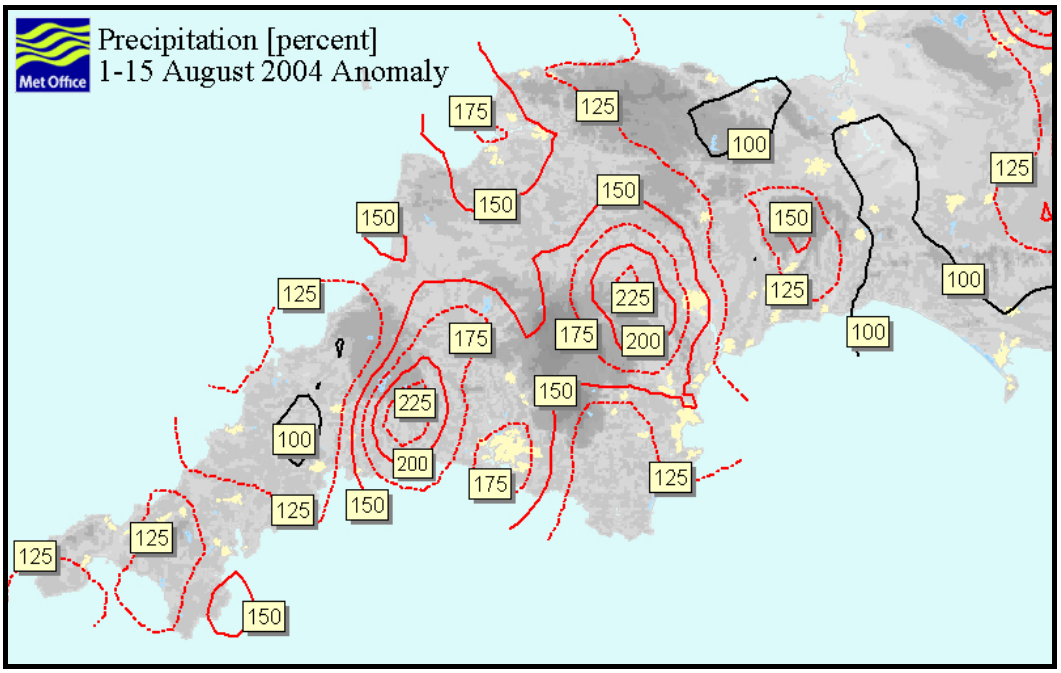

Figure 4 Precipitation anomaly map for SW England, 1-15 August 2004, relative to 1961-90 averages

The higher rainfall in August will have reduced the soil moisture deficit from that obtained following the dry spring and June, but in highly vegetated areas, evapo-transpiration would be expected to dominate at this time of year, tending to maintain the high deficit.

The standard Met Office soil moisture estimation scheme, MORECS (Meteorological Office Rainfall and Evaporation Calculation System: Hough & Jones, 1997) computes daily values on a 40km grid, using daily rainfall and sunshine totals interpolated from Met Office observing sites. On this very coarse grid, soil moisture deficits (SMDs) in the Boscastle area were 82mm on 1st August, increasing to 100mm on 7th then falling to 75mm on 15th.

A new soil moisture estimation scheme, MOSES-PDM (Smith et al, 2004), based on the MOSES (Met Office Surface Exchanges Scheme) land surface scheme in the Met Office's Unified Numerical Weather Prediction (NWP) Model, coupled with the PDM (Probability Distributed Model: Moore, 1985) for heterogeneous run-off generation, has recently been brought into operational use. This computes hourly values on a 5km grid, using hourly radar rainfall and satellite-derived cloud cover as the primary inputs. It uses an updated representation of soil physics which does not involve soil moisture deficit, so it has been necessary to generate a diagnostic algorithm which produces SMD values comparable to those produced by MORECS. Figure 5 shows the resulting distribution for midnight on 16th August. The most notable feature of this map is the high variability, consistent with the large variations found in the precipitation anomaly maps. Within the area of the MORECS 40km grid square, SMD values ranging between 40-180mm are shown, with the smallest deficits over Bodmin Moor. Undoubtedly, much finer scale variability is also present, unrepresented by the MOSES-PDM 5km grid. Like MORECS, MOSES-PDM showed a reduction in SMD between 1st and 16th August, the range of values around Boscastle dropping from 80-220mm SMD to 40-180mm SMD. However, in the immediate vicinity of Boscastle, the SMD remains fairly high, with values in excess of 100mm on 16th August.

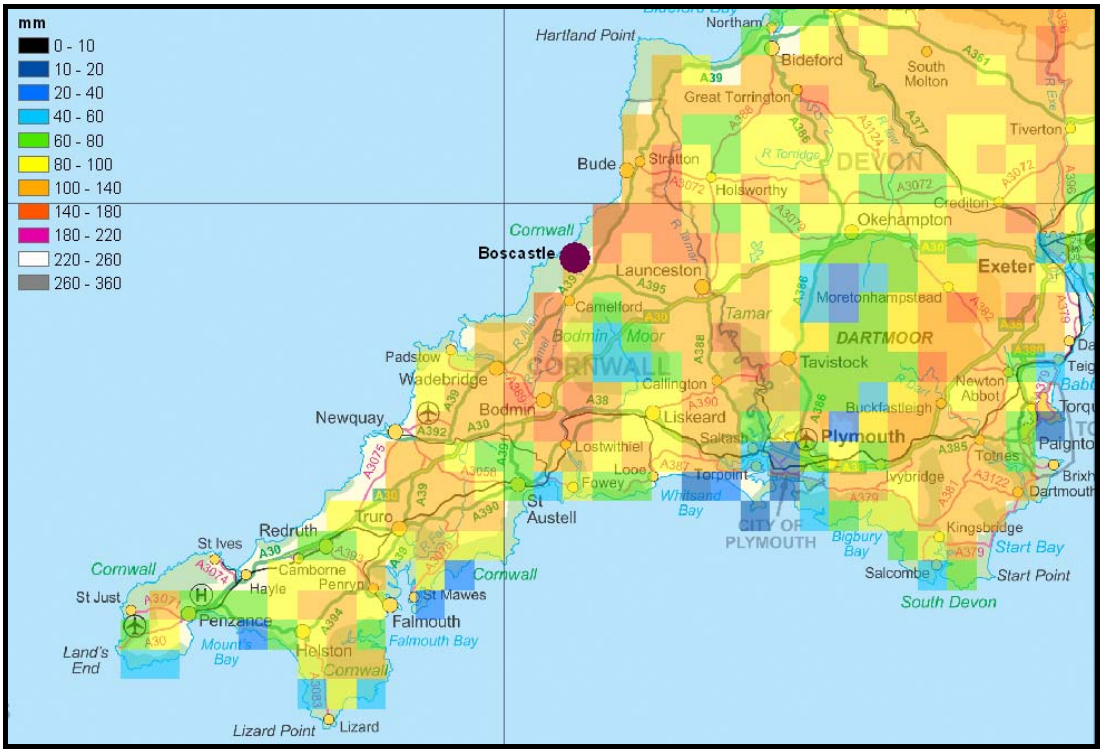

Figure 5 Diagnosed soil moisture deficit from MOSES-PDM for 0000UTC 16/8/2004

Examination of MOSES-PDM diagnostics during the storm itself shows that, given the modelled soil moisture, surface run-off was 20-30% of precipitation in the heaviest rain and 10-20% elsewhere. However, these results should be treated with considerable caution, as they depend on the value of the heterogeneity parameter in the PDM formulation. At present this is set to a uniform value (0.5), whereas it is likely that in hilly terrain such as the North Cornwall Coast, the soil properties would be more heterogeneous, leading to increased surface runoff.

In summary, weather anomalies experienced up to the beginning of August generated a dry soil moisture anomaly for the Valency and neighbouring catchments. Subsequent weather prior to 16th August was significantly wetter than average, but with a highly variable distribution, leading to soil moisture deficits in the range 40-180mm in North Cornwall and just over 100mm in the Valency catchment itself.

3. Meteorological overview

The influences of importance in the development of a storm can be very diverse, reflecting both the structure of the air mass within which it occurs, and the motions being generated by imbalances in the forces acting on it. In this analysis we look at the atmospheric structure as a cascade of scales, starting with the largest which occupy the whole eastern Atlantic, then moving down to the mesoscale, occupying the south west approaches and neighbouring land areas. We then look at the ability of the air mass to support storm development. Then we address the storm scale, looking at the evolution of the train of storms that affected northern Cornwall and Devon. At each scale, we explore the information that can be gained from analysis of all available sources of data.

However, to set the scene, we start with the sequence of surface synoptic charts for 16 August in Figure 6 which show the southwest of England on the forward side of a slowly deepening area of low pressure situated to the west of Ireland. An air mass boundary, indicated by the front symbols, is marked as lying across Biscay and northern France, and two shear zones, marked by curved lines without symbols, are shown in the vicinity of southwest England. All of these features contributed to some degree in determining the development of weather in Cornwall.

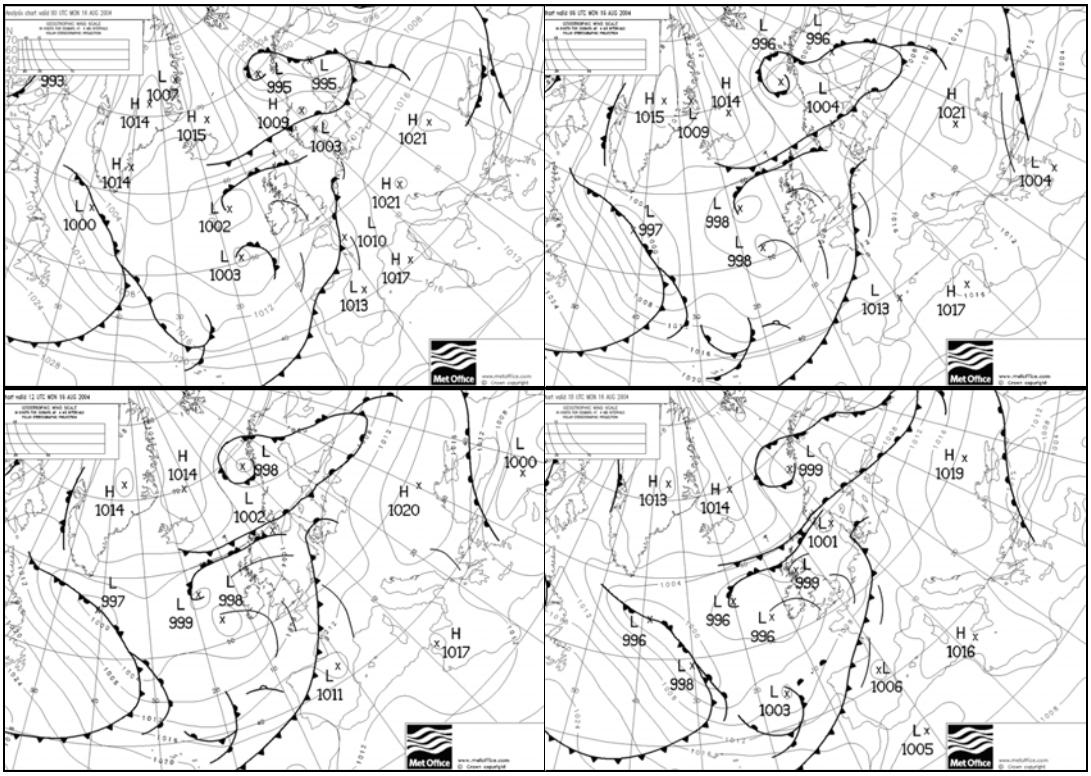

Figure 6 Surface Analysis Charts for 0000UTC, 0600UTC, 1200UTC & 1800UTC on 16th August 2004

3.1. Large scale synoptic environment.

The large scale environment must be addressed in terms of the whole troposphere, and is best understood by focussing first on the upper levels, particularly on the jet stream structure, and then on the middle and lower levels.

Figure 7 and Figure 8 show the parts of the automatic plotted charts of observations at 250hPa for 0000UTC and 1200UTC used in the Met Office Operations Centre. Superimposed on them is the 6-hour model forecast valid at the same time, and used as the first guess in the NWP data assimilation process.

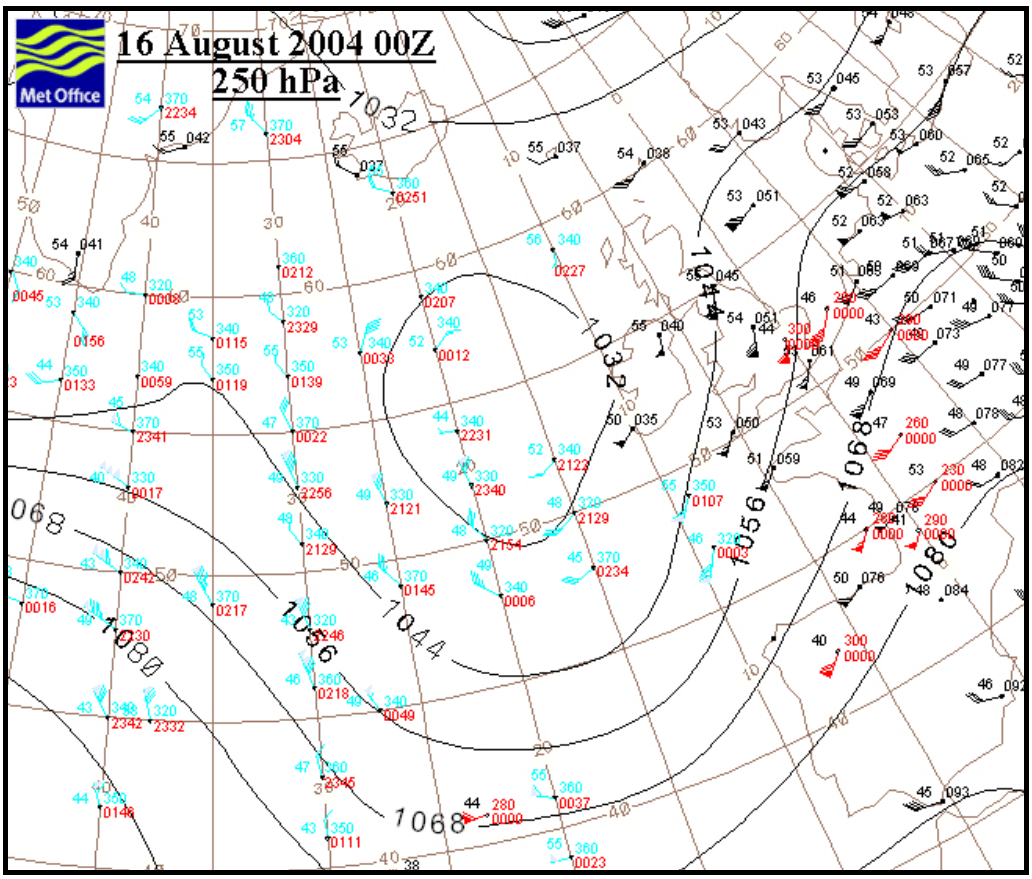

Figure 7 250hPa analysis for 0000UTC 16/8/2004

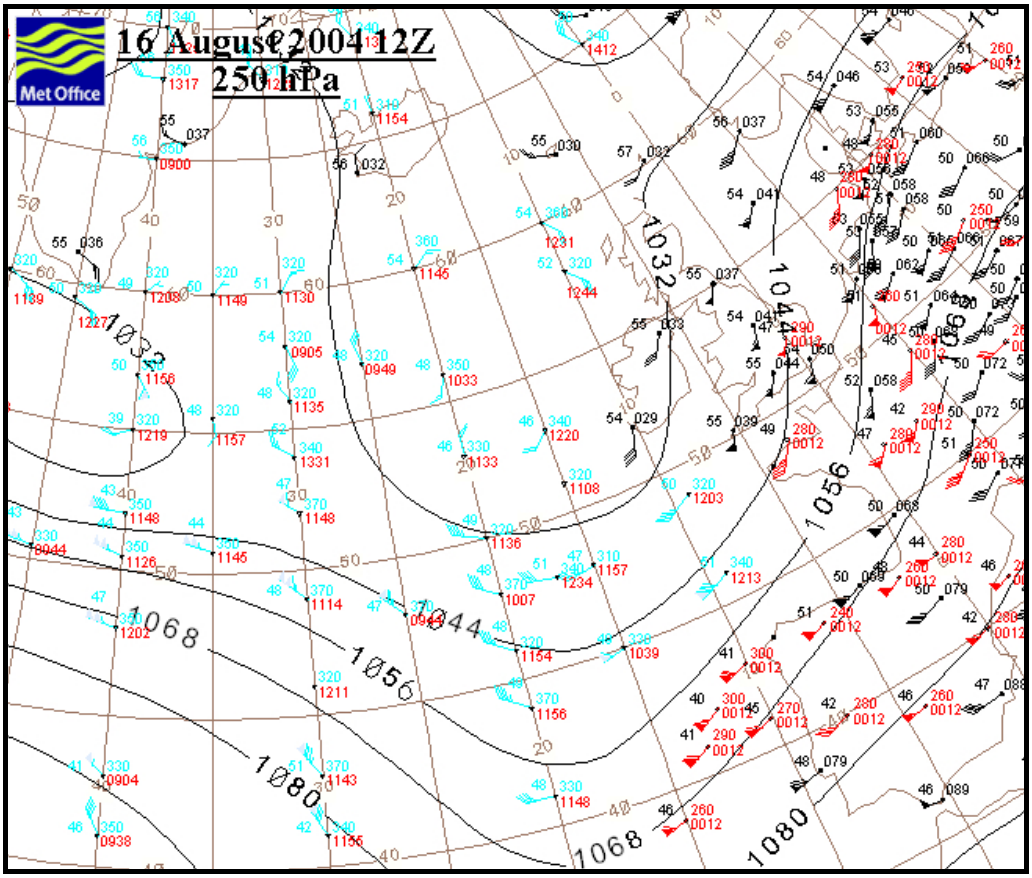

Figure 8 250hPa analysis for 1200UTC 16/8/2004

Figure 7 shows a large cut-off upper vortex centred around 55^{O}N 20^{O}W. Its shape is distorted by troughs extending east over Northern Ireland and England, southeast towards Spain, and southwest into the tropical central Atlantic. This complex structure reflects a history of successive pulses of tropical air becoming absorbed in the circulation, including former Hurricane Alex. Maximum winds of 60-70kn are evident from observations in the areas of tightest gradient to the south and south east of the centre. By noon, Figure 8, the centre of the vortex has moved east to 15^{O}W the south east oriented trough has swung round into Southwest England, and a jet streak has moved into the west of Biscay, between this and the succeeding trough. Due to the influence of the earth's rotation, the velocity changes implied by entrance and exit from the jet streak and by the curvature of the flow in these locations, lead to forces that drive vertical motions and the generation or destruction of vorticity in these areas. The most active area for generation of surface vorticity and uplift is to the left of the jet exit, which at 1200UTC is situated over the western end of the English Channel and adjacent land areas.

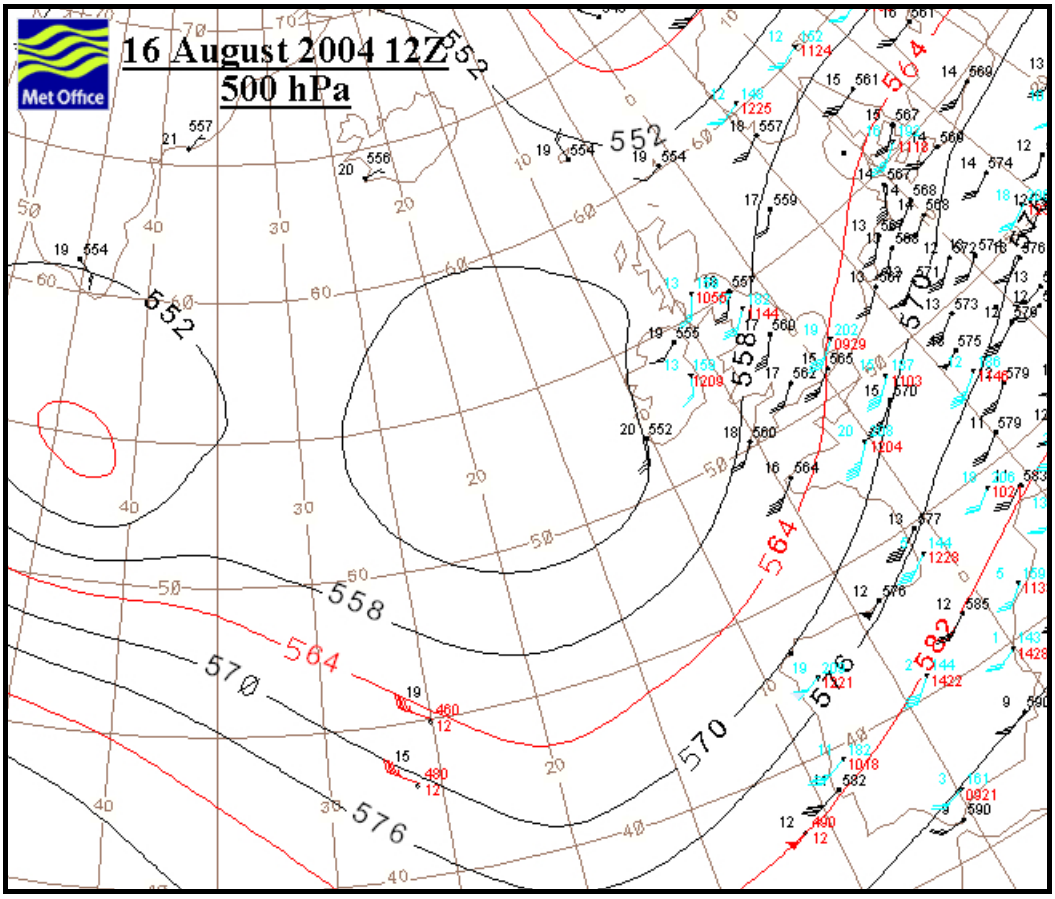

Figure 9 500hPa analysis for 1200UTC 16/8/2004

Moving down to 500hPa, the mid-tropospheric level, Figure 9 shows a similar pattern to that at the higher level. Referring back to Figure 6, we see that the surface low pressure centre to the west of Ireland is also centred at about 15^{O}W indicating a non-developing barotropic structure.

In order to study further the large scale dynamics identified in the analysis above, we now turn to diagnostic quantities derived from a 12-hour forecast using the global configuration of the Met Office Unified NWP Model. This model is used both for forecasting and for climate prediction, and represents the complex interactions between wind, temperature and moisture that determine the evolution of weather systems around the globe. Detailed representations of clouds, radiation and the earth's surface are included, and the initial state of each forecast is updated to

provide a statistically optimum fit to the thousands of observations obtained from worldwide weather observatories and satellites. Figure 10 shows the model structure at 300hPa with the major upper vortex situated south of Iceland surrounded by a complex circulation with major troughs to the east, across mid-Scotland, and to the southeast, across the southwest approaches to the UK, Brittany and southern France. A west-southwesterly jet streak is evident at ~45°N crossing Biscay and terminating at the location of the second trough. These features confirm that the model forecast reproduces the features identified earlier in the observations.

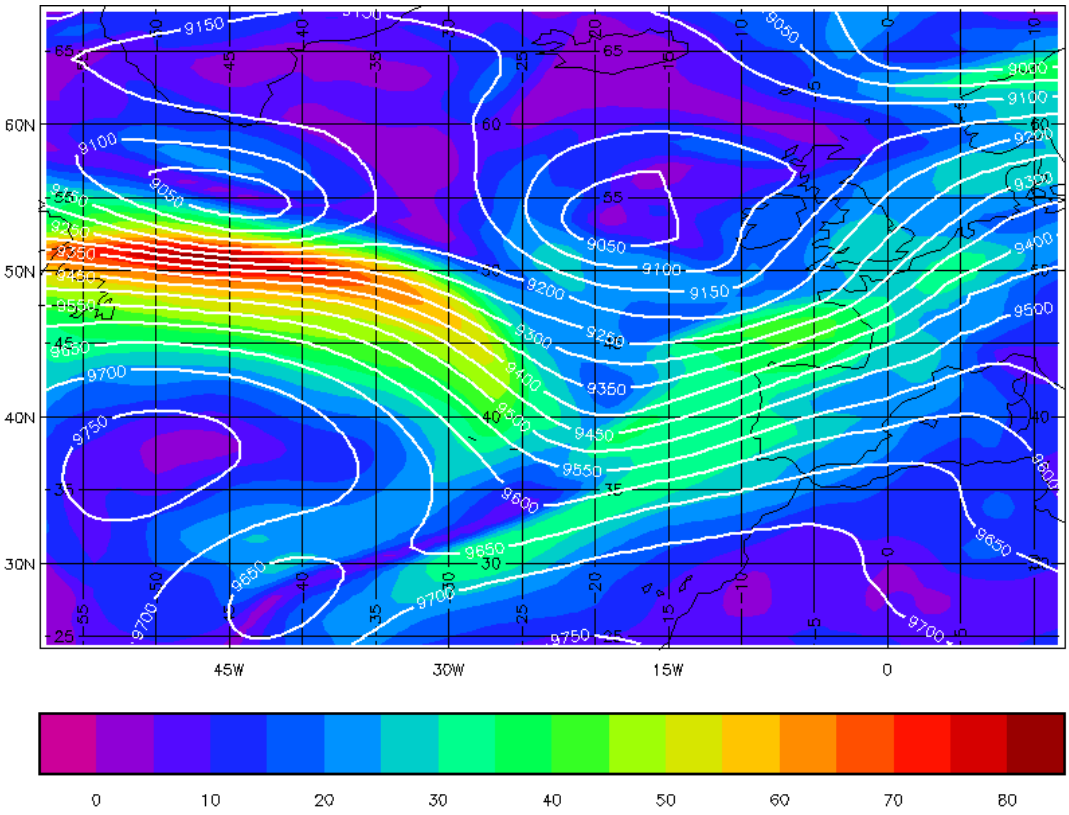

Figure 10 300hPa height (contours) and wind speed (colours) at 1200UTC 16/8/2004

This structure is reflected in the Potential Vorticity (PV) field, in Figure 11, which shows a maximum in the centre of the upper low, with arms extending along the two troughs. The more significant one is the second, with values in excess of 4.10^{-6} s^{-1} to the southwest of Ireland. This curves southward to meet an along-flow maximum oriented west-southwest to east-northeast, associated with the north side of the Biscay jet, with peak values of ~3.10^{-6} s^{-1}. At its forward end this jet maximum has another slight peak associated with a weak north-south oriented maximum through southwest England and Wales. The two north-south maxima in the western approaches to the UK mirror the two troughs drawn by the forecaster in Figure 6.

At 850hPa (Figure 12), there is a very clear maximum of humidity running north from the south of France to southwest England and lying on the forward side of the first trough. A much smaller maximum is situated further west along the line of the second trough, the two joining to the south of Ireland. These maxima are also evident at 500hPa, providing a moist environment suitable for the development of high rain rates.

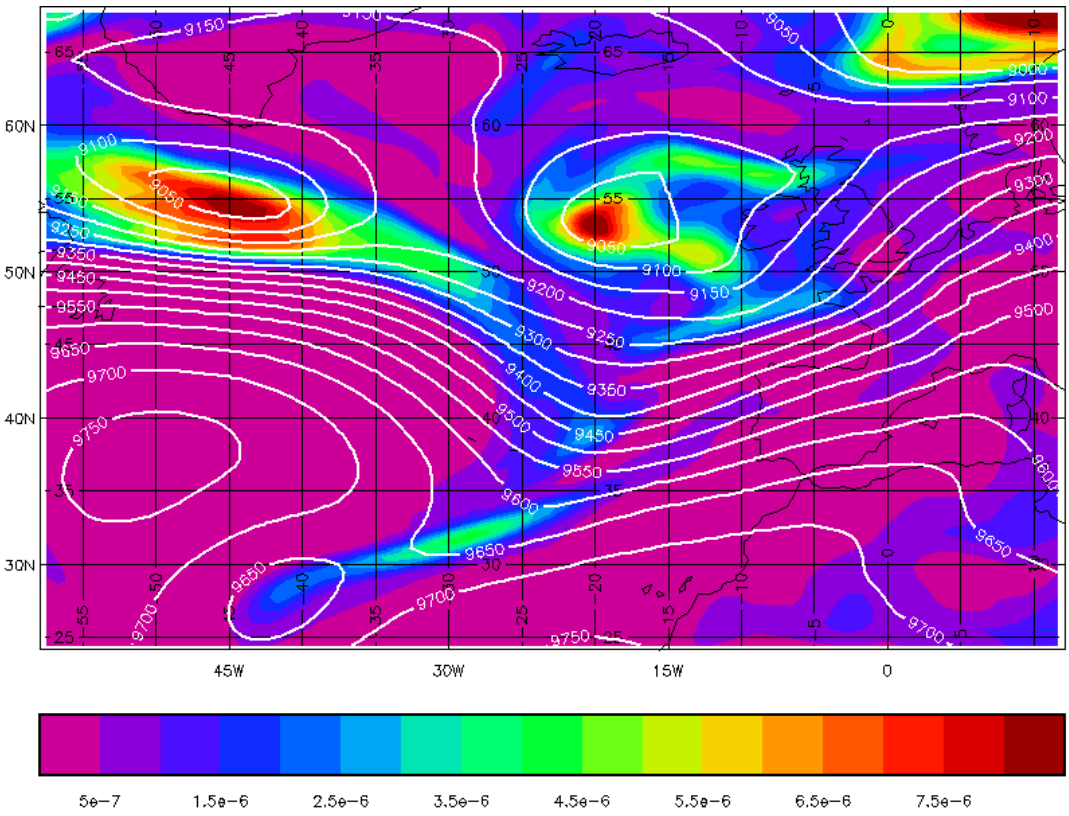

Figure 11 300hPa height (contours) and Potential Vorticity (colours) at 1200UTC 16/8/2004

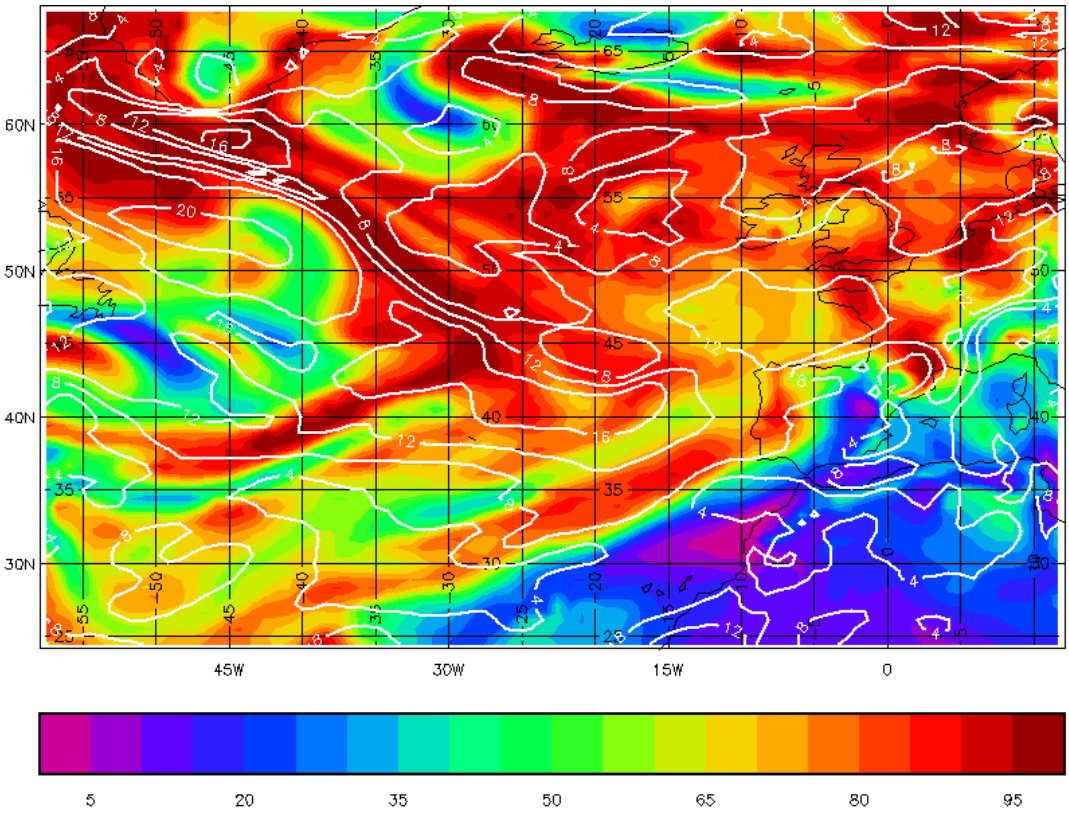

Figure 12 850hPa Relative humidity and wind speed 1200UTC 16/8/2004

In summary, the large scale synoptic situation is very complex, with key features for the Boscastle area being the tongues of warm moist air ahead of the two troughs,

especially the first, and the forcing of uplift in the left exit region of the jet streak approaching Biscay.

3.2. Mesoscale 3-D environment from satellite imagery.

The principal source of satellite information is the SEVIRI instrument on board the newly operational Meteosat-8 satellite. This is owned and operated by European Meteorological Services through the European Meteorological Satellite organisation, EUMETSAT. It is the first of a series of four satellites (Meteosat Second Generation) which mark a significant advance on earlier ones. It was launched in August 2002 and became operational in January 2004. It is a geostationary satellite which is located 36000km above the Greenwich Meridian and the Equator.

The satellite observes the earth's surface in steps from south to north, using its 100rpm spin to scan from west to east. The full earth disk is observed every 15 minutes in 11 spectral channels giving a total of 3712x3712 samples, with a resolution at the sub-satellite point of 3km. In addition a high resolution visible channel provides partial cover with resolution at the sub-satellite point of 1km. At southern English latitudes, the pixel size observed by Meteosat-8 is about 1.5 times that at the sub-satellite point: 5km for most of the channels, and 1.5km for the high resolution visible channel. Each channel registers the intensity of radiation reaching it in a particular band of electromagnetic frequencies. It may be either reflected solar radiation, for short wavelengths, or emitted radiation, for long wavelengths, or a mixture. Some wavelengths are unaffected by passage through the cloud-free atmosphere, allowing clouds and the ground to be viewed, while others are dominated by emissions from atmospheric constituents such as water vapour and so can be used to analyse variations in their concentration.

At this stage in the study, we focus on the 6.2 μm wavelength infra-red channel, situated in a water vapour absorption band, to look at variations in upper tropospheric moisture content associated with vertical motions generated by mesoscale disturbances. Figure 13 shows images in this channel from the period of storm development. Note that the grey scale has been adjusted to emphasise areas of dry air (dark shades) indicating downward motion of stratospheric air (Roberts, 2000). To achieve this, the areas contaminated by cloud have been over-lightened. In order to assist interpretation, the same rescaling has been applied to each of the images shown.

The 1030UTC image depicts a very complex structure of upper tropospheric disturbances. To the west of Ireland, parts of a pair of rings can be seen. These are related to the surface vortex marked on the noon surface synoptic analysis in Figure 6. The north-south oriented dark streak to the west of Ireland marks an area of low tropopause height associated with cold air to the rear of a front and can be associated with the trough marked south of Ireland in the surface analysis. A particularly dark area at the southern end of this band is marked "A" where it joins another dark streak oriented west-east. Further east again is a pair of dark streaks, the darker southern one (B) is joined to "A" and marks the back edge of the active cloud over Brittany. The northern one (C), which lies over the western tip of Cornwall, is separated from "B" by only a very small band of moister air. The main features identified in this figure align with the global model PV structure shown in Figure 11.

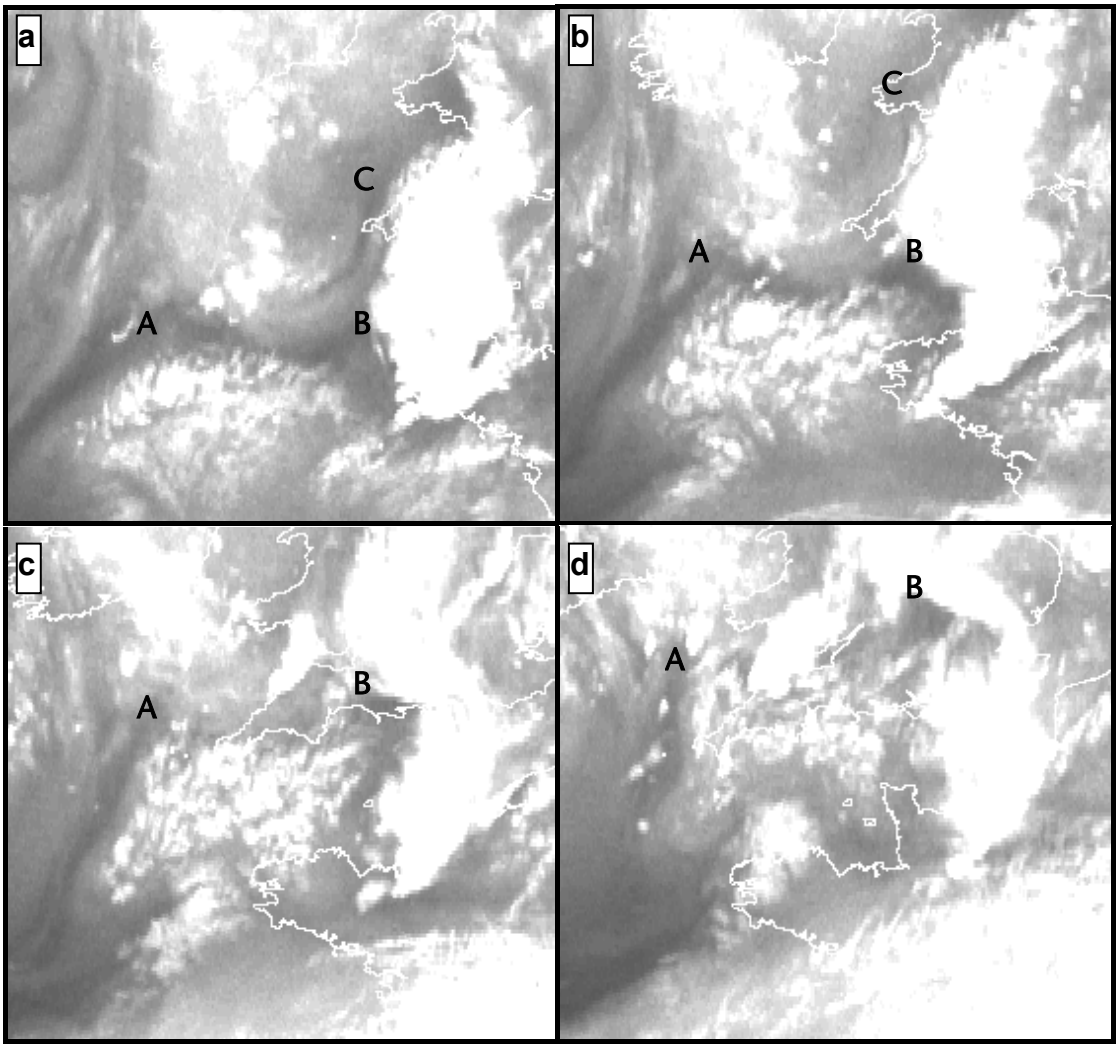

Figure 13 Meteosat-8 images in the upper tropospheric water vapour band at (a) 1030, (b) 1230, (c) 1430 & (d) 1630UTC, 16th August 2004. Note that each image is offset to the East.

By 1230UTC the main area of marked subsidence (B) has pushed rapidly northeast into the English Channel, rotating the cloud band on its forward edge to give a sharp apex over southern Cornwall. Band C, further north, has moistened and moved away, but still shows a weak dark line immediately behind the developing cloud north of Boscastle. Both the forward edge of band "C" and the apex of the rotation associated with "B" are areas where mesoscale uplift might be expected, supporting convective development. In the subsequent frames at 1430 and 1630UTC, the rapid northeasterly movement of "B" continues, taking the dry descending air into central England, and continuing to generate rotation of the apex of the cloud. At the same time, band "A" also moves northeast behind the second trough, approaching southwest Wales by 1630UTC.

Figure 14 summarises the upper tropospheric dry (dark) features identified in Figure 13, and their movement. Comparison with Figure 6 indicates that band A is associated with the second trough and band B with the first trough. However, the analysis in Figure 6 has not captured the orientation and northeastward movement of the head of band B.

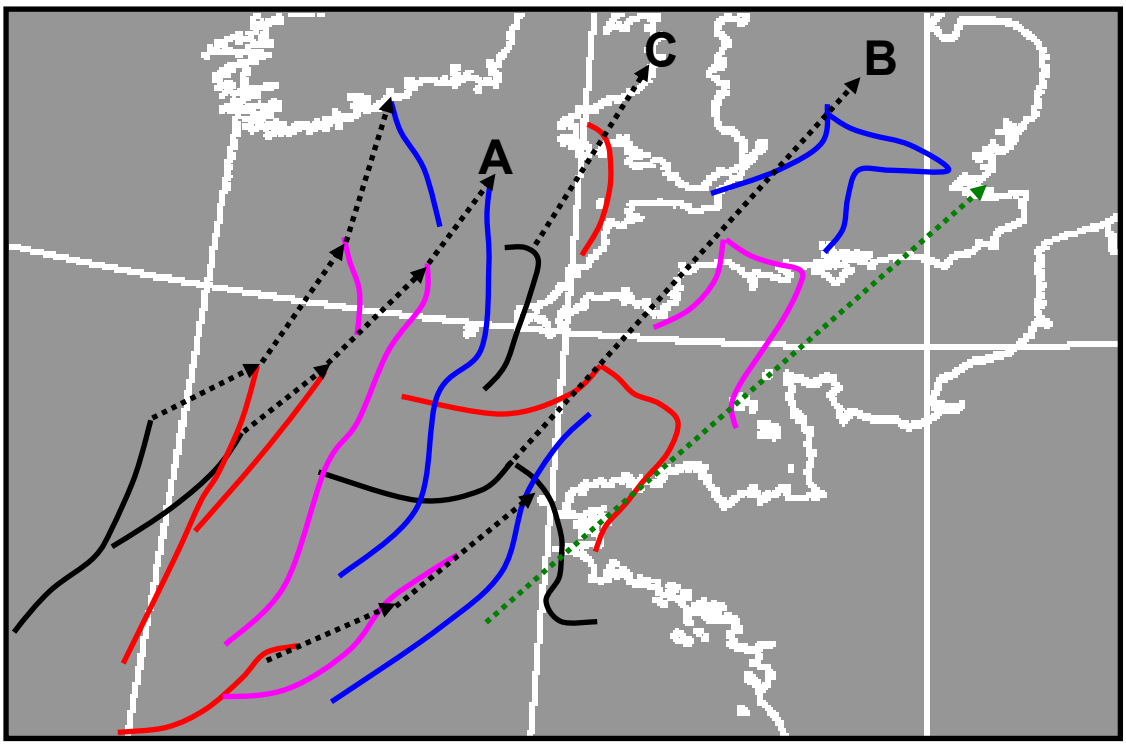

Figure 14 Tracks of features identified in the water vapour imagery, Figure 13. Colours show locations at 1030UTC (black), 1230UTC (red), 1430UTC (purple) & 1630UTC (blue). Green dotted line is approximate track of feature equivalent to B in the mesoscale model forecast, Figure 15.

3.3. Mesoscale 3-D structure from forecast model.

The mesoscale configuration of the Met Office Unified NWP Model has a grid length of about 12.3km and has a domain covering the British Isles and neighbouring parts of Europe and the eastern Atlantic. It is constrained to follow the large scale evolution of the global model through its boundary conditions, but small scale detail can be generated within this framework.

Figure 15 shows the modelled evolution of the upper troposphere as indicated by the "dynamical tropopause" in the potential vorticity (PV). This bears a strong resemblance to the water vapour imagery presented above, with values below 8.5km relating to the dark regions in the imagery. However, the propagation of the high tropopause ahead of the second trough, marked by the area >9.5km over Ireland at 0900UTC, appears to be rather too fast, and this may also affect the eastward movement of the first trough.

Looking in more detail, we see the rapid progression of the tongue of low tropopause heights into northern France, and the much slower movement to the north over Cornwall. There is also some raising of the tropopause height (to >10km) evident on the back edge of the pre-trough air over southern England, which is slightly separated from the main area to the east. This development of a separate area of tropopause maximum close to an existing wave vortex on its cold side is similar to that observed in cold air cyclonic development (Bader et al, 1995). If we shift the location of these features according to the positions of the head of band B in Figure 14, we can see that the area around the apex of the cloud over North Cornwall may have been influenced by the sort of upper tropospheric development exhibited further east in the mesoscale model.

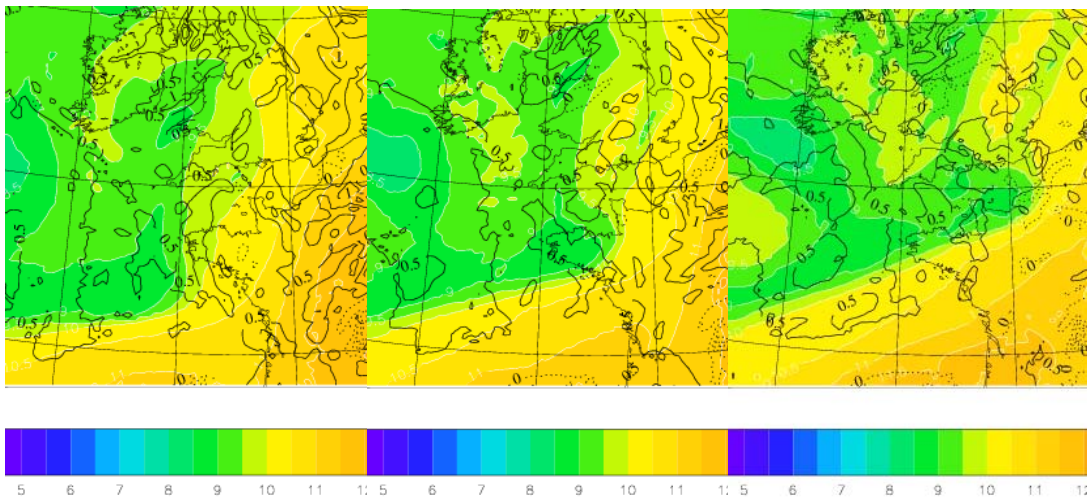

Figure 15 Output from 0000UTC run of the UK mesoscale model at 0900, 1200, 1500UTC 16/8/2004: colours indicate height in km of PV=2 surface (the dynamical tropopause)

Moving to the lower troposphere, Figure 16 shows the 900hPa wet bulb potential temperature at 1200UTC. The area of maximum values over the English Channel is well behind the leading edge of the upper tropospheric dry slot shown in Figure 15, indicating that the upper flow is over-running the lower flow, with the potential for creating unstable conditions favouring deep convection. On the other hand, there is relatively low wet bulb potential temperature air over the Celtic Sea in the immediate vicinity of Boscastle.

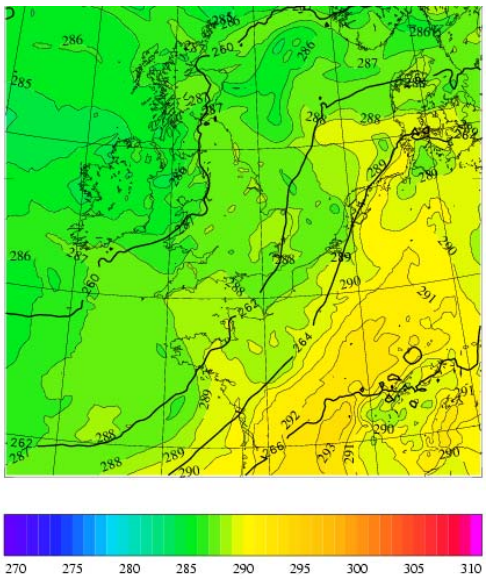

Figure 16 Output from 0000UTC run of the UK mesoscale model at 1200UTC 16/8/2004: colours indicate 900hPa wet bulb potential temperature (K)

In summary, we postulate, on the basis of the model PV diagnostic and the water vapour imagery, that the large scale forcing identified in the region of the left exit of the jet streak, is manifesting itself in a complex structure of upper tropospheric overturning focussed around the area of upper cloud and moisture rotation centred over Cornwall at 1230UTC.

3.4. Mesoscale rainfall structure from radar.

Radar is a key tool for observing mesoscale weather developments in the vicinity of the UK. In this section we look at the broad scale evolution, using a composite of several radars, extended by the use of satellite and lightning data.

Figure 17 depicts the coarse scale evolution of precipitation in the southwest approaches to the British Isles. The images are Nimrod 5km analyses, produced by combining fully corrected radar images from the UK, Irish and French networks with calibrated Meteosat satellite imagery, lightning reports and in situ observations. A description of the methodology employed for radar processing is given in section 3.8. Here we note that the radars are composited by using the radar beam which has the lowest elevation at each location. While carrying out the radar processing, a flag is set to indicate whether the radar would be expected to see any rain present in each pixel. At longer ranges, where the radar beam is high, this may be unlikely. Beyond this range, alternative data sources are used. These are combined using a variational analysis algorithm. The two principal data sources are satellite visible and infra red images which are jointly calibrated, at four rain rate thresholds, using comparisons with coincident radar rainfall rates over a recent period, and lightning reports, which are used to set a minimum rain rate of at least 2mm.hr^{-1}. It should be noted that the

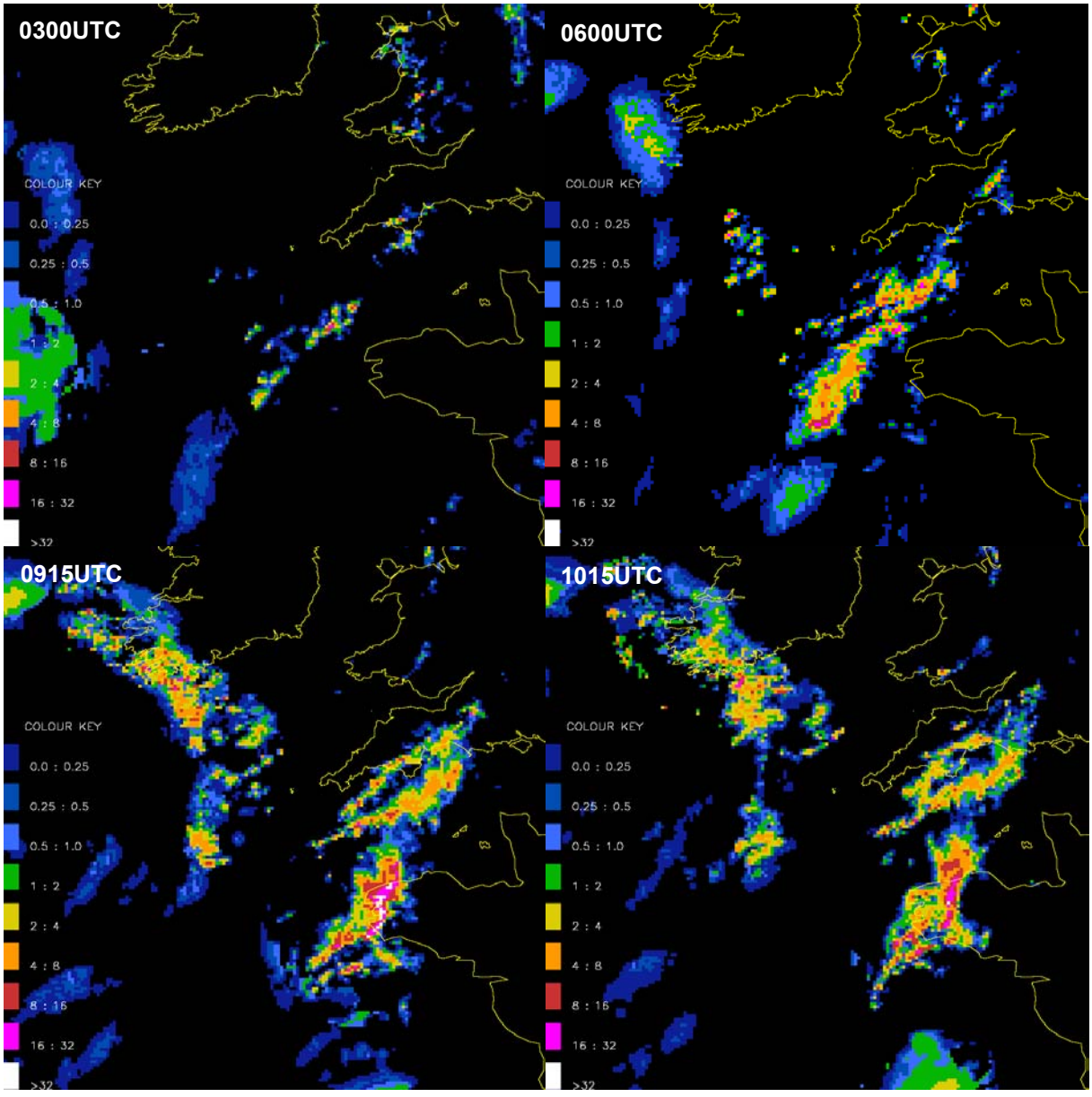

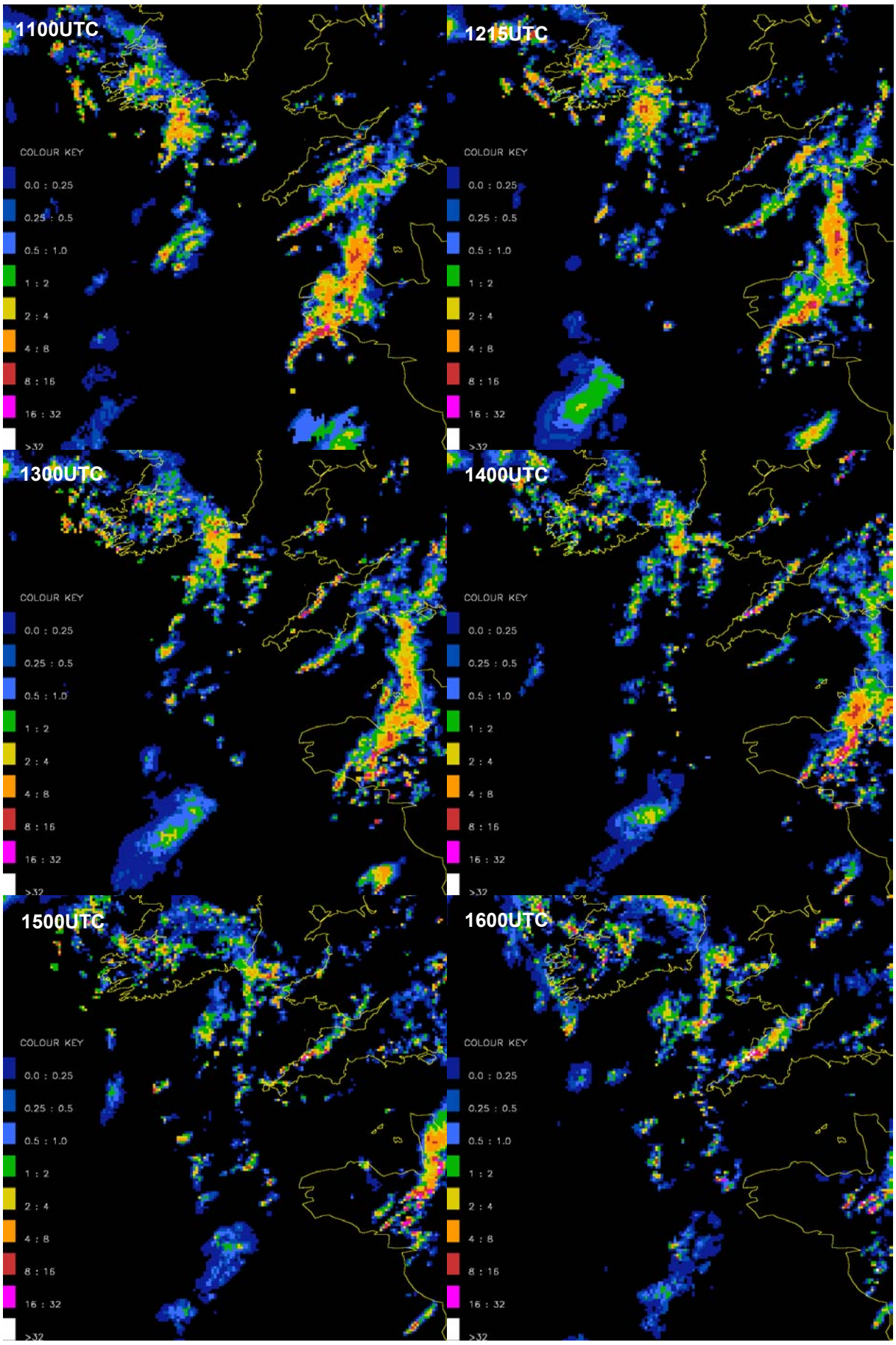

Figure 17 Hourly composite radar/satellite images 0900-1400 UTC on 16/8/2004

satellite calibration works well at low rain rates of 0.125mm.hr^{-1} & 0.5mm.hr^{-1} but lack of coincident radar data locations makes the performance at higher rain rates (2mm.hr^{-1} and 8mm.hr^{-1}) much poorer.

On some occasions the Irish images arrive too late for inclusion in the analysis produced on the hour. On those occasions, the analysis produced 15 minutes later has been selected for Figure 17 so that the additional detail available from radar is included. Note also that the first 3 images are spaced at 3-hour intervals, with the remainder at hourly intervals. Finer scale detail will be discussed later in section 3.8.

Inspection of the sequence shows several features of interest. There are two main bands of rain and showers that cross the area during the day. The first is initially oriented southwest to northeast and intersects the coast of south Devon in the first image at midnight. Pulses of convection develop along this band, and then move northeast. Between 0600 & 0900UTC, two point sources of convection develop on the band in the English Channel south of Cornwall and then persist, creating long plumes of precipitation with their heads in the band, but their sources left far behind. A similar plume develops later, between 1000 & 1100UTC to the south of Brittany. Note that there is no obvious surface forcing for these plumes, as they all form over the sea. Inspection of the English Channel plume in animated radar imagery indicates that its source is not fixed, but moves east and west on timescales of an hour or so, perhaps indicating intermittency and/or variation in the location of its source. As the main band moves east, it takes on a more north-south orientation, the northern end being fixed for a time over Somerset, while the southern end moves rapidly east over France. This band clears away east from our area of interest in the mid-afternoon.

Further west there is an eastward curved band of rain, which first hits the southwest Irish coast at about 0900UTC. This can be identified with the second trough marked in the synoptic chart, Figure 6, and with the band of cloud noted in the satellite image, Figure 13. This moves steadily eastward, reaching Cornwall at about 1500UTC, when it first reinforces, then terminates the Boscastle plume. There is a suggestion in the later images that this second band is retarded as it approaches Cornwall, while moving steadily eastwards to the north and south.

3.5. Mesoscale surface airflow.

Figure 18 shows the standard surface synoptic analyses for southwest England on 16th August 2004. The maps record the in situ observations available to the Met Office on the day. Information contained in each observation is plotted as a group of numbers and symbols centred on the cloud observation, if present. For manual observing stations, the cloud is depicted in a circle, while for automatic stations, a triangle is used. The amount of the circle or triangle that is filled indicates total cloud cover. To the left of the cloud a pattern of dots indicates continuous rain, with more dots indicating heavier rain, while an inverted triangle indicates showers. Temperature is plotted to the upper left and dew point to the lower left, both in degrees Celsius. Wind is shown by an arrow in the direction from which the wind is blowing, with the each full fleche indicating 10 knots of wind speed. On top of the observational information, isobars are shown by green and magenta lines at 2hPa intervals, and the locations of troughs are indicated by black lines. Charts are displayed for the intermediate and main hours of 0900, 1200 & 1500UTC, but the observations were analysed for all hours.

At each of the times displayed, the main surface wind direction is predominantly south-southwest. The main exceptions are some French observations, and those in the north of Devon, which are from the southwest. The lack of observations along the north Cornish coast makes analysis of developments very difficult. However, the

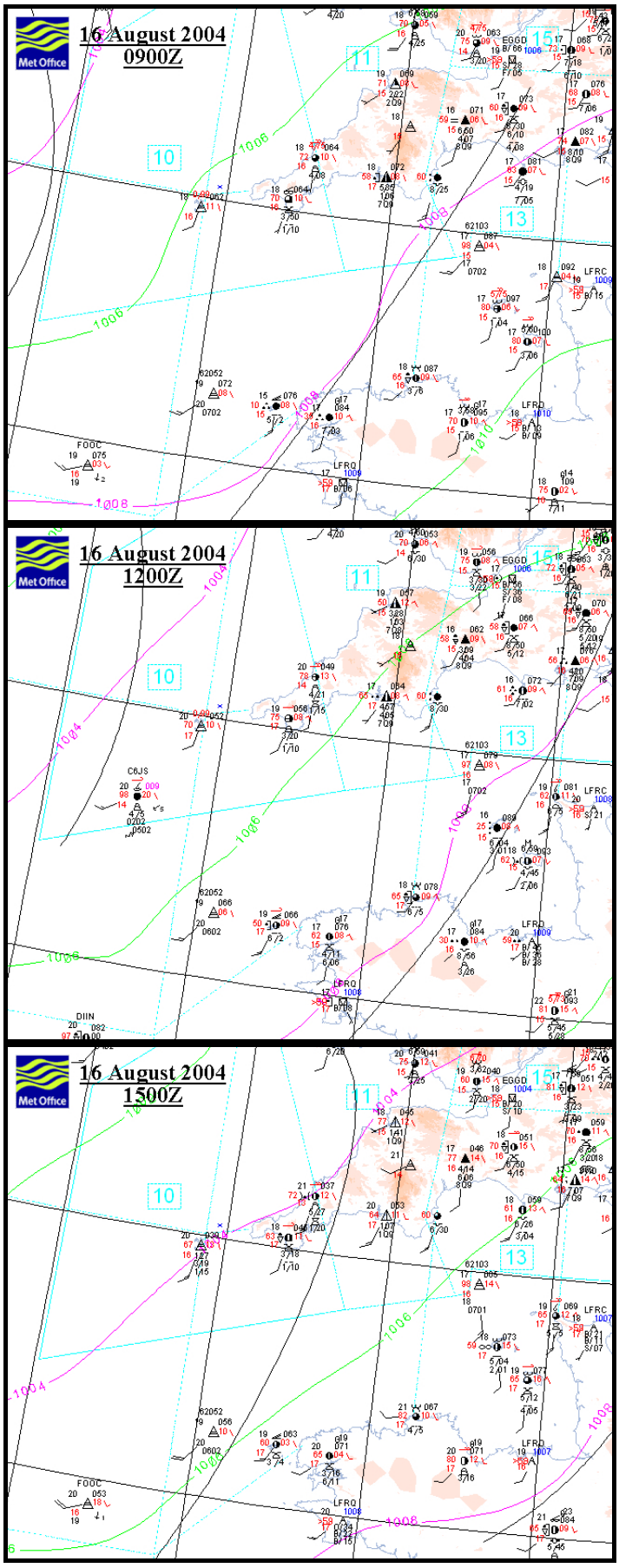

Figure 18 Surface observations for 0900, 1200, 1500UTC 16/8/2004

observation at St. Mawgan, near Padstow, shows that the temperature rose from 18°C at 0900UTC to 20°C at noon and then to 21°C from 1300-1500UTC. The nearest sea temperature is from the buoy marked 62052 west of Brittany, which is recording 20°C. The humidity is initially high, with a dew point of 16°C at 0900UTC, but this falls irregularly through the day, reaching 13°C by 1500UTC. Of more interest is the evolution of the surface pressure which is falling almost everywhere throughout the period, but with two areas of maximum falls. Inspection of the 3-hourly pressure tendency observations shows one area of maximum fall of 1.0hPa in western Cornwall at 0900UTC, which spreads up the coast and increases to 1.3hPa at 1200UTC and then shifts east into Dorset and further increases to 1.5hPa at 1500UTC. The second area starts in Brittany at 0900UTC with 1.0hPa falls, moving east and increasing to 1.5hPa at 1200UTC and then moving up to the Channel Islands and increasing further to 1.6hPa at 1500UTC. This pattern of falls does not fit well with the manually plotted trough lines, but it is on too large a scale to be explained by the convection itself. Bearing in mind the structures identified in the water vapour imagery and the mesoscale model diagnostics, it is suggested that the enhanced pressure falls over Cornwall are associated with the upper tropospheric development around the apex of the cloud band.

Unfortunately, the absence of further wind observations prevents any deeper analysis of mesoscale structure. It is sometimes possible to obtain additional observations of surface wind from satellite remote sensing. However, the overpasses of the Quikscat scatterometer on 16th August were not conveniently located, and no useful information can be deduced on the wind structure around Cornwall.

3.6. Local air mass analysis.

At this point in the meteorological analysis, we switch from looking at the dynamical structures that may have provided forcing to the convection, to the vertical structure of the air mass in which the storms themselves developed. This will be largely based on information from Camborne radiosonde ascents, supplemented by diagnostics from the model.

The basis of stability analysis is to discover whether a parcel of air from the lower part of the atmosphere, normally the boundary layer, will continue to rise, forming a convective cloud, if displaced vertically. Typically, a boundary layer air parcel will be sub-saturated, and will need to be lifted a substantial distance (to the Lifting Condensation Level: LCL) for the air to saturate. At this point it would probably be cooler than the surrounding air, and would need to be lifted further (Convective Inhibition: CIN) to initiate free ascent (at the Level of Free Convection: LFC). Free ascent will only take place if there is positive Convective Available Potential Energy (CAPE) – also indicated by appropriate values of other instability indices such as the Lifted and K indices. The depth of the convection is determined by the height at which the kinetic energy gained from the CAPE has all been used up in raising the parcel beyond the level where it becomes cooler than its surroundings. This is complicated by the modification of parcel characteristics during ascent through mixing. Falling precipitation exerts a drag on the air, and may cool it though evaporation, leading to development of a downdraught. The downdraught outflow at the surface is often important in initiating succeeding updraught development. Where there is significant wind shear, the locations of the updraught and downdraught can be separated in a way that permits long lived convective structures. The Bulk Richardson Number (BRN), which relates CAPE and wind shear, is therefore a descriptor of the character of the convection.

Figure 19 is a tephigram of the full resolution ascent from Camborne at noon. This displays observed thermodynamic variables on rotated axes of temperature and

potential temperature, an arrangement in which area on the graph corresponds to energy. It shows a surface temperature (T) of 20°C surmounted by a shallow super-adiabatic layer to a potential temperature of about 19°C. The surface dew point (Td) of about 16°C drops quickly to ~13°C, suggesting that the unmodified marine air has characteristics T, Td of 19°C, 14°C. Above this there is a clear mixed layer with a constant potential temperature of 19°C and a slight fall in moisture content. It is capped by a shallow layer almost at saturation, which, given the typical response of radiosonde moisture elements, may be taken to indicate a shallow cloud layer at 910hPa, 800m, a very low cloud base. Above this, the temperature trace is close to the 15°C wet bulb potential temperature, but with reduction, indicating strong instability around 800hPa (2km) and again around 650hPa (3.5km), then some shallow stable and dryer layers which might indicate possible cloud tops. The equilibrium level, at which most convection would be expected to terminate, was computed to be at 450hPa (6.5km). The freezing level is crossed at 710hPa and the -15°C level, at which clouds typically start to freeze, at about 530hPa. A cloud top at 450hPa would therefore be only just cold enough to initiate ice processes, without which the observed heavy rain seems unlikely. A lapse of slightly less than the saturated adiabat continues up to the tropopause at 250hPa, which marks the cloud top height of the most vigorous clouds. Humidity remains high as far as the tropopause, indicating layers of liquid water cloud at low levels, and continuous ice cloud at higher levels.

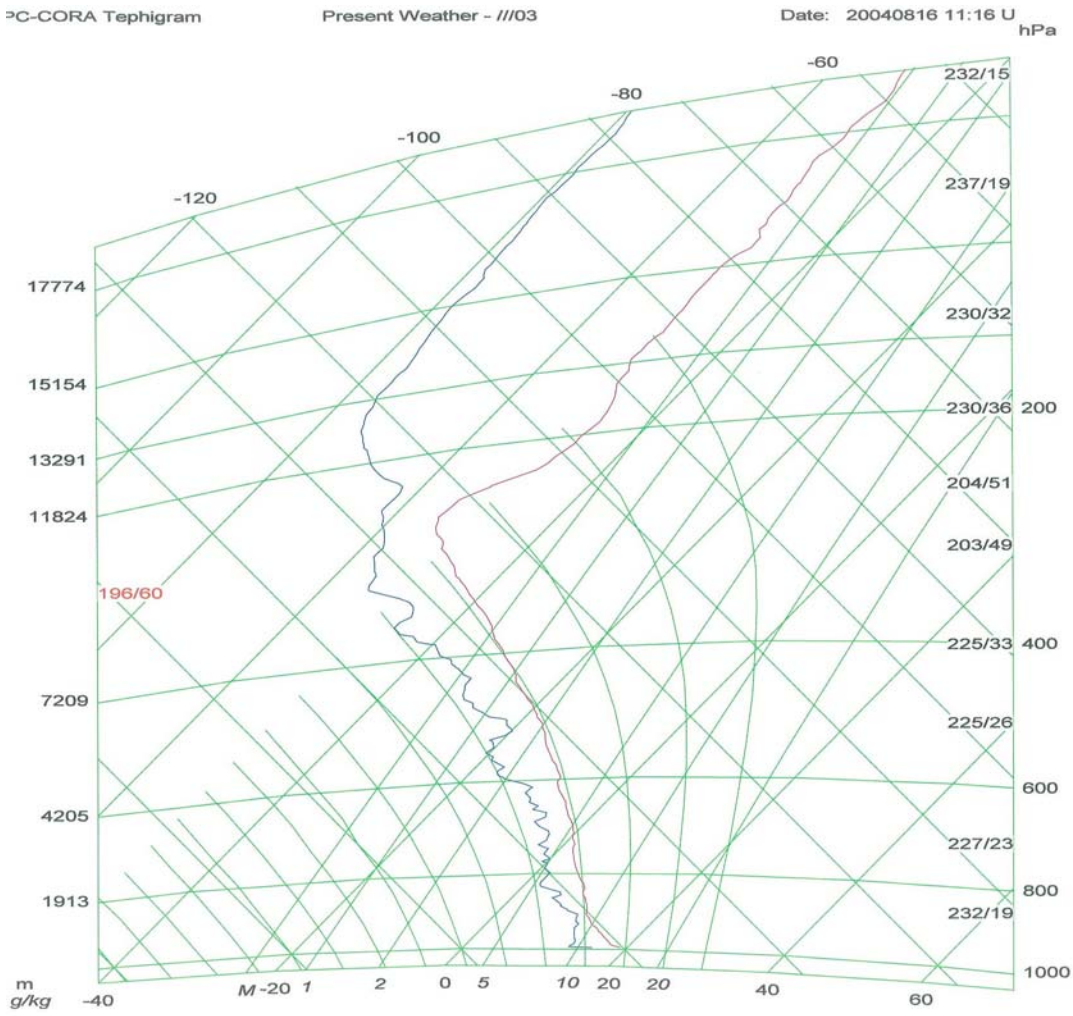

Figure 19 Tephigram from the radiosonde ascent at Camborne, 1200UTC 16/8/2004

Standard measures of instability in this ascent, and others on the same day, are summarised in Table 2. The sounding is very unstable, having substantial Convective Available Potential Energy (CAPE: 170J.kg^{-1}) and minimal Convective Inhibition (CIN: 2J.kg^{-1}). Undilute convection with CAPE of 170J.kg^{-1} gives a maximum vertical velocity of about 18m/s, so after allowing for entrainment and averaging over the depth of the cloud, a mean vertical velocity of 5m/s is probably appropriate. This is supported by the absence of observed hail in the storm. At this speed it would take 15minutes for air from the boundary layer to reach the equilibrium level, and another 15 minutes to reach the tropopause. We can use this information as the basis for calculating a possible rain rate. If we assume that the total column of air is lifted until there is no water left in it, we can calculate that the rain rate is given by the precipitable water divided by the lifting time. 26mm of precipitable water lifted to dryness in 15 minutes corresponds to about 100mm.hr^{-1} rain rate. In real clouds, much of the rainfall is evaporated into the surrounding air. This is expressed as the efficiency of a cloud, and is typically less than 50%. The maximum 15-minute rates observed by raingauges and the radar were 80-100mm.hr^{-1}, indicating an unusually high efficiency, while hourly accumulations of up to 60mm indicate that this high efficiency was being maintained over multiple cloud lifecycles without break.

Table 2 Diagnostics of the Camborne radiosonde ascents computed using the University of Wyoming package.

	00UTC 16th	12UTC 16th	00UTC 17th
Showalter index	2.18	2.05	1.51
Lifted index	-0.78	-0.50	-1.20
LIFT computed using virtual temperature	-1.06	-0.60	-1.43
SWEAT index	174.80	128.79	163.99
K index	28.90	28.00	28.60
Cross totals index	23.00	23.10	23.50
Vertical totals index	24.70	25.90	26.10
Totals totals index	47.70	49.00	49.60
Convective Available Potential Energy	233.29	170.17	297.80
CAPE using virtual temperature	289.23	217.22	360.48
Convective Inhibition	0.00	-1.18	-0.21
CIN using virtual temperature	0.00	-0.33	-0.03
Equilibrium Level	455.23	373.72	350.66
Equilibrium Level using virtual temperature	452.14	372.71	338.89
Level of Free Convection	964.73	905.20	926.47
LFC using virtual temperature	964.90	908.41	932.01
Bulk Richardson Number	20.71	11.86	22.49
Bulk Richardson Number using CAPV	25.67	15.14	27.22
Temp [K] of the Lifted Condensation Level	288.06	284.49	286.46
Pres [hPa] of the Lifted Condensation Level	969.52	913.15	945.32
Mean mixed layer potential temperature	290.63	291.98	291.11
Mean mixed layer mixing ratio	11.12	9.32	10.27
1000 hPa to 500 hPa thickness	5562.00	5552.00	5553.00
Precipitable water [mm] for entire sounding	28.93	25.87	26.03

Figure 20 shows a plot of the wind profile from the Camborne ascent. The near surface wind is southerly, veering to southwesterly 7.5 m.s^{-1} (15kn) at the top of the boundary layer. There is weak, unidirectional shear from there up to cloud top – the wind remaining southwesterly, increasing to 17.5 m.s^{-1} (35kn) at 400hPa. This is a structure that ensures that any downdraught will be down wind of the initiation point. It does not favour development of either multi-cell or supercell storms, which require directional shear of more than 20-30 degrees between cloud base and the height of

origin of the downdraught (Pierce and Cooper, 2000). The wind at the middle of the storm layer (~500hPa), is southwest 12.5 m.s^{-1} (25kn) consistent with the observed movement of the storms.

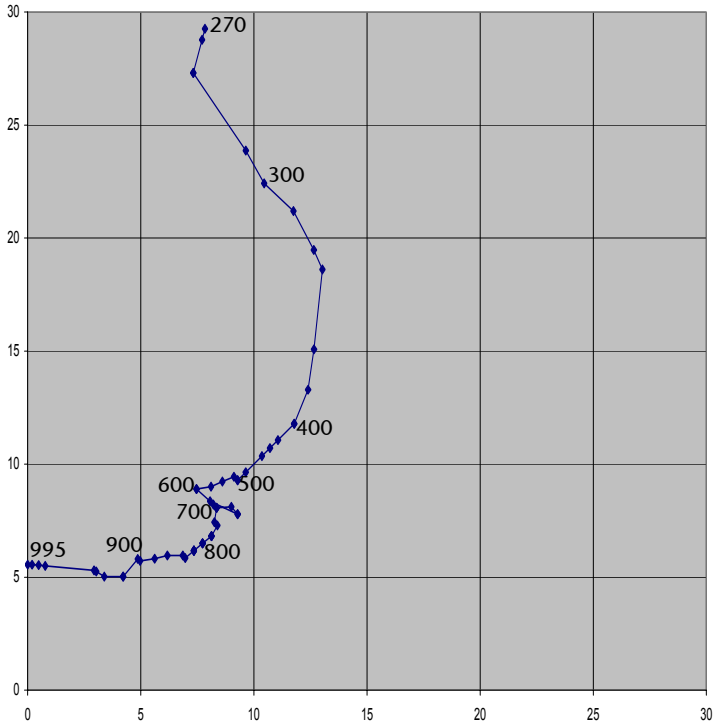

Figure 20 Hodograph from the Camborne 1200UTC sounding. Axes are in m/s. Values are pressure in hPa.

Figure 21 illustrates the time evolution of the vertical atmospheric structure, using four available soundings from Camborne. The early afternoon sounding was an additional sounding, made for experimental purposes, but to the same standard as the regular operational soundings. Note however, that in these plots the normal soundings are plotted using the reduced vertical resolution of official coded reports, whereas the additional sounding has the full resolution received locally. Potential temperature (temperature adjusted to 1000hPa) is used for the first plot to emphasise differences, that would otherwise not be visible on the scale of the temperature difference between tropopause and surface. Evolution of the temperature structure is very slight over the 24 hour period, with the expected day-time development and decay of a super-adiabatic surface layer and well mixed boundary layer at the bottom, and a steady cooling of the top of the troposphere, associated with a slight lowering of the tropopause. The humidity is expressed as a % relative humidity, and is characterised by a high level of small scale variability. The boundary layer again responds to the diurnal heating cycle, being nearly saturated throughout at night, but with a much dryer surface during the day. However, the top of the boundary layer and much of the lower troposphere remain near saturation throughout the period. The main changes can be seen in the upper troposphere, at levels where cloud would most likely be in the form of ice. Here there is a marked increase in relative humidity during the middle of the day, which decreases again later. This agrees with the moistening evident in the water vapour imagery, Figure 13, that was associated with distortion of the moist tongue ahead of the first trough. Finally, we see a maximum of humidity at all times in a thin layer immediately below the tropopause, indicating moisture outflows from deep convection. The wind speed profiles show the diurnal change from a low level nocturnal jet to a well mixed day time boundary layer. There is also a more marked reduction of wind speed in the upper troposphere, mainly occurring over the morning period. The wind direction profile changes rather little during the period, with a

constant southwesterly over most of the troposphere and frictional backing to southerly at the surface. However, there is a very marked backing to almost southerly

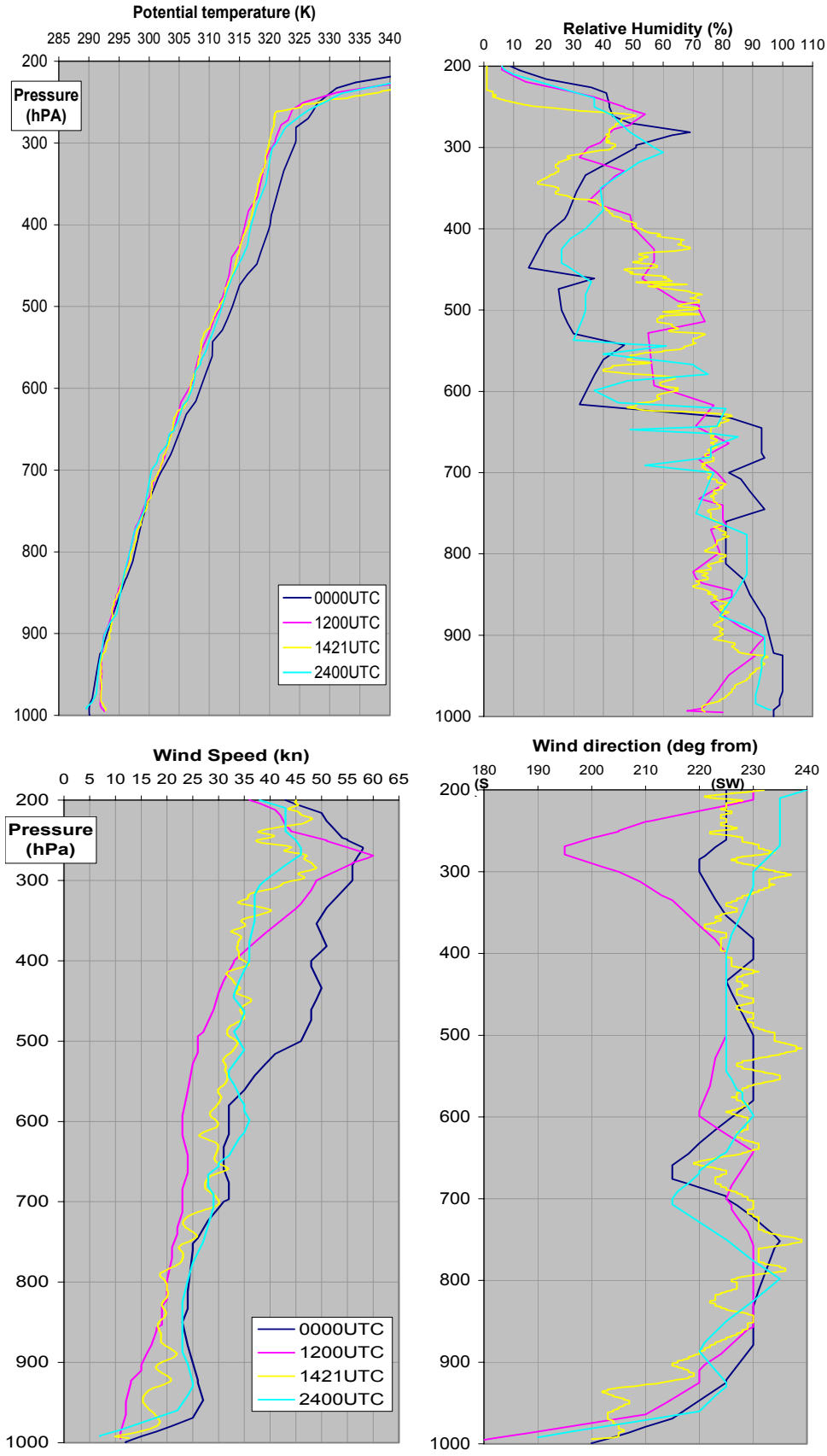

Figure 21 Time sequence of upper air potential temperature, humidity, wind speed and direction profiles observed at Camborne on 16th August 2004

in a shallow layer near the tropopause at noon, which is associated with a peak of 60kn in wind speed. This cannot be a result of the initial Boscastle convection, as the sounding is upstream of that. It seems likely therefore, that this is again associated with the upper vortex noted in the water vapour imagery.

Further analysis of the expected response of the atmosphere to the observed vertical structure can be obtained by looking at mesoscale model diagnostics produced as part of the Convection Diagnosis Procedure (CDP), implemented on Nimrod to support broad scale forecasting of convection. The highest CAPE value in the model midnight run was 144 $J.Kg^{-1}$ at 1400UTC on the coast south of Boscastle. The sounding shown in Figure 22 is from the model forecast for 1200UTC at a location

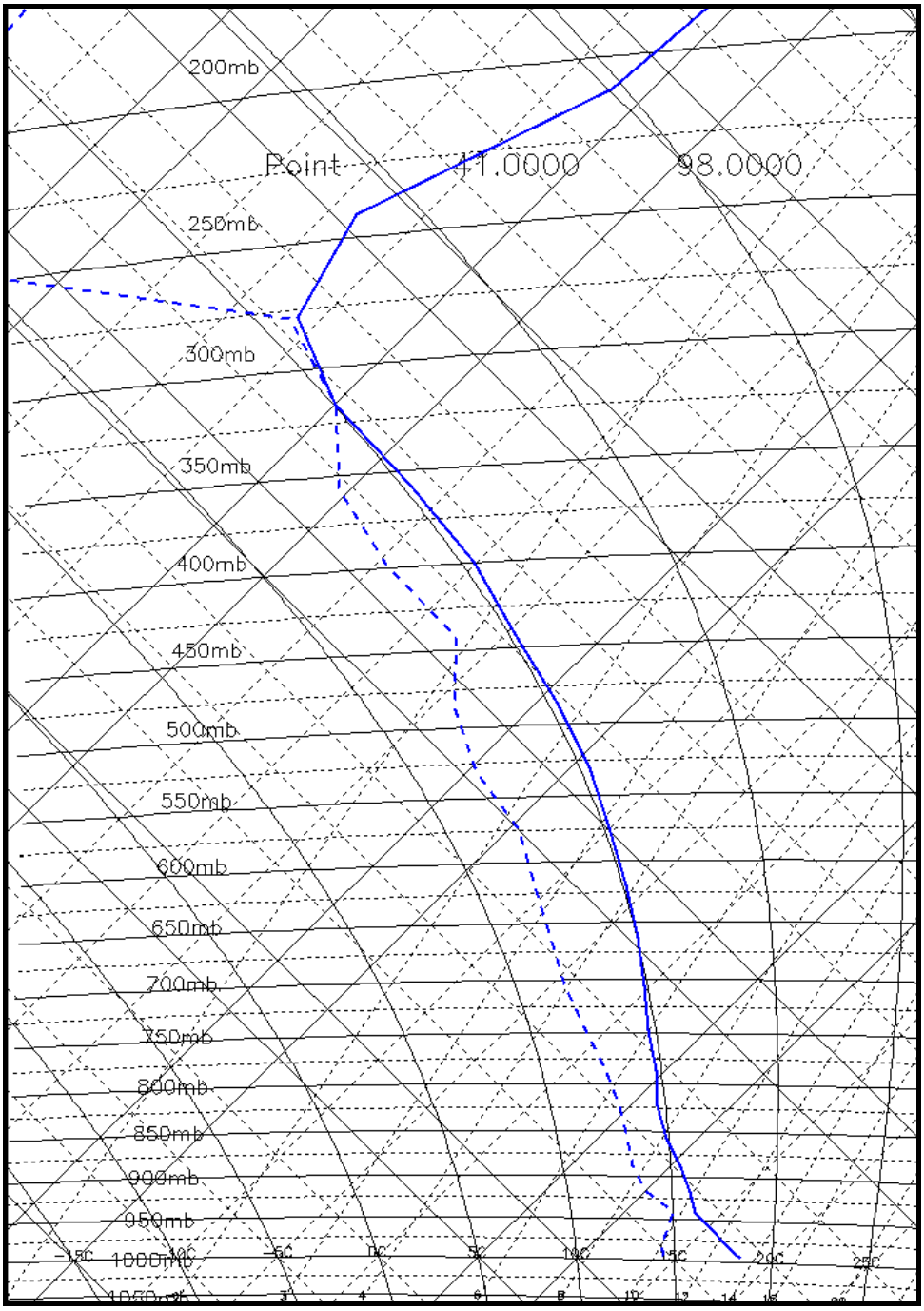

Figure 22 Tephigram from mesoscale model T+6 forecast for 1200UTC from a location 10km east-southeast of Padstow

about 10km east-southeast of Padstow. It reproduces the structure seen in the Camborne soundings, though the coarse vertical resolution means that much of the detail is missing, especially in the humidity structure. Diagnostics computed from model soundings of this sort should be consistent with the real atmosphere.

The largest peak rainfall rate deduced by the CDP was 40 $mm.hr^{-1}$, which is consistent with the upper end of expected rainfall efficiency, given the lower CAPE than that observed.

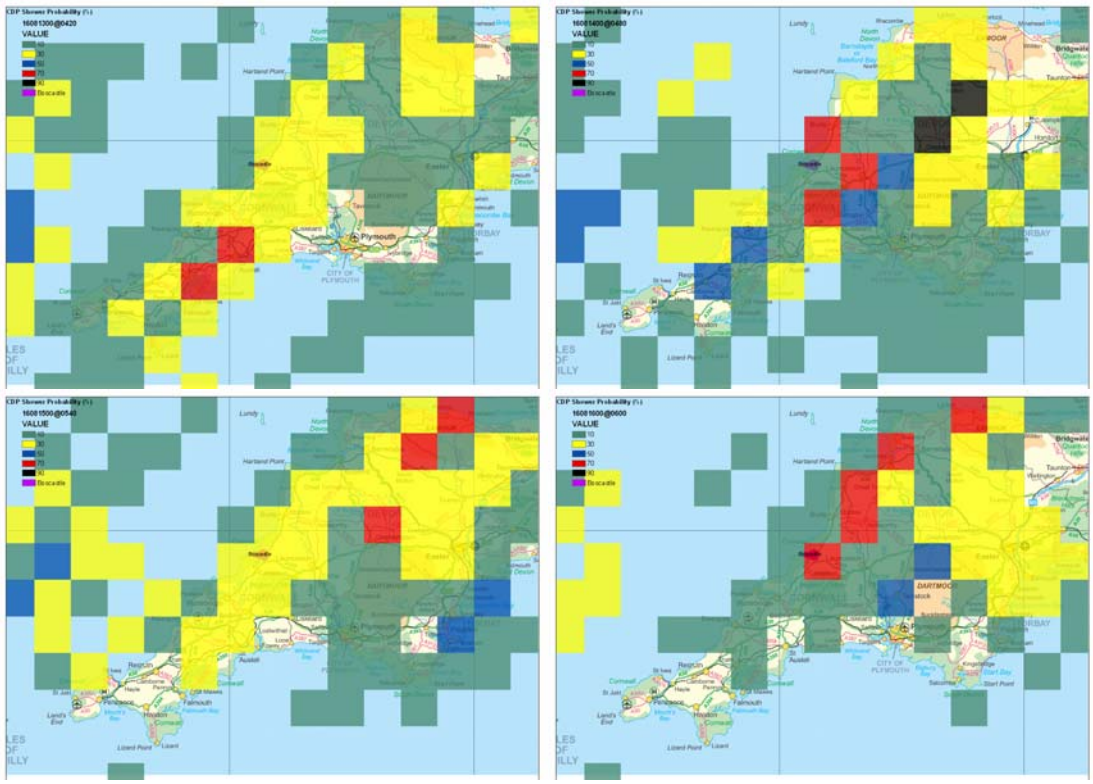

Figure 23 Probability of convection occurring in 15km squares for 1300, 1400, 1500, 1600UTC, diagnosed from the mesoscale model using the Convection Diagnosis Procedure (CDP). Values shown are black (>90%), red (>70%), blue (>50%), yellow (>30%) and green (>10%)

Figure 23 and Figure 24 show estimates of probability and intensity of precipitation produced by the CDP, given the air mass characteristics represented in the model. Note the apparent random variation in the locations over land with highest probability in the 60-70% range and maximum rain rates in the range 16-32mm/hr. The high probabilities reflect the very small values of CIN present both in the model and in reality, while the rain rates largely reflect variations in CAPE.

A set of predictors has also been assembled for extreme rainfalls in the UK, based on extreme events in the period 1900-2000 (Hand et al, 2004). Applying this to model fields for 16th August 2004 gives the results shown in Figure 25. Peak probabilities of a 100 year return period event reach 10-15% in Cornwall, consistent with earlier evidence that the model forecast structure could support heavy, but not extreme, individual thunderstorms. The algorithm does not include a representation of the features that resulted in repeated generation of convective storms along the same line.

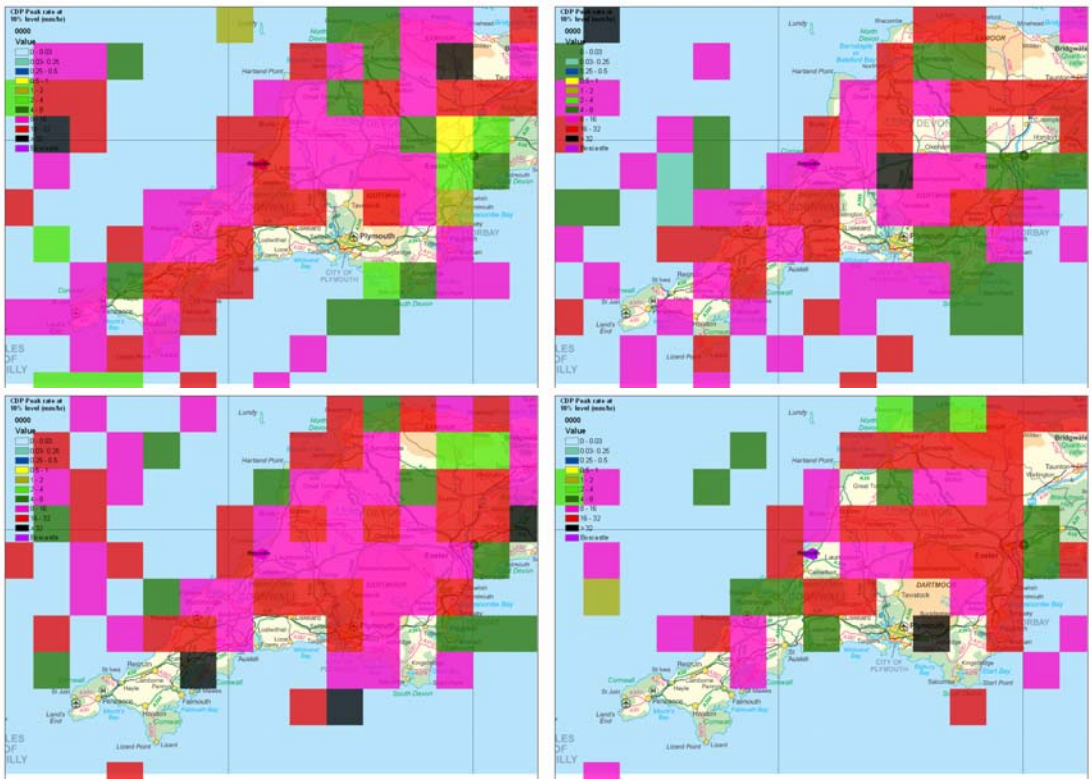

Figure 24 Peak convective rain rates for 1300, 1400, 1500, 1600UTC, diagnosed using the Convection Diagnosis Procedure (CDP) from the large scale conditions in the mesoscale model in 15km squares. Heavier values shown are black: >32mm/hr, red: >16mm/hr, pink: >8mm/hr, dark green: >4mm/hr.

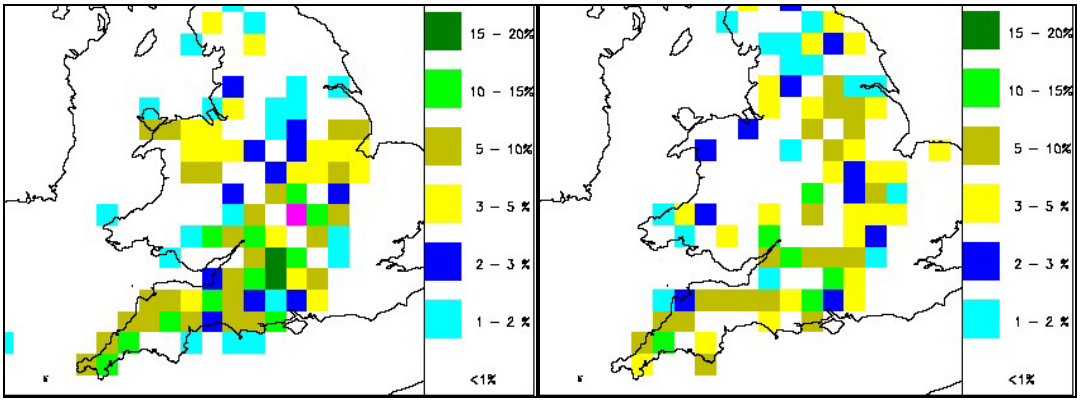

Figure 25 Probability of extreme (1:100 year) rainfall at 1200 & 1500UTC obtained using the method developed in the Extreme Event Recognition project.

3.7. Storm analysis using satellite data.

There is much that can be learned about the storms from the satellite imagery available from the Meteosat-8 SEVIRI instrument described in section 3.2. For the storm scale analysis, we focus on the high resolution visible channel for cloud structure and the far infra-red channel at 10.8μm for cloud top height.

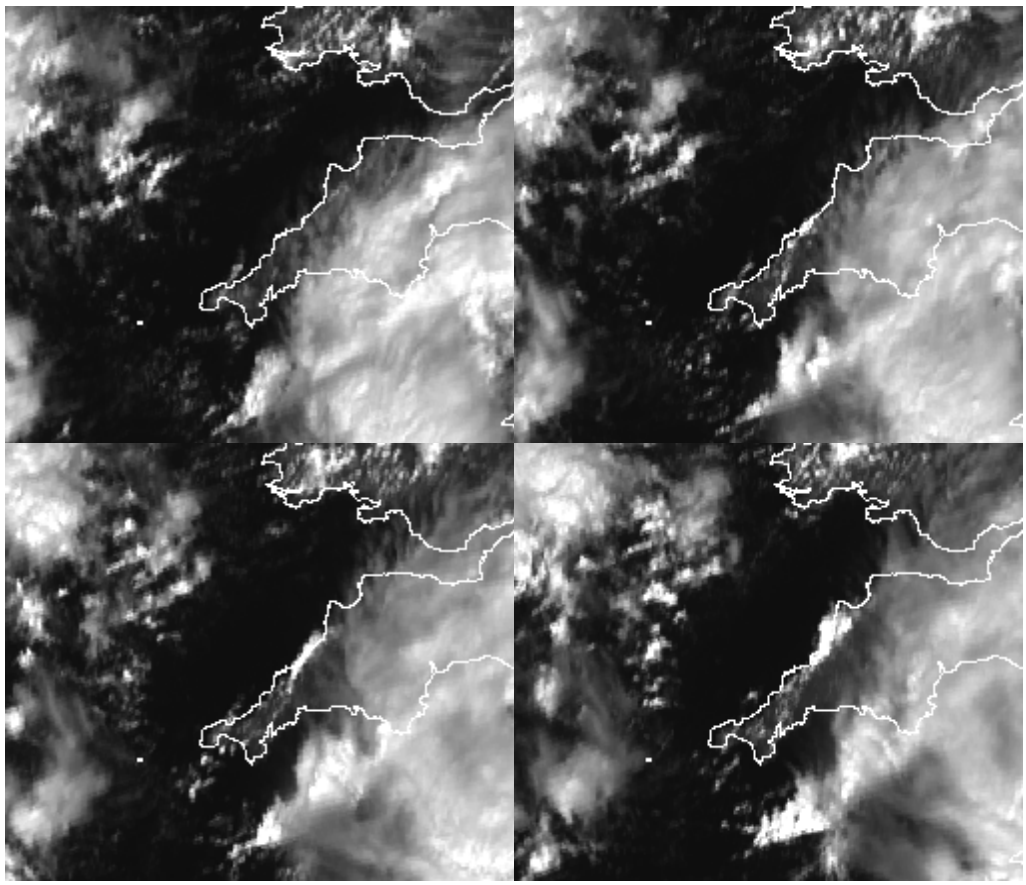

Figure 26 Meteosat-8 high resolution visible images for 1030, 1100, 1130 & 1200UTC 16th August 2004

Figure 26 shows expanded sections of the Meteosat-8 high resolution visible images taken just before and after the appearance of the first radar echoes in north Cornwall. The images shows bright clouds as white where they reflect sunlight strongly. The brightness depends on the concentration and size of the water drops or ice crystals. The brightest clouds are composed of large numbers of large water drops, while light grey clouds have lower concentrations of water, and the fuzzy areas are thin layers of ice crystals. The eastern part of each image is dominated by thick bright convective cloud associated with the storms in Brittany and the English Channel, the latter also affecting south Devon. Bright convective cloud is also present to the south of Ireland. At 1030UTC, the precipitation plume identified in the radar pictures in the western English Channel can be identified clearly. Over the far west of Cornwall, a line of cloud can be seen forming on the east side of the Lands End peninsula, and advecting northeast. Further east, over northern Cornwall, a line of cloud cells can be detected to the northwest of the main cloud plume. At this stage they are not very bright, indicating a modest thickness of cloud. By 1130UTC, the eastern line of cells has developed into a bright cloud plume along the north Cornwall coast, with a darker tail of smaller clouds extending from the Falmouth estuary to its start, near Wadebridge

Later development is shown in Figure 27. The main cloud plume over France has moved away to the east, while the part of it remaining over southern England has become less bright, indicating that it is largely formed of cirrus. The origin of the cloud plume near the Camel estuary is clearly identifiable in the 1330UTC image. Note that there is a second, less bright line of cloud to the southeast at this time, which was remarked on by the eyewitness at St. Breward. Further northeast beyond Bude, two elements to the structure can be identified: a broad cloud shield over the Hartland peninsula and a narrow arc of storm cells to the east. The most intense precipitation

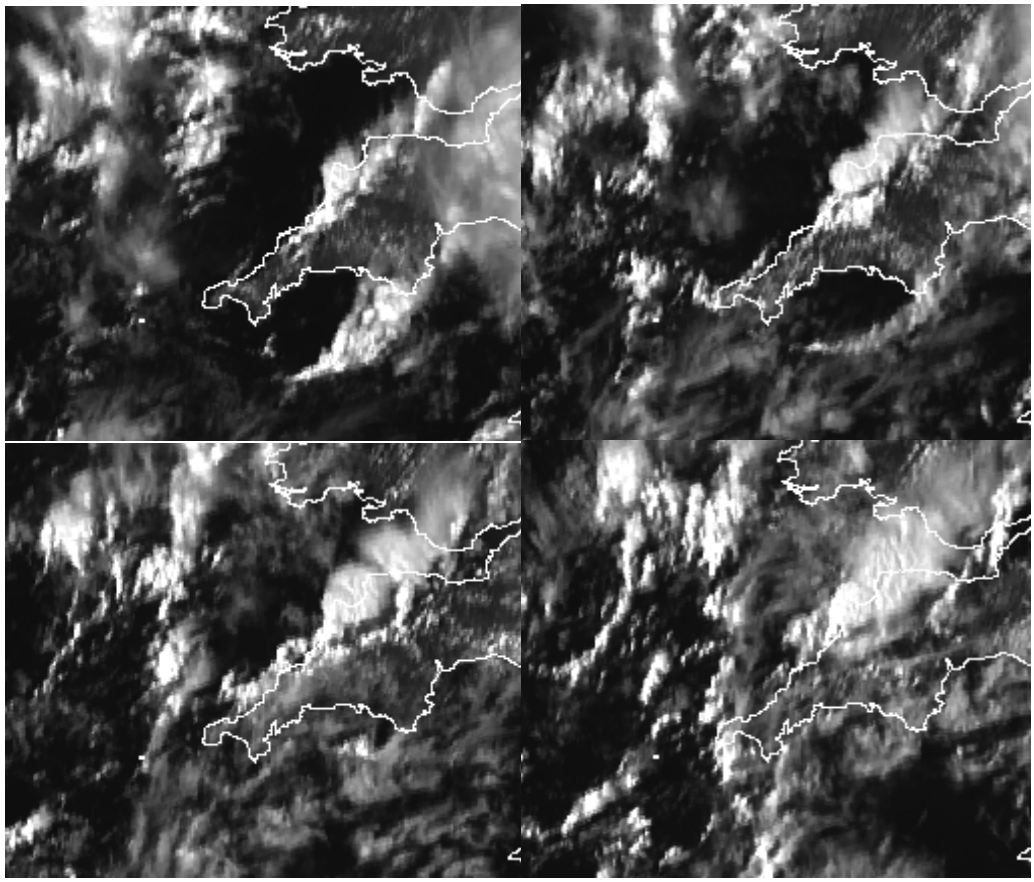

Figure 27 Meteosat-8 high resolution visible images for 1330, 1430, 1530 & 1630UTC 16th August 2004

in this area is associated with the eastern arc of cloud. Later on, this separation becomes more marked, with the eastern arc of cloud broken into individual storm elements, while the shield covers a much larger area extending to Morte Point in northwest Devon.

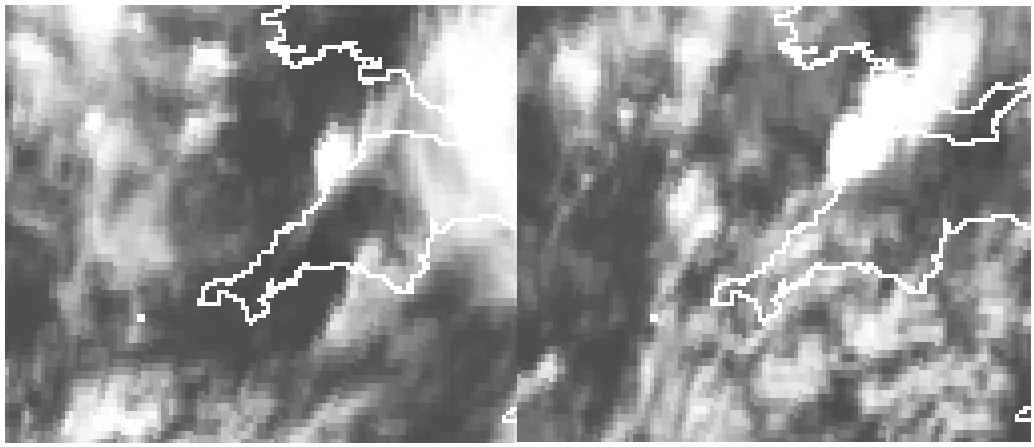

Figure 28 Meteosat infra red images for 1330UTC & 1530UTC 16th August 2004

Figure 28 shows images from the10.8μm infra red band, which primarily responds to the cloud top temperature. Note that images from this channel have poorer resolution than those from the high resolution visible channel discussed above. At 1330UTC, the eastern part of the image is dominated by the plume of cloud swirling north-east from the Brittany storms. This plume, like subsequent ones, has cloud tops in the range 9.2-10.6km (30-35kft), consistent with the tropopause height found earlier. At

this time, the coldest cloud over north Cornwall is significantly warmer than that found in the main plume, indicating that cloud tops are not as high. Also note that this cloud is located over Hartland and out to sea, whereas the cloud associated with the heaviest rain to the south near Boscastle is hardly evident. This indicates that the storms developing near Boscastle are not reaching their greatest vertical extend until they reach the vicinity of Bude, and that by this time the upper parts of the cloud have been blown to the west of the newly active parts at the ground. In the later image, the same pattern is evident, but the plume of high cloud downwind of Boscastle is now much more extensive, and the cloud top temperature is comparable with that found in the other major plumes.

3.8. Storm analysis using rainfall radar data.

Radars emit pulses of microwave radiation and observe the back scattered radiation from precipitation particles. The back scatter is dependent on the number and size of droplets. By observing the back scatter at various times from its transmission, a range dependent measurement is made. The antenna scans in a horizontal plane so as to obtain measurements in all directions from the radar site. The useful range for quantitative measurement of rainfall rate depends on cloud depth, and hence on the climate of the region and the time of year.

Operational weather radars, around the world, are operated in the S, C, & X bands, in order of increasing frequency and decreasing wavelength (~10cm, 5cm & 3cm respectively). The low frequency S band radar suffers less from attenuation but requires a bigger dish and higher power, making costs much higher. X band radars are only suitable for small area surveillance due to high attenuation losses. Most European countries use C band radars which provide a compromise of cost and range. The sources of error associated with radar observation of precipitation are dealt with in section 4.4. The major advantage of using radar is that it provides areally averaged rainfall estimates, which do not suffer from the spatial sampling problems of rain gauges.

Two C-band radars cover the area of interest: the Predannack radar near the tip of Cornwall, which is owned by the Royal Navy, and the Cobbacombe Cross radar in North Devon, which is jointly owned by the Met Office and the Environment Agency. Both are operated by the Met Office. A programme of continuous improvement to processing of the data is carried out in the Met Office, with periodic changes implemented to the operational equipment and processing procedures when improvements have been proved in trials. Both radars have an unobstructed view of the Boscastle area, at a range close to 100km. Cobbacombe is slightly the nearer. As the range increases, the increasing height of the beam leads to the estimate of surface precipitation becoming more indirect and the increasing spread of the beam leads to increasing volumes being observed in each sample,. As a consequence, there is a limit to the resolution of the basic data. At the range of Boscastle, this effect limits the minimum observable scale to about 2km, so products are not made available at finer resolutions.

Development of the storms is traced using single site images from both radars: Predannack for the initiation and early development from 1100-1430UTC in Figure 29, and Cobbacombe from 1200-1630UTC in Figure 31. Each display shows corrected rain rate in 2km pixels up to the limit of 2km processing at 100km radar range. Looking at the whole sequence, note the very small scale of the event. The width of the plume does not exceed 10km throughout its life. As a result, the 5km radar analyses shown earlier give a poor indication of peak rates and accumulations with only isolated pixels exceeding 16mm.hr^{-1}. By contrast, the 2km displays of the same data here show extended features of more than 32mm.hr^{-1}.

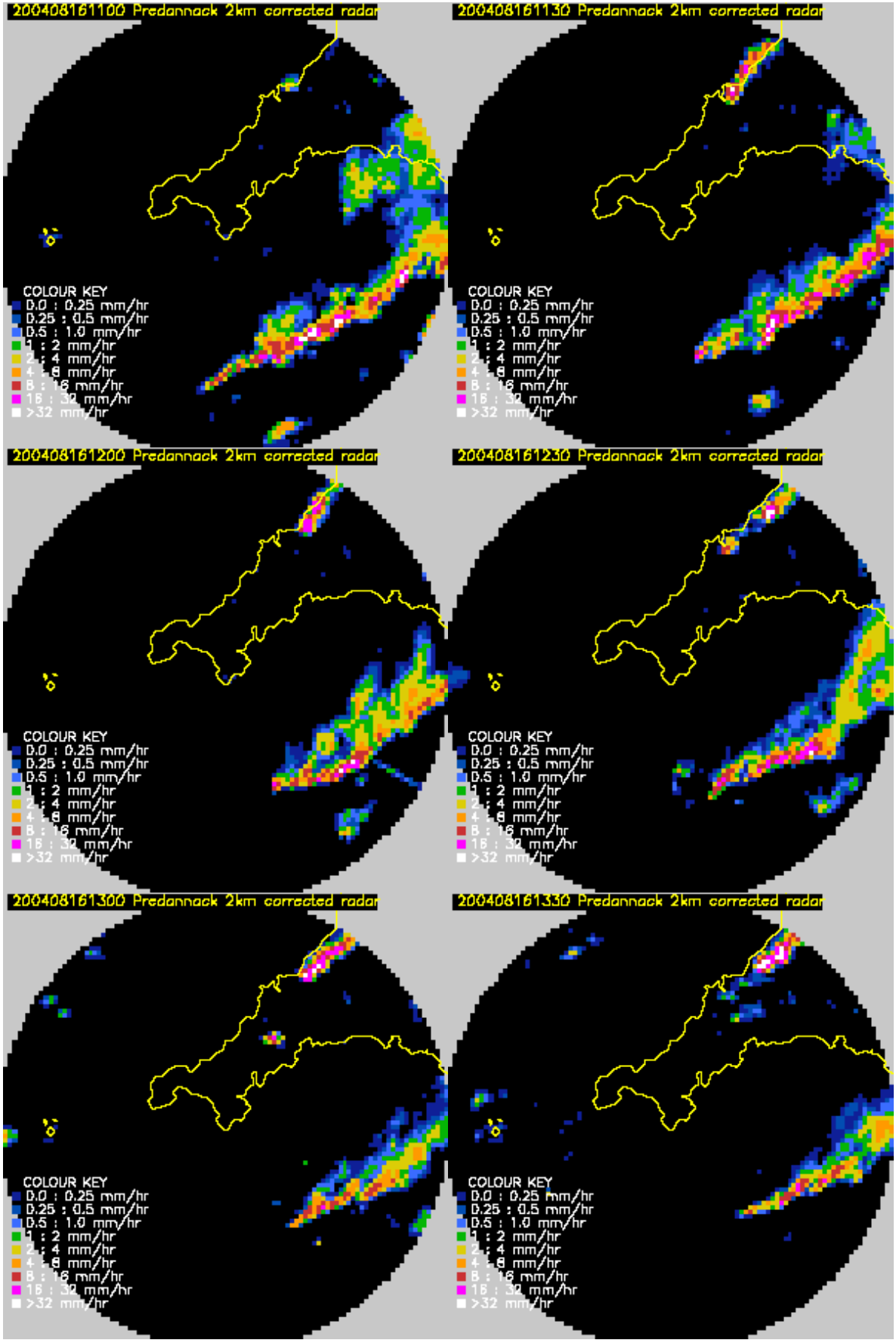

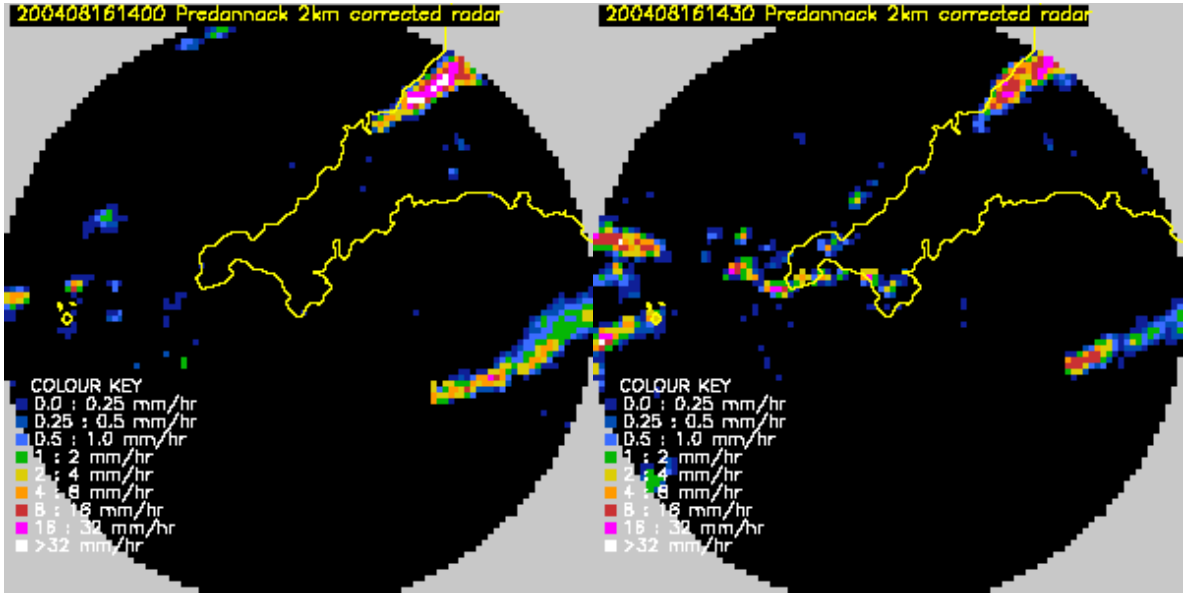

Figure 29 Predannack corrected 2km radar surface rain rates 1100UTC - 1430UTC

The conditions for radar observation were good on 16th August, and both radars produced clear images of the event. The Predannack radar gives a clear view of storm initiation, and Figure 29 shows the evolution of this early stage of storm development from the first cell at just before 1100UTC through to the arrival of more general convection associated with the second trough at 1430UTC. The first echo of the first cell was seen on the coast, northeast of the Camel Estuary. Given the timescale between initial cloud development and first precipitation, it would appear that the trigger for deep cloud development was uplift associated with convergence in the vicinity of the high ground there. The fact that cloud development is occurring along the whole of this part of the coast, with other precipitating clouds further north-east, suggests that it is a mesoscale feature associated with the land-sea contrast, that is the trigger. However, it is also possible that the synchronised timing is a result of upper level forcing or a gravity wave train. By 1130UTC, this first storm has spread along the coast, with most of the rain falling over the sea and a second, much more intense storm has developed over the Camel with maximum rates exceeding 32mm.hr^{-1}. The first echo of this cell was seen south-west of the Camel Estuary, and further inland than the first cell. The next cell to develop independently can be seen in the 1230UTC image, and is first located south west of the Camel Estuary at 1215UTC. The next to develop can be seen much further south between Newquay and St Austell at 1300UTC, after first appearing at 1250UTC. This remains further east than the others and decays. From 1310UTC, a sequence of small cells develops across the Camel Estuary at 1310-1320UTC, and can be seen as the last three cells in the 1330UTC image, of which the first has developed to rates greater than 32mm/hr. Further cells develop in succession after this time, maintaining the upstream end of the convection close to the Camel Estuary until shortly after 1400UTC.

Each of the main cells followed a similar development, starting as an isolated precipitation echo near the Camel estuary, then moving up the coast and developing into a line of precipitation. Figure 30 illustrates this development, using 5-minute, 2km radar images of the first two cells (marked A & B respectively) observed by the Predannack radar. Each active precipitating element propagated northeast at a speed of about 10ms^{-1}. However, the figure shows that the first cell, A, actually spread out with its forward edge propagating at 15ms^{-1} and its back edge stationary. Within this envelope, development of three secondary cells can be identified which link with each other, and with cell B, to create a continuous line of heavy precipitation. The result of this evolution was to turn two 5km cells separated by about 15km into an unbroken

string of four 5km cells. With each cell moving at 10ms^{-1}, the point frequency would have been one cell every 7 minutes, consistent with the periodicity evident in the rain gauge analysis in Figure 37.

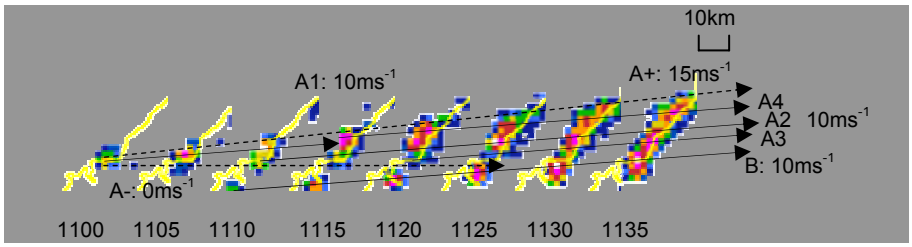

Figure 30 Initial evolution of the 1st & 2nd storm cells, 1100-1135UTC. Each time is shifted right by an additional 25km for clarity

Figure 31 shows half-hourly single-site images for 1200-1630UTC from the Cobbacombe radar. The 1200UTC image shows a train of showers right up the coast from Tintagel into north Devon. Reference back to Figure 29 shows that only those cells from southwest of Bude have developed from the vicinity of the Camel. The others appeared further northeast at the same time as the first cell around the

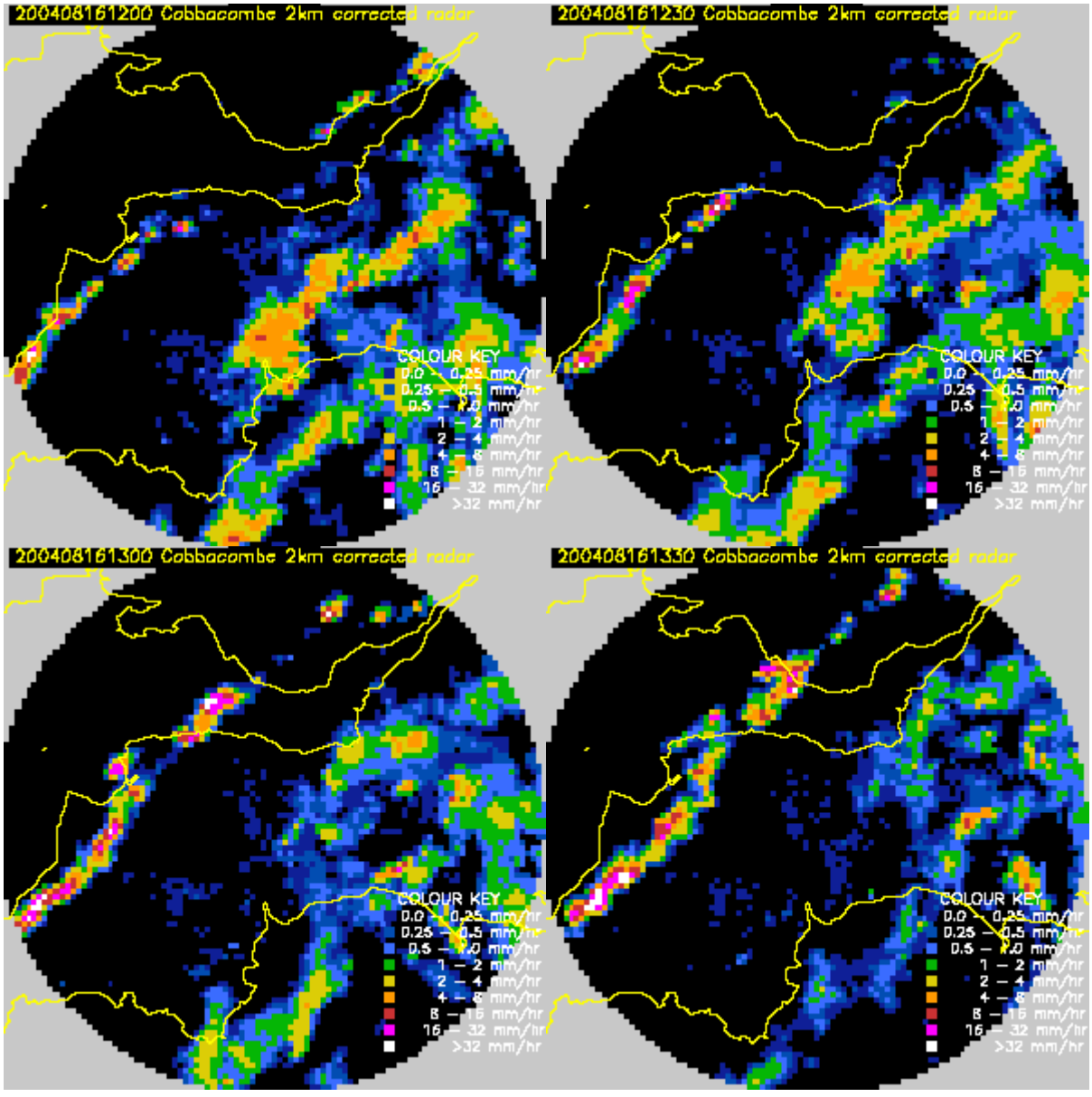

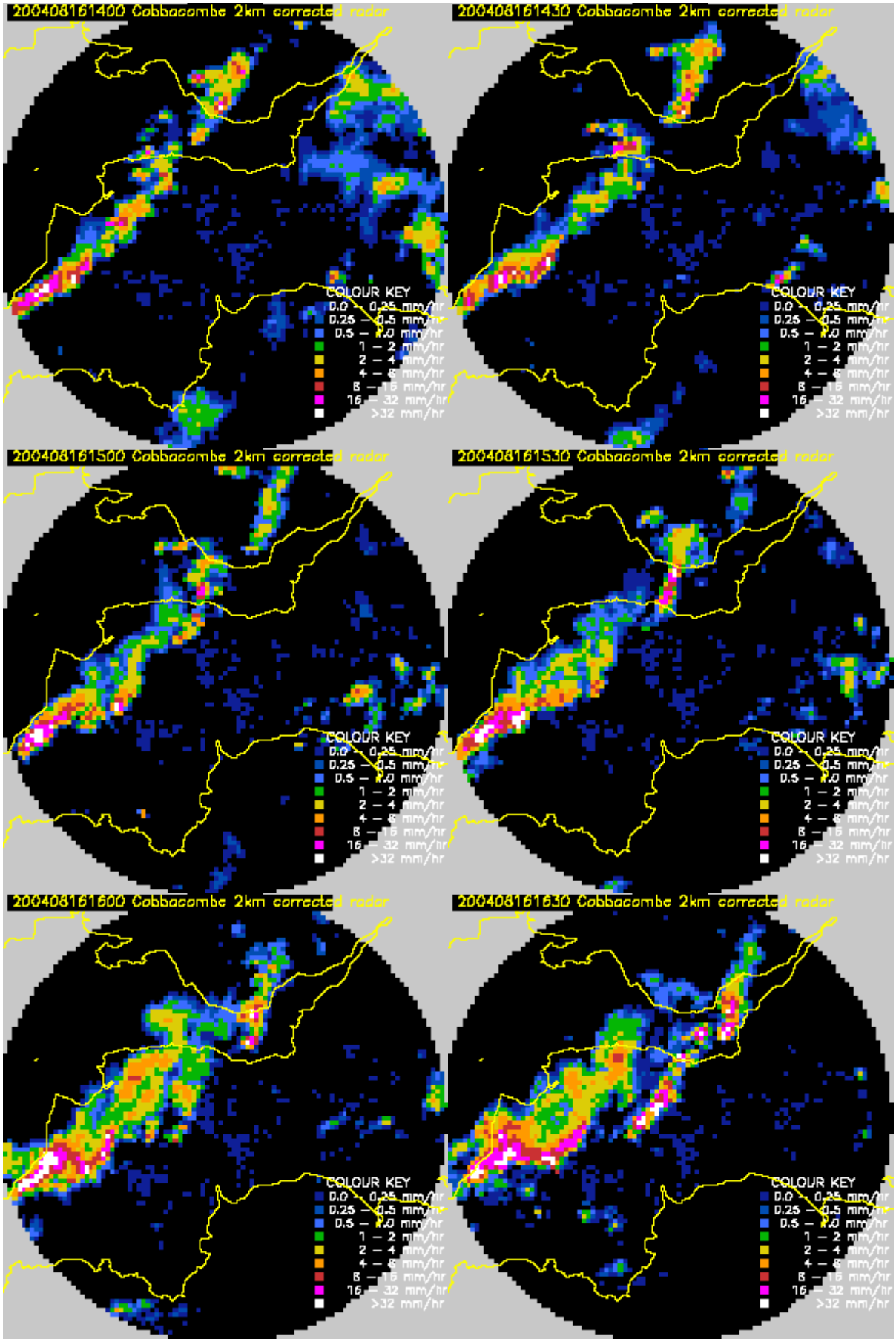

Figure 31 Cobbacombe corrected 2km radar surface rain rates 1200 - 1630UTC

Camel, and have developed independently. Inspection of the images from 1200-1300UTC indicates a string of showers with maximum rainfall covering about 4x6km, elongated in the direction of flow, with gaps of about 10km between and moving about 2km every 5 minutes (10ms^{-1}). The structure is very fluid, with separate maxima merging into a continuous plume and then separating. Later at about 1400UTC, a more definite plume structure appeared at the southwest edge of the image, which did not break into separate features until about 15km into the image. By this time, there is also a suggestion of slightly longer gaps between shower maxima. By 1430UTC this plume appears not to progress but to meander to the right by about 10km. As will be shown below, this is related to the development of a downdraught outflow boundary. Subsequently, a pattern is established of a plume of intense rainfall reaching to the vicinity of Bude, which then breaks up with arcs of high precipitation moving away to the east.

Details of individual storm elements, extracted from the Cobbacombe and Predannack radar images, are presented in Figure 32, Figure 33 & Figure 34 at 15 minute intervals. Each storm element starts from a single cell in the vicinity of the Camel Estuary and propagates downstream. In each case, the cell develops multiple maxima after about 30 minutes of precipitation, with the downstream component accelerating, and the upstream component becoming almost stationary for a while. This is interpreted as indicating that the downdraught from the first cell has generated new updraughts on its up- and down- wind sides along the coastal convergence line. However at this stage, the downdraught is not strong enough to modify the front. This process of splitting and redevelopment continues for some time. Later, after an intense phase of this process, a distortion of the precipitation plume occurs, indicating that the downdraught has taken over from the coastal convergence as the dominant forcing. This occurs at about 1234UTC in storm 1, at about 1315UTC in storm 2, and at about 1515UTC in storm 4. Ultimately, these arcs of expanding convective activity forced by the storm outflows, join up to form a squall line over northeast Devon from about 1630UTC onwards. Note that the first storm remains over the sea until it reaches the vicinity of Bude.

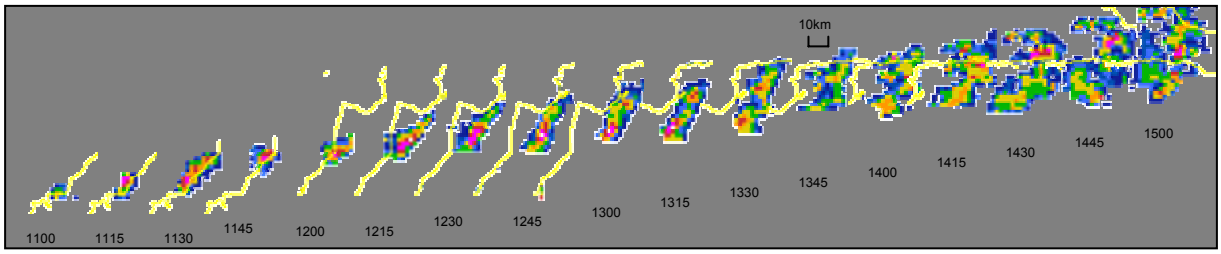

Figure 32 Evolution of the 1st storm cell, 1100-1500UTC. Each time is shifted right by an additional 30km for clarity

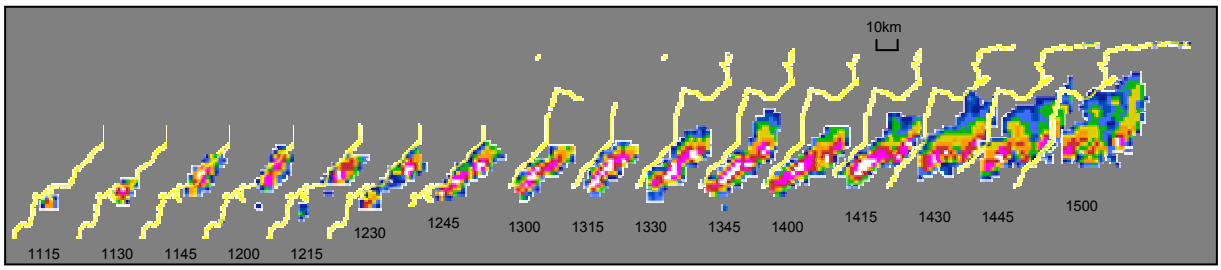

Figure 33 Evolution of the 2nd & 3rd storm cells, 1115-1500UTC. Each time is shifted right by an additional 30km for clarity

This evidence for the location and nature of the development along outflow boundaries is consistent with the satellite imagery in Figure 27, which showed that to

the northeast of Bude, thick cloud with low tops formed an arc along the eastern side of the plume, with the high topped cirrus outflows to the northwest.

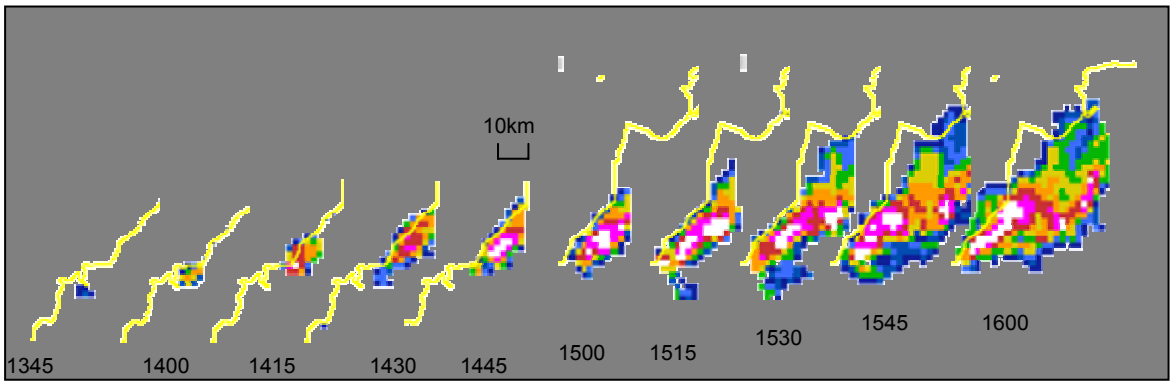

Figure 34 Evolution of the 4th & 5th storm cells, 1345-1600UTC. Each time is shifted right by an additional 30km (40km for the last) for clarity

3.9. Storm analysis using lightning data

Lightning flashes are recorded by the Met Office's Arrival Time Difference (ATD) network. This detects the waveforms of electromagnetic disturbances from cloud-to-ground strikes, and by matching those received at different locations can identify the location to within about 2km over the UK. The system has a limit on processing capacity which means that it typically located about 1 in 5 flashes, although it is tuned to give priority to processing flashes that are distant from others, so as to optimise the detection of storm cells. The resulting information is processed in Nimrod to create maps of lightning frequency, expressed in flashes per minute (scaled by 100) on a 5km grid co-incident with the radar analysis grid. For each map, lightning strikes are accumulated over 30 minutes. For presentation purposes, the resulting flash rates are colour coded as low, medium and high risk, with low (blue) being indicated where a flash has occurred nearby or where forecast conditions favour lightning, medium/low (green) where flashes have occurred recently, yellow for rates of one per 15 minutes, red for one per 5 minutes, and white for more frequently. It should be noted that the sampling of the ATD system means these represent a fraction of the true rates, and are useful mainly as relative measures. Note also that cloud-to-cloud strikes, which typically exceed cloud-to-ground strikes by a factor of five of more, are not observed by the ATD system.

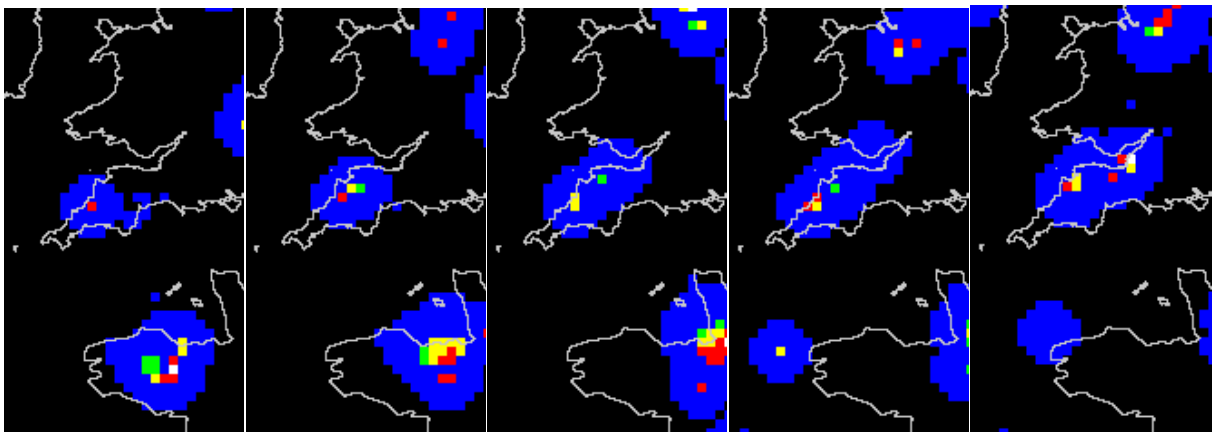

Figure 35 Hourly lightning frequency analyses expressed as flashes per 100 minutes for the 30 minute periods centred on 1300-1700UTC: green (1), yellow (3-5), red (6-20), white (>20).

Although precipitation started at 1100UTC, no lightning was recorded until after 1200UTC. Only one 5km pixel contained lightning in the hour 1200-1300, and this was directly over the precipitation maximum at this time. In the following hour, the main maximum shifts NE by one pixel, and further activity occurs further downstream. In the following two hours, the main centre of activity returns to Boscastle and immediately SW, where the heaviest rain is located. At no time do recorded cloud-to-ground flash rates exceed 1 per 5 minutes. Finally at 1700UTC the lightning activity along with the heaviest rain, has move NE into the Hartland and the Barnstaple area of N. Devon.

More comprehensive information on lightning locations and frequency is available from the EA Technology lightning detection network, used by the electricity distribution industry. These data corroborate the spatial distribution indicated by the ATD data, but provide additional information on frequency. During the period 1200-1300UTC, two flashes were observed: one near Padstow and one near Boscastle. None were observed in the following hour. Seven flashes were observed between 1400-1500UTC, mostly between Wadebridge and Camelford. Nine flashes were recorded between 1500-1600UTC mostly grouped between Camelford and Boscastle, but with outliers towards Holsworthy. The numbers of flashes increased rapidly after 1545UTC. Between 1600-1700UTC there were 36 flashes, mostly between Padstow, Wadebridge, Bude and Holsworthy. Between 1700-1800UTC 46 flashes were observed, but by then most were over the sea, or further away over north Devon. However, a group of four were recorded close to Boscastle.

3.10. Storm analysis using rain gauge and other in situ data

The traditional basis for estimating the actual rainfall accumulation has been to collect it in a suitable container and to measure the collected water at regular intervals, typically daily. The measurement process is laborious and requires care. For more frequent and less laborious measurements, automatic rain gauges are widely used, which record the amount of rain collected and periodically empty themselves. In both cases the observations form a spatially sparse sample. In a standard rain gauge, rain is collected at the orifice and fed through a funnel into a collecting bucket. From there it is periodically emptied into a measuring device. The most common type of automatic rain gauge uses a tipping bucket, both to record the amount of rain, and to remove it.

Information on the storms of 16th August 2004 comes mainly from 5 tipping bucket rain gauges in the area: at Slaughterbridge in the River Camel catchment, at Woolstone Mill, Tamarstone and Crowford Bridge in the Bude catchment, and at Lesnewth/Trevalec in the Valency catchment. All use 0.2mm buckets. The first four record the number of tips at fixed time intervals, giving 15 minute rainfall accumulations, while the last records individual tip times with a precision of 10 seconds. At times in the peak of the storm, when the instantaneous rain rate exceeded 120mm.hr^{-1}, up to four tips were being recorded at each time stamp, indicating instantaneous, local rates in the vicinity of 300mm.hr^{-1}. For the Lesnewth/Trevalec location, data are also available from a daily check gauge, which was read manually at 1730UTC. Manually read daily gauge reports are also available from Otterham, which gave the highest available total, and from several other daily gauges as shown in Figure 36. These confirm the small scale of the main rainfall area.

Additional information about storm structure can be obtained from the tip time data recorded by the Lesnewth TBR, shown in Figure 37. The data displayed in this figure have been smoothed to show the rate of fall of each 1mm of rain, so as to remove artificial peaks in the data due to the lack of precision of the time recording. In interpreting the results, it is important to bear in mind that the radar images show

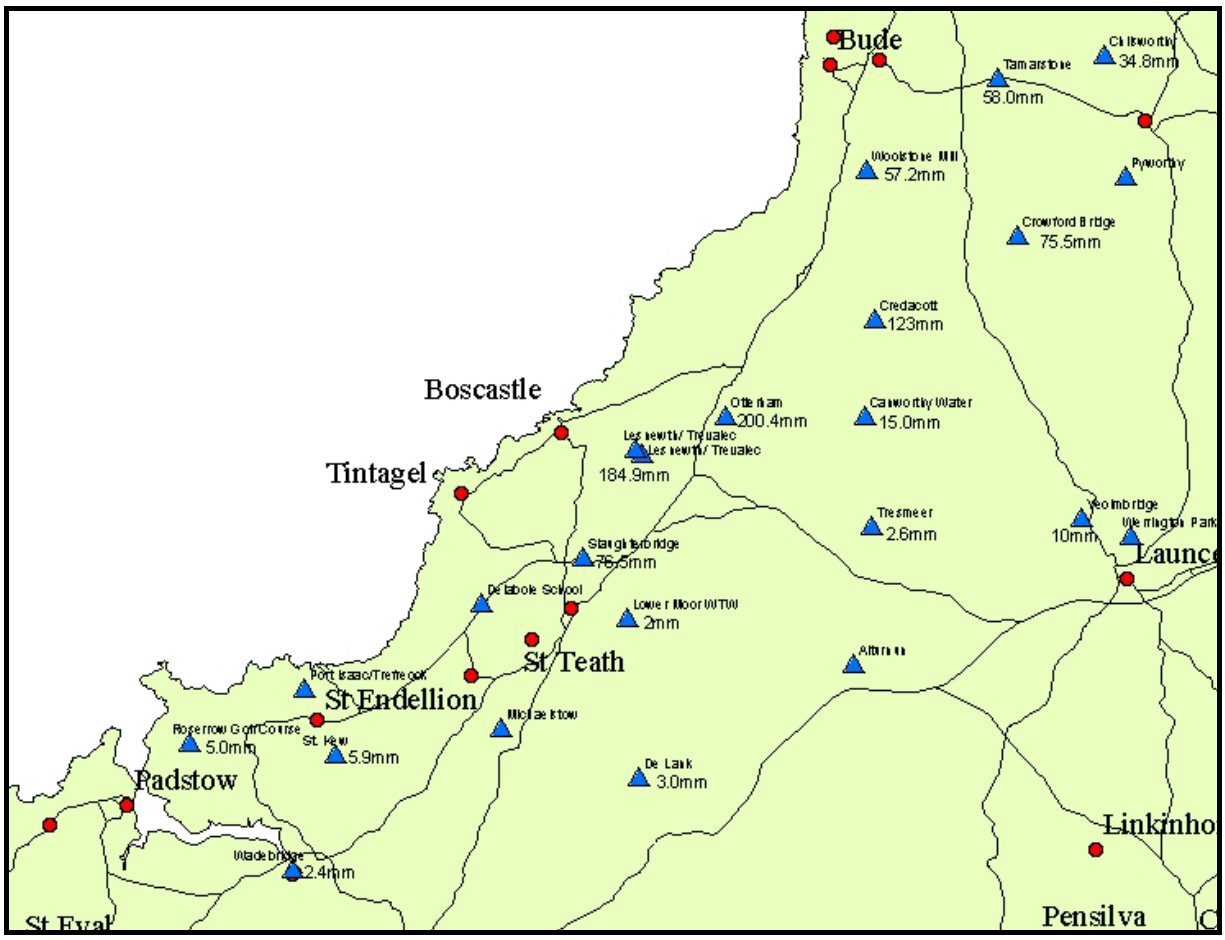

Figure 36 Available rain gauge locations, with 24 hour totals for 0900UTC 16/8/2004 – 0900UTC 17/8/2004, in relation to roads and settlements

Lesnewth to have been west of the main storm activity in the first part of the afternoon, so that only the period after 1445UTC represents the core of the rain band. The main characteristic of the period from 1445 to 1615UTC is the frequency of the peaks which approach or exceed 100mm.hr^{-1} every 5-10 minutes. The spatial scale of these features would be expected to be close to the resolution of the radar. The intensity of the largest peak, reaching nearly 300mm.hr^{-1} and exceeding 100mm.hr^{-1} almost continuously for 5 minutes, is outstanding, and clearly does not fit with the expectation of a peak undiluted rate of 100mm.hr^{-1} from the air mass analysis.

There are a number of possible explanations for the intensity of the observed precipitation. The calculations of expected intensity are based on the noon Camborne ascent, and it is possible that conditions at Boscastle were rather different. For this to be the case, we must also assume that the structure indicated by the mesoscale model in the vicinity of Boscastle is also not representative of the true conditions. The only evidence to support this is the presence of the upper tropospheric disturbances. These would be expected to generate enhanced mesoscale uplift in the region of north Cornwall during the afternoon. The main effect of this would be to raise the humidity of the atmosphere, reducing the evaporation of falling precipitation. However, there are also a number of features of the storm system itself that might be expected to lead to enhanced efficiency of rainfall production. It has been shown that the clouds were initially of modest height, and did not develop an anvil until much later. Thus there was no loss of ice crystals blown away in the anvil. Also, the forcing at cloud base in the coastal convergence line was evidently quite strong and interacted with the storms to generate the quasi-continuous line of precipitation shown earlier. Normally such a precipitation line would propagate perpendicular to its length. However, here, the storms were running along the length of the line, so that

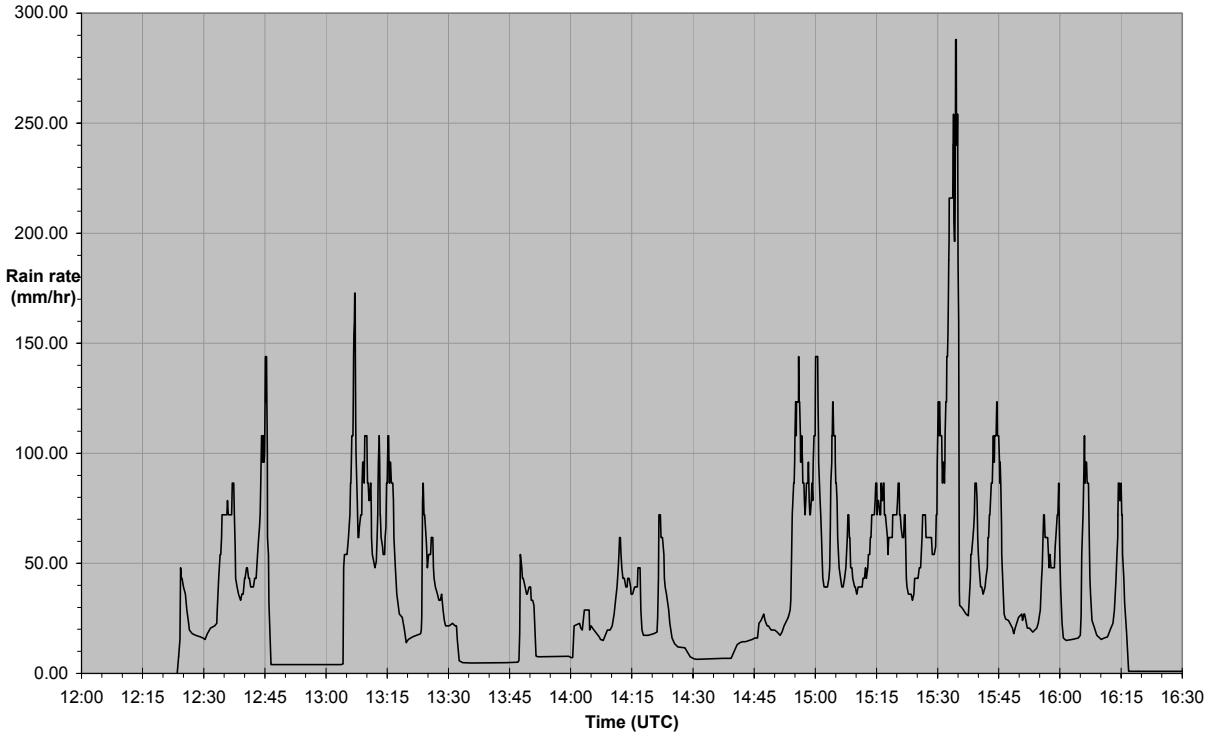

Figure 37 Smoothed rain rate profile from the Lesnewth Tipping Bucket Raingauge on 16th August 2004

new storms were able to draw on the moisture reservoir left from previous ones. Taken together, these provide plausible arguments for a much higher storm efficiency than in a normal isolated thunderstorm. However, it is not possible to identify which were critical to the extreme accumulations observed.

3.11. Storm analysis using convective scale model.

In carrying out the analysis so far, we have been unable to address the cause of storm initiation at the mouth of the Camel. There are no observations of the wind field that might indicate the cause and location of the near surface convergence that undoubtedly led to storm development. In this section we use the output from the newly developed Met Office convective scale model to provide this information, bearing in mind that this is a simulation and may not reproduce what really happened.

The convective scale model is a configuration of the Unified Model, with which all Met Office forecast and climate simulation work is carried out. It has a 1km horizontal grid and enhanced vertical resolution and physical parametrizations relative to the standard UK forecasting configuration. The model is extremely costly to run, and so was applied over the small domain shown in Figure 39 for this study. It is run with initial conditions obtained by interpolation from coarser scales, without the addition of fine scale observations. In order to relate it to these larger scales, it is run nested in a 4km grid length configuration, which is itself nested in the 12.3km mesoscale configuration shown earlier.

The strengths and weaknesses of the mesoscale evolution of the 12.3km configuration have already been noted. It was unable to resolve all of the processes leading to storm development in north Cornwall.

By contrast, the 4 km model was both remarkably accurate and quite consistent, at least in the region of triggering, between forecasts. This suggests a high level of

predictability, which further suggests that a strong surface influence (i.e. land/sea contrast, orography and land surface cover) is likely, as these inputs are quite well known. Figure 38 shows the forecast 10 m wind and its convergence at 1100UTC after 8 hours of forecast, immediately before precipitation first formed. The first precipitation formed to the southwest of Boscastle. The figure shows divergence over the sea, and convergence over the land along the north Cornish coast, modulated by the orography. The low level flow is southerly over land while to the north the flow is closer to the geostrophic south westerly. The convergence is stronger on the northeast (leeward) side of hills. Strong low level convergence formed in the region of the Camel valley where rain initiated both in the model and in reality. Strong convergence also happened elsewhere, later associated with rain and largely lined up with the cell movement direction.

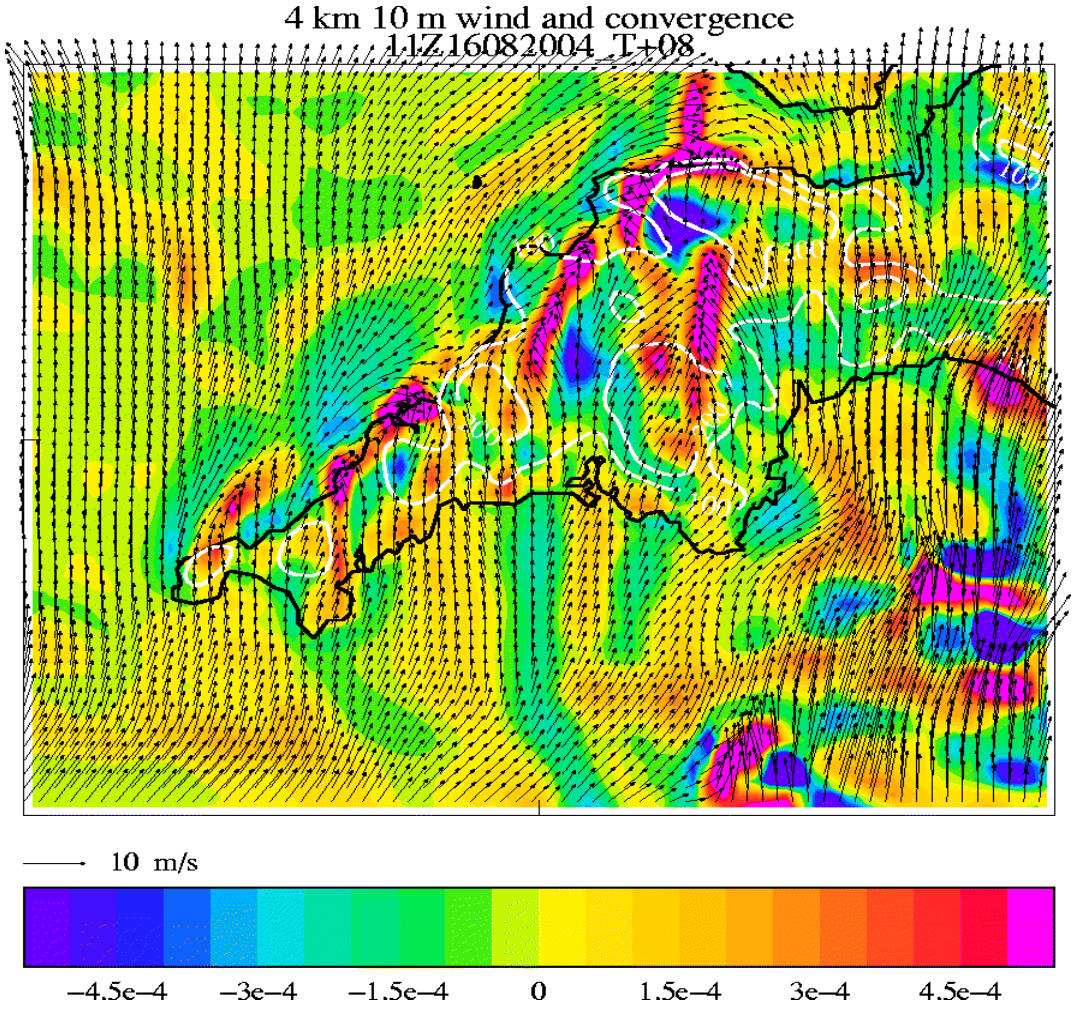

Figure 38 Surface wind and convergence at 1100UTC, 16th August 2004 from a 4km grid length integration of the Unified Model

Proceeding down to the finest scale, 1km model configuration, Figure 39 shows the evolution of the 1km grid length configuration in two hour steps from 1000UTC to 1600UTC. The wind and convergence patterns are similar to those shown for the 4km configuration, but with the structures at finer scale. At 1000UTC, the main convergence line is over the sea, to the northwest of Cornwall, associated with a coastal jet, and with maxima in the vicinity of Lands End and Hartland Point. The rainfall in the model simulation at this time is largely spurious, especially that in the convergence zone offshore of Hartland. By 1200UTC, a convergence line has begun to develop just inland of the coast, with its strongest development at the Camel estuary. This appears to be associated with the coastal jet, which is turning inland, presumably due to the pressure gradient caused by diurnal heating of the land, and a

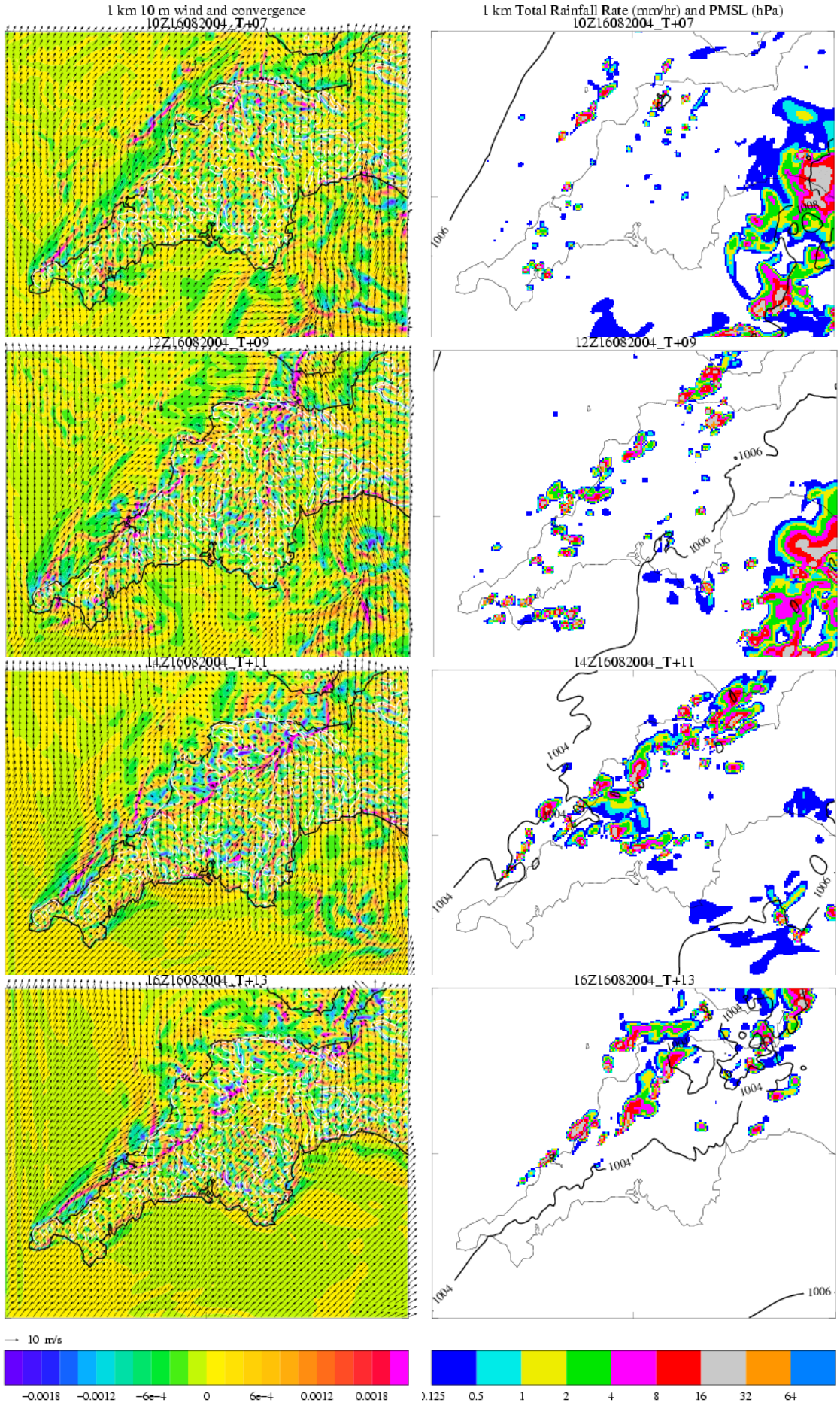

Figure 39 Wind flow & precipitation from a 1km model simulation initiated at 0300UTC

localised flow across the peninsula, accelerating down the northward slope of Bodmin Moor. It would appear that the sea breeze is insufficiently strong to propagate inland. Further convergence lines can be seen further northeast, and the rainfall rate image shows that the model develops precipitation on each of these, as occurred in reality. Peak rates of 32-64mm/hr are found at the cores of the model storms offshore of Tintagel and near Bude. By 1400UTC, the convergence line near Bude has propagated inland, consistent with observations. However, the precipitation distribution in this region is not quite consistent with the outflow structure identified in the radar and satellite imagery. Further southwest, the storms continue to have a realistic structure, but are less constrained in track than observed. Finally, by 1600UTC, the organisation of the convergence line and associated precipitation is very close to that observed.

Although the structure of the precipitation elements has a rather more discrete appearance in the model simulation than in the radar images, the cumulative effect of the storms is very similar, as shown by the total model accumulation through the event in Figure 40.

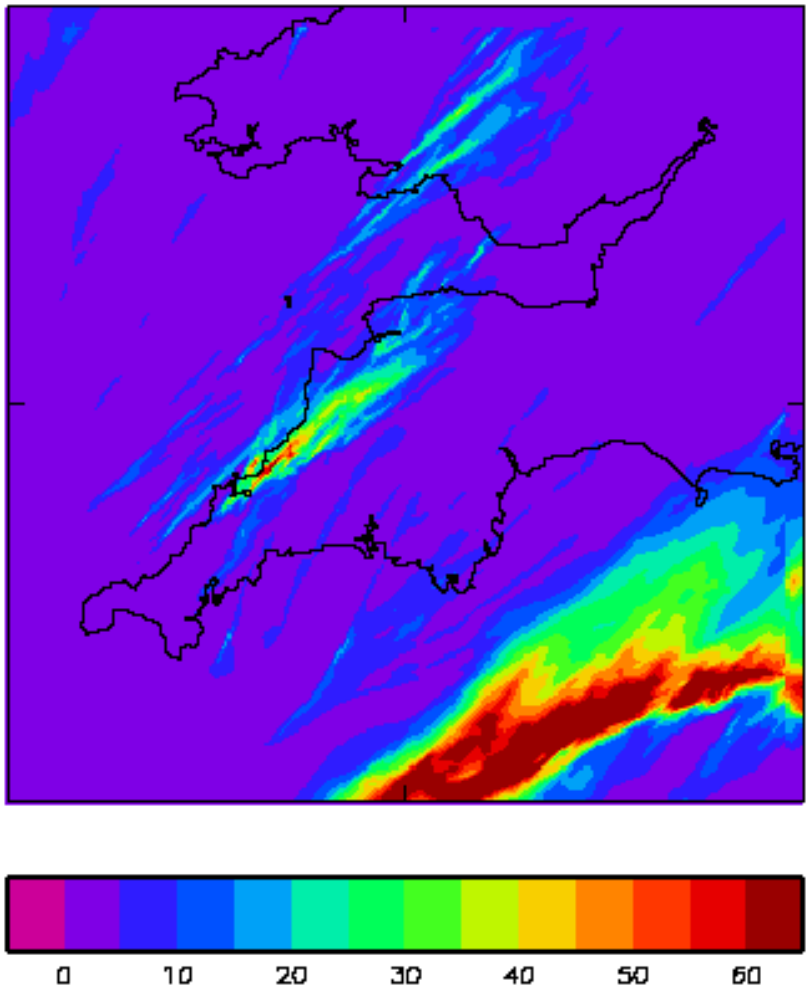

Figure 40 Total rainfall accumulation 0300-1800UTC from the 1km grid model

Figure 41 shows the sensible heat flux from this model integration. It is significant over land, as would be expected, but does not show a great deal of geographical variation. The main variation is a tendency for higher fluxes (by a few 10s of W m^{-2}) over the high ground, consistent with ideas of elevated radiative surface heating. Essentially, the surface energy balance is dominated by temperature, and is only weakly dependent on altitude. Surface temperatures are similar at altitude compared

with low down, but the air temperature is colder (by adiabatic cooling), leading to a larger temperature difference so a larger sensible heat flux. The pattern is not strong enough to directly explain the convergence pattern, though it may have contributed to stability effects. We therefore postulate that land/sea roughness contrast and overall thermal contrast dominated the coastal convergence, modulated strongly by local orography.

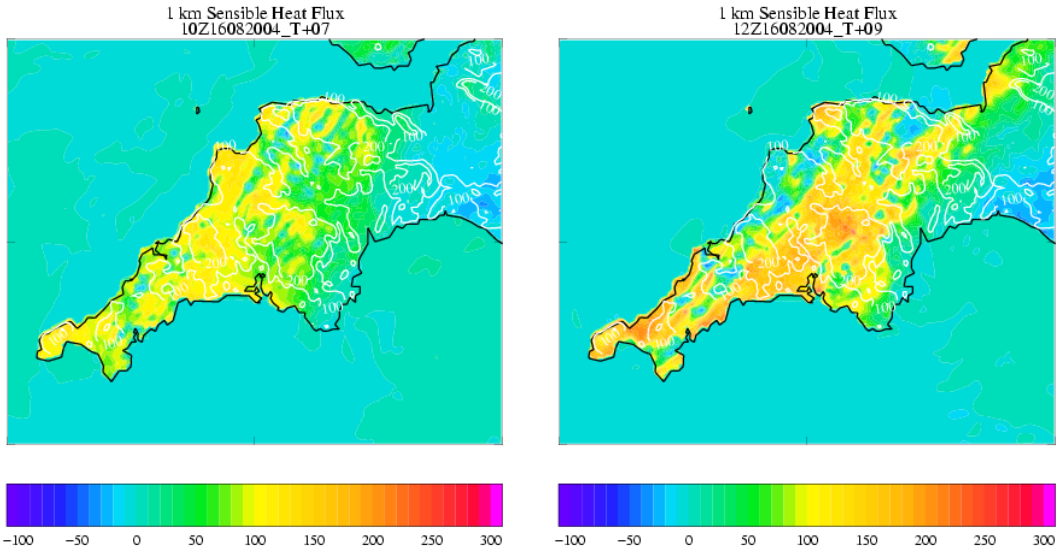

Figure 41 Sensible heat flux from the 1km model simulation at 1000 & 1200UTC

We have re-run the 1 km model, first removing orography over the SW peninsula (i.e. setting the height to sea level) and, in addition, setting the surface heat and moisture fluxes and the surface temperature over land to values typical of the sea. Figure 42 shows that the influence of orography on the precipitation is small. If anything, the pattern is more organised and pushed slightly further towards the sea, so that some rain falls over the sea. However, it should be remembered that this is the impact of numerous convective cells, and even very small changes in flow leads to small, essentially random, changes in cell development, so this difference may simply be sampling error. Figure 43 shows that the convergence line is also a little more organised and a little closer to the coast. There is also a stronger suggestion of a second line originating near Falmouth and merging with the primary line. Removing the enhanced surface fluxes removes the Boscastle peak in precipitation almost completely. This is expected, as the surface heating is clearly contributing to the instability. However, Figure 43 also shows much weaker coastal convergence. We conclude that the convergence line is largely driven by surface buoyancy fluxes over land, and exists near the N coast only (rather than near both coasts) because of the backing of the wind due to surface friction, aided, perhaps, by orography. The exact position is a subtle balance between frictional and thermal effects. One might speculate further that the triggering occurs where it does because at this point low level air from travelling from the SSW has had maximum fetch over land to be influenced by surface heating. Having said this, it is evident that the Land's End region has a particular impact on surface convergence so may have had a strong down-stream influence.

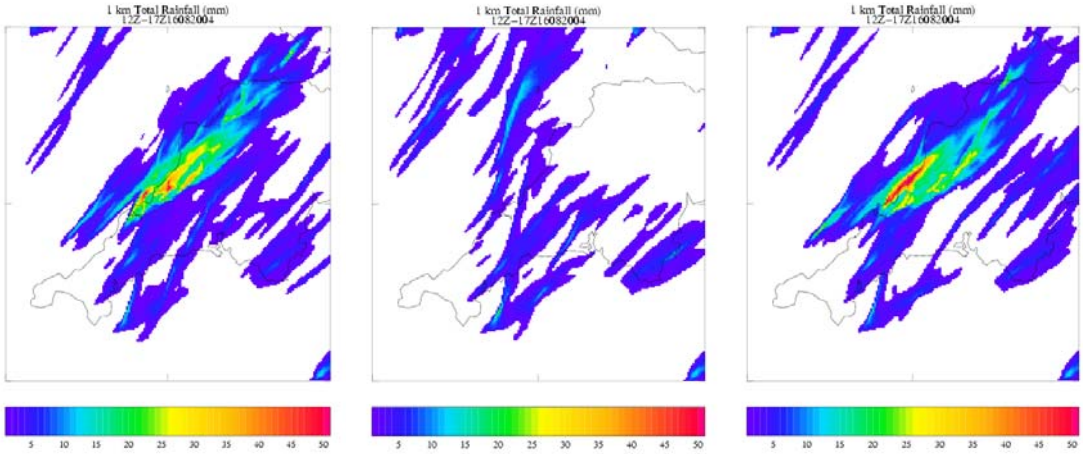

Figure 42 Accumulated precipitation from 12 to 17 UTC 16th August 2004 from 1km grid length integrations of the Unified Model. Full simulation (left), flat orography (centre), flat orography and surface fluxes and temperature over land fixed to sea values (right)

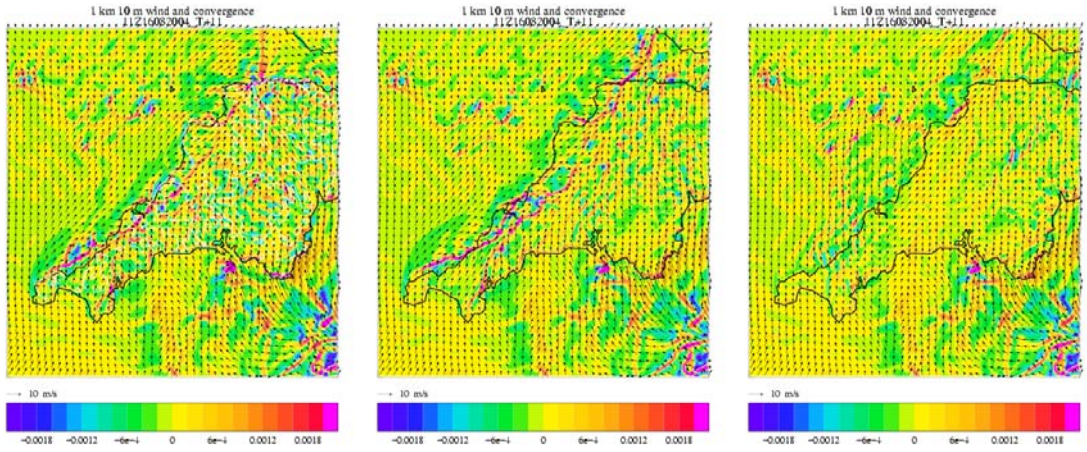

Figure 43 Surface wind and convergence at 1100UTC, 16th August 2004 from 1km grid length integrations of the Unified Model. Full simulation (left), flat orography (centre), flat orography and surface fluxes and temperature over land fixed to sea values (right).

3.12. Eye witness observations

An eyewitness with meteorological training observed the storm from St. Breward, located to the southeast of the storm. At 11am he noted that St. Breward was located in a sunny slot between two cloud lines, of which the one to the northwest, over Boscastle was the more threatening. In the cloud band to the northwest, he noted a pileus (or cap) cloud above the rapidly growing cumulus. The cumulus cloud then grew through the pileus cloud . The presence of the pileus indicates lifting of the ambient air above a developing cumulus and is consistent with the observation that the cloud was growing remarkably rapidly. His observation also noted that winds were light and the air was very warm.

Photographs of the storm are shown in Figure 44. The image taken from the sea shows no evidence of anvil development and is consistent with the satellite analysis presented earlier. The image taken from Davidstow, looking northeast towards Boscastle, was taken at 1400UTC and emphasises the narrowness of the rain band, with clear sky visible on its far side.

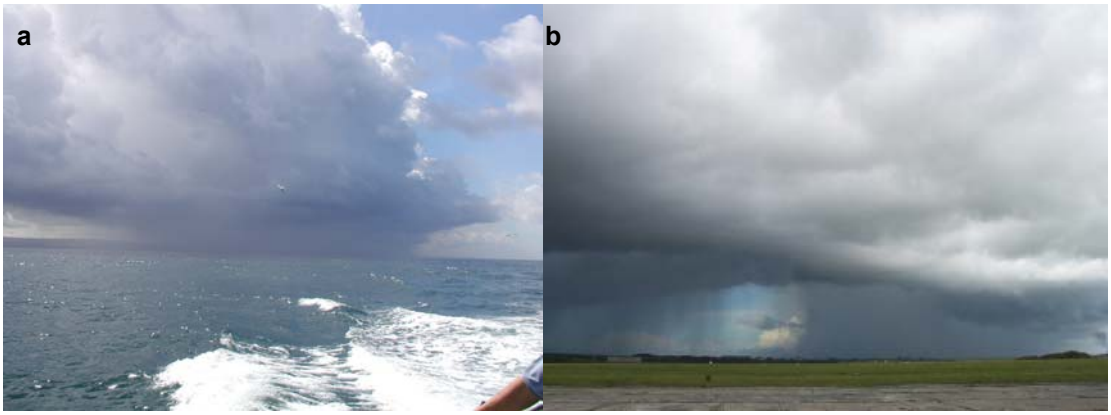

Figure 44 Views of the storm from (a) the sea (© J.Rowlands), (b) Davidstow airfield (© Mr. Wallace).

3.13. Summary of meteorological analysis

The analysis presented above has demonstrated how the storms can be set in a hierarchy of meteorological scales of activity reaching up from an individual hill or river valley to the structure of the extensive low pressure area over the eastern Atlantic.

The extreme rainfall accumulations, observed in the Valency catchment, resulted from prolonged very heavy rain over the four hour period 1200-1600UTC. The exact track of the heavy rainfall cells varied slightly during this period, but between the Camel Estuary and Bude the variation was sufficiently small to ensure that the heaviest rain fell into the same coast-facing catchments throughout the period.

Using evidence from satellite and radar imagery, we can synthesise the storm development in the following sequence of events. Each storm element started as a non-precipitating cumulus either near the Fal Estuary, or further north between there and the Camel Estuary. From there it moved northeast, developing slowly. As it approached the north Cornish coast near Padstow, it started to grow rapidly and to produce precipitation at the ground. From here it moved parallel to the coast and spread out into a line of storm elements, all precipitating heavily, but with cloud tops at mid-tropospheric levels. The continuous nature of this precipitation and its constancy of track resulted in the extreme accumulations observed in the Valency catchment. A few of these storm elements developed more strongly as they moved up the coast towards Bude, reaching the tropopause, and initiating an arc of storms propagating to the east across north Devon, while the anvil cloud shield from the original storm was sheared away northwards over Hartland, producing only moderate rain. As a result, rainfall to the north and east of Bude, while being as heavy as that further southwest, did not remain in one place long enough to produce extreme accumulations.

The mechanisms that produced the evolution outlined above can be understood in terms of the structure of the airflow over Cornwall. However, without detailed three-dimensional wind observations we have to rely heavily on model simulations and theoretical understanding. Initiation of the slow growing non-precipitating cumulus

clouds can be related to the lee convergence indicated in the model simulations to the east of the Lizard and the high ground around Redruth. Given the extremely small convective inhibition, the uplift of 0.5ms^{-1} at the top of the boundary layer, implied by the convergence field, was sufficient to initiate convection. However, since the prevailing wind was not parallel to this convergence, individual clouds would have lost this forcing as soon as they moved away northeast. The origin of the convergence can be understood in terms of distortion of the low level airflow crossing the Cornish peninsula around the areas of high ground.

The next phase of development occurred when these clouds, still of modest size and non-precipitating, reached the north coast near the Camel Estuary. The model simulations all generate a strong convergence line along the north Cornish coast, with local enhancement linked to specific topographic features. The values of convergence in the 4km model run, Figure 38, are sufficient to provide 1-2ms^{-1} of uplift at cloud base. The strength of this convergence line arises from the alignment of the prevailing wind with the boundary between the rough surface of the land and the smooth surface of the sea. Over land the rough surface results in a backing of the surface wind from southwest to south-southwest, but when it reaches the sea, it accelerates and turns to the right under the influence of the Coriolis effect due to the earth's rotation. The result is a coastal jet that may be significantly stronger than the ambient wind (Hunt et al 2004). The boundary between the backed flow over land, and the coastal jet, is marked by strong convergence and uplift. This is reinforced by an onshore pressure gradient resulting from solar heating over land. The synchronised initiation of showers along the whole coast at about 1100UTC is consistent with friction-induced coastal convergence as the primary cause. The exact position of the convergence relative to the coast varies with the ambient wind direction and the thermally induced pressure gradient. Initially the storms developed just offshore, consistent with pure frictionally driven convergence. The subsequent move inland and then back to the coast may be associated with a response to the late morning solar heating, followed by subsequent cooling due to heavy cloud cover in the afternoon, or may merely reflect minor changes in the ambient wind direction.

This phase of development produced rapid growth to mid-tropospheric depth with cloud tops probably in the vicinity of the equilibrium level in the Camborne ascent at 450hPa (6.5km). This implies a cloud top temperature of around -15^{o}C to -20^{o} which is only just cold enough to initiate ice processes in the cloud. However, the satellite images in Figure 13 indicate that it is possible that the clouds were being adequately seeded with ice from the outflow cloud shields of the earlier storms over Brittany. If so, the seed crystals would have grown rapidly by contact freezing. Whatever its microphysical origin, the precipitation resulted in downdraughts being generated, which stimulated new cell development along the convergence line as shown in Figure 30, resulting in a quasi-continuous line of closely packed storm cells. The small size of these cells is consistent with the low altitude of the cloud tops. The secondary cells were characterised by very rapid growth, as observed by the eyewitness at St. Breward, and rapid development of intense precipitation. In general these secondary cells grew to the same limited height as the primary ones. However, a few were sufficiently energetic to exceed this, and grew to reach the tropopause at around 250hPa (9.7km) where the temperature was -54^{o}C. At these levels remaining water droplets would be turned to ice crystals, and these are visible in the growth of the large cloud shield over the Hartland area. The greater vigour of these storms is reflected in their precipitation intensity at the ground, to the north of the main precipitation line. This precipitation was accompanied by a strengthened downdraught, resulting in a gust front which distorted the convergence line, causing it to bow in an eastward arc to the north of Bude. A succession of such arcs is visible in the satellite and radar imagery, generating new rows of storm cells as they spread east into north Devon and across the Bristol Channel into south Wales.

The extreme precipitation in the vicinity of Boscastle appears to have been related to the fact that while convection was strong enough to generate heavy precipitation, it was shallow enough to enable the development of closely packed storm cells, and with downdraughts that were weak enough not to distort the coastal convergence line in this region. Further north the influence of the stronger downdraughts caused more variation in the location of the heavy precipitation, resulting in much lower point accumulations.

While these local processes are the primary influences on the intensity of the precipitation, it is clear from the earlier analysis that there were larger scale forcing processes at work which may have added to the observed intensity. It is not possible to quantify the extent to which these processes were significant to the outcome. At the largest scales there was a large scale forcing mechanism arising from the dynamical response in a jet exit region. It has been proposed that the influence of this was mainly through development of an upper vortex associated with the first of the troughs identified on the surface chart, and that this was reflected in the pressure falls observed at the surface. In addition there was a weak trough which approached the north Cornwall coast at around 1200UTC and then moved away northeast. The effect of these larger scale processes on the storm development would have been to create an environment of weak uplift which would support the retention of cloud water in the atmosphere, leading to accretion on the falling raindrops from the locally generated convection.

4. Assessment of the Quality of the Rainfall Data

4.1. Error Characteristics of Rain Gauge Data

Internal instrumental errors contribute little to the error of a well designed and maintained rain gauge, such as those operated by European National Meteorological and Hydrological Services and other professional hydrological bodies. The principal issues dealt with in design are that evaporation and splash should be minimised, and that the rainfall should all be measured. Evaporation is minimised by keeping the interior air of the collecting bucket at high humidity, through use of the funnel. Losses on the funnel are minimised by using a suitable material with a steep slope and by keeping it clean so that drops are not held on the funnel by accumulated dust. The slope also helps to minimise splashing of large drops out of the gauge. The opposite problem of drops splashing into the gauge is minimised in most cases by raising the orifice above the ground surface - typically by 0.3-0.5m. In locations where this is not possible due to wind effects, alternative precautions are taken to avoid splashing.

Of more significance for official readings is the impact of the rain gauge on the airflow. This results in progressive under-collection of rain by standard gauges as the wind speed rises, due to distortion of the air around and over the gauge which carries small drops with it. This is a problem even for modest wind speeds, and studies have shown that long term records using standard gauges are almost certainly underestimates by a few percent due to this effect (Robinson & Rodda, 1969). In upland locations that are exposed to a windy climate, the effect can be much larger and official observing stations provide protection to minimise it. In the UK, this takes the form of a turf wall, built to the height of the gauge orifice, at a radius of 1.5m from it (Met Office, 1982). In other areas, the gauge may be sunk in a pit, with appropriate measures taken to avoid splashing, or a shield may be provided around the gauge to break up the wind field.

A particular problem with automatic tipping bucket gauges arises from the finite tip volume. This results in the start of rainfall being delayed until a bucket-full has accumulated. At the end of a period of rain the bucket may be left partially full, making the end of precipitation appear earlier. In cases of light rainfall, this may result in significant errors in hourly rainfall totals. In heavy rain, a tipping bucket rain gauge also underestimates the rainfall amount due to the "dead time" while the bucket is emptying. At a rain rate of 200mm.hr^{-1}, this occurs every 3 seconds. The bucket may also “bounce” giving a false double count.

A well sited gauge should provide an estimate of rainfall accumulation equal to the mean actual accumulation over a small area surrounding the gauge. The size of the area for which the gauge is representative will, of course depend on the local topography and the nature of the precipitating weather system. In order to achieve this it is important, for instance, that the gauge is not sheltered by trees or buildings. In the UK it is recommended (Met Office, 1982) that such obstacles are separated from the rain gauge by at least twice their height. While these recommendations are adhered to at many official observing sites, it is often not possible to find suitable locations that meet them. Even when a suitable site is found, it is often the case that subsequent changes make it less so. For this reason rain gauge records should be interpreted in the light of information concerning the changing characteristics of the site.

The principal problem arising with the use of rain gauges is, however, their lack of representativity. Gauges are rarely sited less than 10km apart, whereas the spatial variance of hourly precipitation accumulations can be at least a factor of two between a point estimate and a 10km mean (implying that a factor of eight difference between points separated by 10km would be expected occasionally). Such variability is most marked in convective storms such as that being studied here.

Conditions were generally favourable for accurate rain gauge accumulations on 16th August, with reported wind speeds low. However, there are no reports from near the storm to indicate whether downdraught winds were sufficient to cause any loss of rainfall catch. At the locations of the heaviest rain, the Tipping Bucket Gauges will have suffered significant losses due to the very high tip rate. This is confirmed by the comparison with the daily gauge at Lesnewth.

4.2. Met Office Rainfall Quality Control (QC) process

The Met Office Rainfall Quality Control process is carried out using the DRAM (Daily Rainfall Assessment Method) software. DRAM uses selected near neighbours' readings to produce what it thinks is a reasonable rainfall value for that station for that day. This is known as the 'plan' value. DRAM compares the observed daily value against the 'plan' value and raises queries, where appropriate. It is the role of the quality controller, using sound reasoning and supporting evidence, to judge the validity of the query and the 'plan' value and either change or verify the observed value, as appropriate.

The vast majority of rainfall data in England & Wales comes from Environment Agency (EA) operated gauges. These gauges are a mixture of manually read, daily and monthly reporting gauges and Tipping Bucket Rain gauges (TBRs), reporting event data. The data are received in Rainark format from most EA areas, however some areas send their raincards to the Met Office and these are keyed by the Met Office's keying contractor. The data from all rainfall stations, be they operated by Met Office, EA or any other agency, are stored on the MIDAS (Met Office Integrated Data Archiving System) database.

There are consistency checks made as part of the ingestion process. These are to ensure that there are no keying errors, that the record reports for the correct number of days for the month, and that the rainfall station is Met Office registered etc. Any queries raised are resolved as they arise.

On a monthly basis, the rainfall data are transferred from MIDAS to DRAM to begin the QC process. DRAM incorporates a mixture of Standing and Observational data files to assist the quality controller:
Standing data files:

- Average annual rainfall (AAR) data set – to compare the monthly total against the station's AAR. Across a relatively small area, stations can have widely differing monthly totals due to height, location, exposure etc. However, in a month with mainly frontal rainfall, the percentage of each station's AAR should be broadly similar.
- Topography – each station's readings are plotted on DRAM, showing location, coastline, mountains, valleys etc.
- Rainmaster – the complete list of Met Office registered rain station details including names, numbers, position, height etc. These details are displayed on DRAM.
- DRAM notes – all changes to a station's data are noted in the station's notes page and are available for the quality controller. These help build a picture of the reliability of the readings and log any recurring errors made by the observer. They are also used to store any pertinent information on the station such as the Network Inspector's report on the gauge and site from their inspection.

Observational data files: Can be overlaid on the DRAM map

- Rainfall radar – three cumulative radar frames matching the 0900 to 0900UTC rainfall day

- Atmospherics or lightning reports (ATD) – any lightning strikes detected during the rainfall day are available.
- Rainfall readings – daily or monthly data from all other registered gauges can be used as a comparison with the subject station's data.
- 'Plan' values – are displayed on DRAM allowing the quality controller to compare the observed reading against DRAM's estimated value.

Also available to the quality controller are:

- Daily weather summary charts – Met Office monthly publication containing synoptic charts, plotted observations, a text summary and data for each day during the month.
- Rainfall postcards – the notes column can contain vital information from the observer on extreme rainfall events.
- Access to MIDAS – to view sub daily data from Met Office SAMOS (Semi-Automated Meteorological Observing System) & CDL (Climate Data Logger) gauges.
- Advice from collecting authorities – EA area staff can be contacted to discuss any issues. Most changes to data are fed back to the EA who can advise if they have additional information, such as river level data, or disagree with the changes made.
- Network Inspectors – with first hand knowledge of the site, the observers and the Agency staff.

The Rainfall Quality Control process is about ensuring that a rainfall reading is the true record for that particular rain gauge. Quality Control staff resist the urge to smooth values over an area, as weather and in particular rainfall, are very often not smooth.

During the QC process, changes are routinely written back to MIDAS. The write-back program, DRAMAMM, also changes the QC Flags and Record State Indicators (RSIs) in MIDAS to indicate that the data have been quality controlled.

4.3. QC Report on the Boscastle Event, 16th August 2004

Figure 45 shows the DRAM display of observed data around the Boscastle area for 16th August 2004 prior to QC. On the right hand side of the display, DRAM is showing the data for station 371899, Tresmeer. The 'Val' column shows the 'as observed' readings. The 'Plan' column shows DRAM's estimate for that day derived from the selected near neighbours. On the map, Tresmeer's reading of 2.6mm is shown in red, with the selected near neighbours' readings shown in blue.

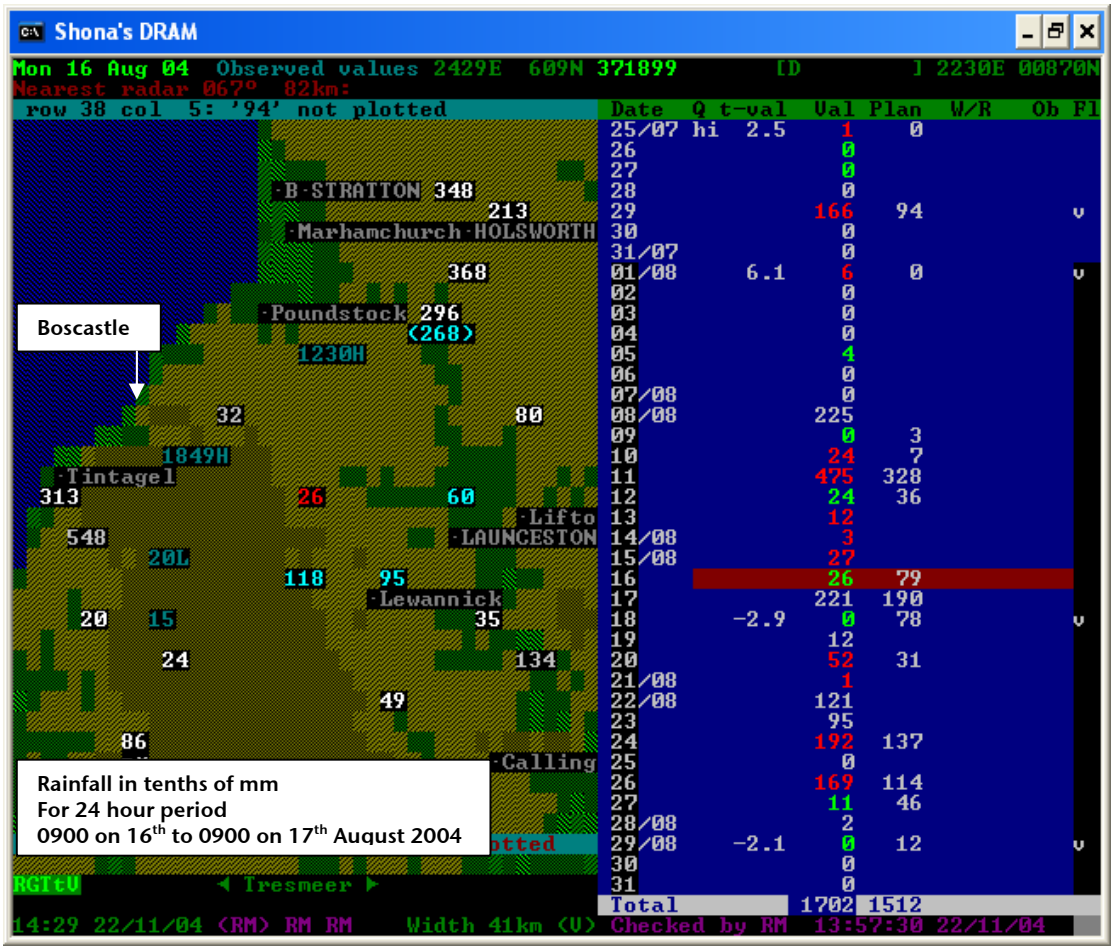

Figure 45 DRAM display before quality control

The recorded observations of the ten nearest neighbours (all check gauges i.e. manual readings) to Boscastle are listed in table 3.

Table 3 Rainfall observations for 16/8/2004 from the ten nearest rain gauges to Boscastle

Station No.	Station Name	Operating Authority	Observed Value (mm)
371160	Otterham	EA Cornwall	~~3.2~~ (200.4)
371374	Creddacott	EA Cornwall	123.0
371899	Tresmeer	EA Cornwall	2.6
373165	Altarnun	EA Cornwall	11.8
384101	Lower Moor W.Wks.	EA Cornwall	2.0
384366	St Breward, Camperdown Farm	EA Cornwall	1.5
384901	Delabole P.Sch.	EA Cornwall	54.8
384966	Michaelstow	EA Cornwall	2.0
385589	Treknow	Met Office	31.3
385700	Lesnewth, Trevalec	EA Cornwall	184.9

The Environment Agency in Cornwall has very few Met Office registered TBRs. Consequently, no TBR data was included in the Met Office QC process, other than being used as additional information. The site at Lesnewth, Trevalec has a non-registered TBR which reported 155.2mm compared to the check gauge reading of 184.9mm. The Agency also has a non-registered TBR at Slaughterbridge (between Delabole P.School & Lesnewth, Trevalec) which reported 76.5mm.

As expected for such an extreme, localised event, DRAM wanted to significantly reduce the extremely high rainfall values and wanted to add slightly to the lowest recorded values, removing almost 500mm of rainfall, from the ten stations listed above, in the process. Despite this, only one QC amendment was made to the ten stations listed on the 16th. All the other queried readings were verified.

At 371160, Otterham, the observer had entered the rainfall on the wrong day on the raincard during the period 11th to 20th August inclusive. The readings had not been thrown back, so the 200.4mm which fell on the 16th had been recorded on the 17th. This was 'thrown back' to 16th during the QC process.

Following the QC, the DRAM display of data around the Boscastle area for 16th August 2004 is shown in Figure 46. The letter 'v' following a value indicates that it has been flagged as suspect by DRAM but has been verified as being correct by the quality controller during the QC process.

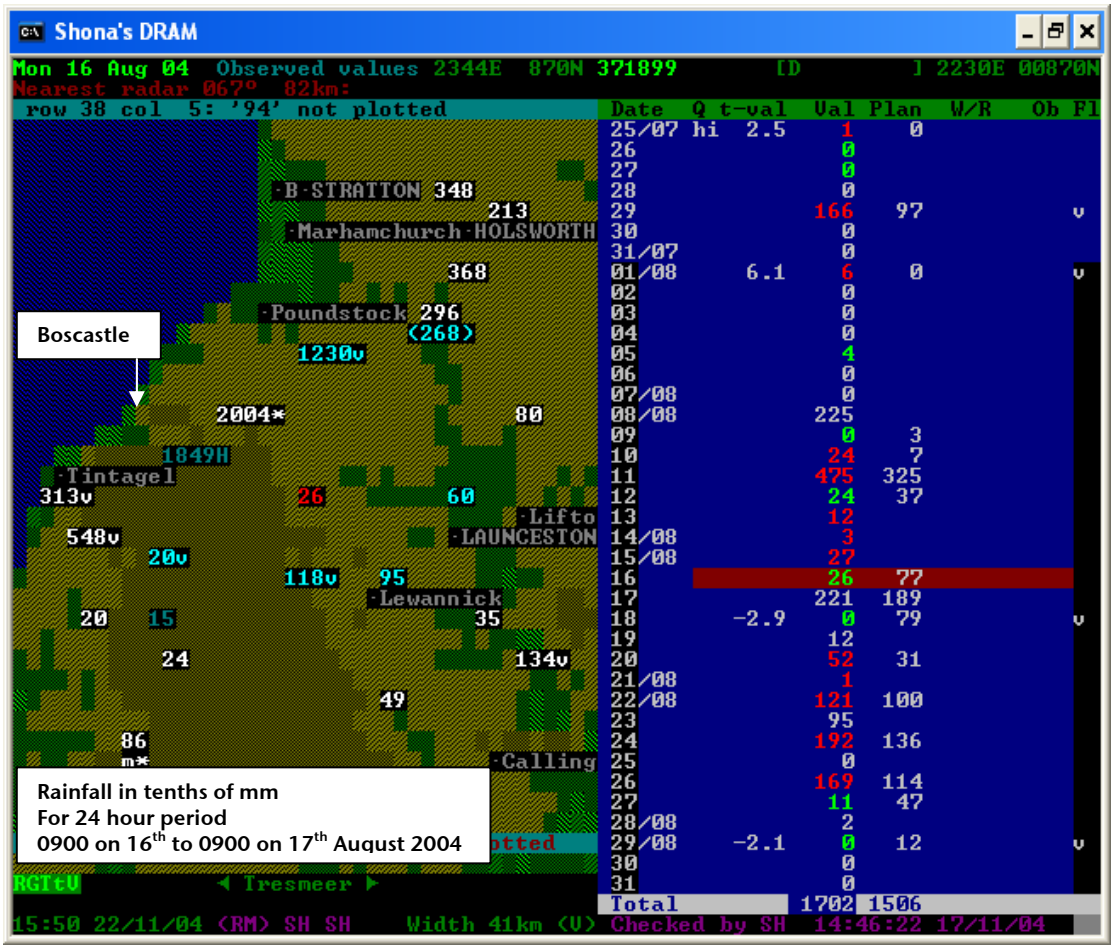

Figure 46 DRAM display after quality control

Unfortunately, there were no DRAM radar data available for August due to storage difficulties. However, the quality controller did have access to half hourly radar frames on the Met Office's intranet site and DRAM ATD data for 16th August.

The QC process was undoubtedly helped by the fact that there are so many reliable, manual, daily reporting stations in the area. Of the 10 stations in the table, eight are rated by the quality control staff as 'excellent'. Otterham and Delabole P.School have a history of occasional errors but are still rated as good stations.

During an extreme event such as this, the observers' comments on the raincard provide extremely valuable information for the quality controller. The following comments were noted on raincards:

- 385700 Lesnewth, Trevalec

Commented on the 16th: "Walls of water fell from 12.30am - 5.30pm"
From the TBR information, it is likely that the observer meant 12.30pm.

- 384901 Delabole P School

Commented on the 16th: "Very heavy rain 2-5pm" and also reported thunder & lightning.

- 371799 Virginstow, Beaworthy

Commented on the 16th: "Ink black clouds and thunder north & west of here but only moderate rain after 4pm."

- 373165 Altarnun

Commented on the 16th: "There was no rain at Altarnun during the time of the Boscastle flood. We had a slight shower at about 1830. The rest of the rain fell after 1930. The local river (Penont Water) remained very low throughout."

It is worth noting that the daily values for the three stations with the highest totals represented the following percentage of the stations' Average ANNUAL Rainfall
371160 Otterham – 17%,
371374 Credacott – 11%,
385700 Lesnewth, Trevalec – 13%.

4.4. Quality review of radar rainfall data

Errors in radar-derived precipitation rates can arise from several sources, including the radar hardware and its siting, conversion of the observed reflectivity to rain intensity and the location of the observed volume of the atmosphere.

Making allowance for these problems in relating radar observations to the surface rain rate is a critical part of achieving useful information from a radar system (Kitchen et al, 1994). Using these corrections hourly rainfall accumulations on 25km^2 squares across the UK are observed by radar with a RMS fractional difference of about a factor of 2 from rain gauge measurements located in those squares. This is close to the difference that would be expected given the different time and space sampling of the two observing approaches, indicating that the quality of measurement is likely to be similar.

For quantitative estimation of precipitation it is important for the radar to have a clear view of the horizon with as few obstacles as possible. In mountainous areas this is a major difficulty and may require a large number of radars to achieve full coverage of precipitation in valleys. The radar should have a narrow beam to optimise resolution, and high power to give clear echoes. The side lobes need to be small and weak to minimise spurious echoes. The transmitter and received circuits must be stable and noise free. If a radome is fitted, it should be treated to avoid attenuation from water collecting on the surface. All of these issues can be addressed with a modern, properly installed, and well maintained weather radar.

Where the beam is obstructed by obstacles, these can be removed by accumulating echoes on known dry days. Those pixels that have a high probability of contamination on these days can be identified, and removed from routine processing. Methods for estimating values for these pixels include use of a higher beam, and interpolation from adjacent pixels. However, where large areas are missing, as in mountainous areas, it may be necessary to use rain gauges or satellite information.

Reflectivity is converted to rain rate using an estimate of the droplet spectrum. Different spectra are associated with different climatic rainfall regimes and with different hydrometeor types, so this conversion may need to vary. Fortunately, the most common situation, where there is snow rather than rain, requires no change to the standard rainfall conversion, since the factor of five difference in fall speed is almost exactly balanced by a factor of five difference in dielectric constant.

However, when snow melts, it reflects like large raindrops. The radar signature of the melting layer is well documented and has a reproducable structure which can be used to deduce what the reflectivity would have been if rain were being observed, provided the height of the bright band can be identified. The most accurate way to do this is to use a short range forecast from a mesoscale Numerical Weather Prediction model. Studies have shown that typical errors in such models are less than 200m, and that this is sufficiently accurate to enable removal of most of the bright band effect on most occasions.

It is more difficult to deal with melting from convective clouds. Graupel does not show a bright band signature, and so should not be corrected, whereas hail intensity is overestimated by standard conversion formulae at all altitudes. It is not possibly to make reliable corrections in these situations with reflectivity only, although it has been shown that the additional information from polarisation diversity radars may help. Fortunately, severe convective storms occur mainly in summer, when the melting layer is higher, and contamination of the observations is less likely.

Finally, in some circumstances, the atmosphere may contain other contaminants that provide a reflection signal strong enough to be mistaken for precipitation. This occurs especially when migrating insects are gathered by convergent wind fields.

As range from the radar increases, the quality of the rainfall estimate falls off due to the increase in the beam width, and hence the variety of conditions that are being aggregated to form a single observation. In addition, at least for C & X band radars, the attenuation of the beam by nearby precipitation is sufficient to significantly decrease the available power for reflection from more distant precipitation. The impact of beam broadening can be minimised by good radar design, using a narrow beam, and good radar siting, ensuring that the distant view is not masked by nearby hills etc.. Where information is available from satellite cloud top heights, for instance, allowance is made for partial filling of the radar beam by precipitation. Finally, a general allowance for the mean effect of distance can be incorporated. Where attenuation by intense rainfall is a frequent problem, the best solution is to use a longer wavelength radar. However, techniques have also been developed for dual polarisation radars that enable the attenuation to be estimated.

The curvature of the earth generally introduces an increase in beam height with range. In order to make an accurate estimate of the surface rain rate, it is necessary to know at what height each pixel is located. This is more complicated, since the rays are not actually straight, but are bent slightly by the mean refractivity gradient in the atmosphere due to its vertical moisture gradient. As mentioned below, local variations in these gradients may also lead to significant departures from the mean ray path.

Having located the height of the radar beam, and correctly deduced the rain intensity at that height, an estimate must be made of how the precipitation at the height observed will alter as it falls to the ground. There are many possible processes to take account of, including wind drift and sub-cloud evaporation, but the dominant one is the growth of precipitation arising when hydrometeors fall through cloud generated by forced uplift of humid air over orography. The effect of this has been found to be well estimated using the low level wind and humidity predicted by a NWP model,

together with an estimate of the vertical deviation of the flow, estimated from a Digital Elevation Model for a variety of wind directions.

Where there are strong moisture gradients in the atmosphere, the radar beam may be anomalously bent, leading to intersection with the ground (anaprop) and resulting spurious echoes. At least four different approaches are used to remove this contamination, and these may be combined. The UK Nimrod system focuses on independent data to estimate the probability of an echo being spurious (Pamment & Conway, 1997). Cloud information from satellite imagery is used to indicate where there is no cloud, and therefore rainfall is impossible, and also to identify thin cloud which is unlikely to be generating rain. Pixels close to a dry surface observation are also assumed to be unlikely to be raining. A second approach uses Doppler velocity information, where this is available from the radar. Whereas rainfall typically moves with the wind, spurious echoes are more likely stationary. There are also signal processing methods that compare the reproducability of the echo over short time periods, relying on the greater variation in precipitation returns to identify them. Finally, some attempts have been made to use ray tracing to actually diagnose when and where spurious echoes will occur. None of these methods is fully satisfactory, and the best systems use a combination.

An additional source of error in very heavy storms arises from the method of data representation, which provides reduced rain rate precision at high rates. UK radars store data with 2mm/hr precision for rates from 32mm/hr to 126mm/hr. Rates higher than this cannot be stored, but are truncated to 126mm/hr.

On 16th August, the conditions were favourable for good quality radar measurements. The storms were within 100km of both radars, there was no anaprop evident and the bright band was too high to cause any problems. Some weak interference from a nearby electromagnetic source was evident early in the day on the Predannack radar, but disappeared by the time of the storms. No hail was reported, so the conversion to rain rate should be good. These general indications are supported by a comparative analysis of the two radars.

The Valency catchment is slightly closer in range to Cobbacombe than Preddanack radars. However, because the Predannack radar is at a lower altitude, the Preddanack radar has the lower beam height for a given range and hence is normally used in preference to Cobbacombe in the composite products in this area. Although Cobbacombe recorded a slightly higher maximum storm accumulation than Predannack in the Valency catchment on Aug 16th , there is very little overall bias evident between the two sets of data. In the areas of common coverage at 2km resolution, Cobbacombe recorded 108 sq km with accumulations exceeding 64mm whereas Predannack recorded 132 sq km. Both Cobbacombe and Preddanack radars recorded 9 pixels (36 sq km) with accumulations exceeding 96mm.

Comparison between the radars suggests that the geo-location of the rainfall data was accurate - certainly to better than the 2km data resolution. A best estimate by eye is that the rainfall recorded by Predannack is perhaps a few hundred metres North and/or West compared to the Cobbacombe data. Of the 9 pixels where Preddanack recorded accumulations exceeding 96mm, 7 of these were common to pixels exceeding this threshold in the Cobbacombe data.

There is some evidence that the Preddanack radar recorded significantly higher rainfall rates than Cobbacombe to the SW of Boscastle - around Tintagel. This is probably a manifestation of some attenuation of the Cobbacombe transmissions during passage through the heavy rainfall further to the east. The Predannack radar transmissions would not suffer this effect because the path-integrated rainfall to the southwest of Tintagel would be much lower.

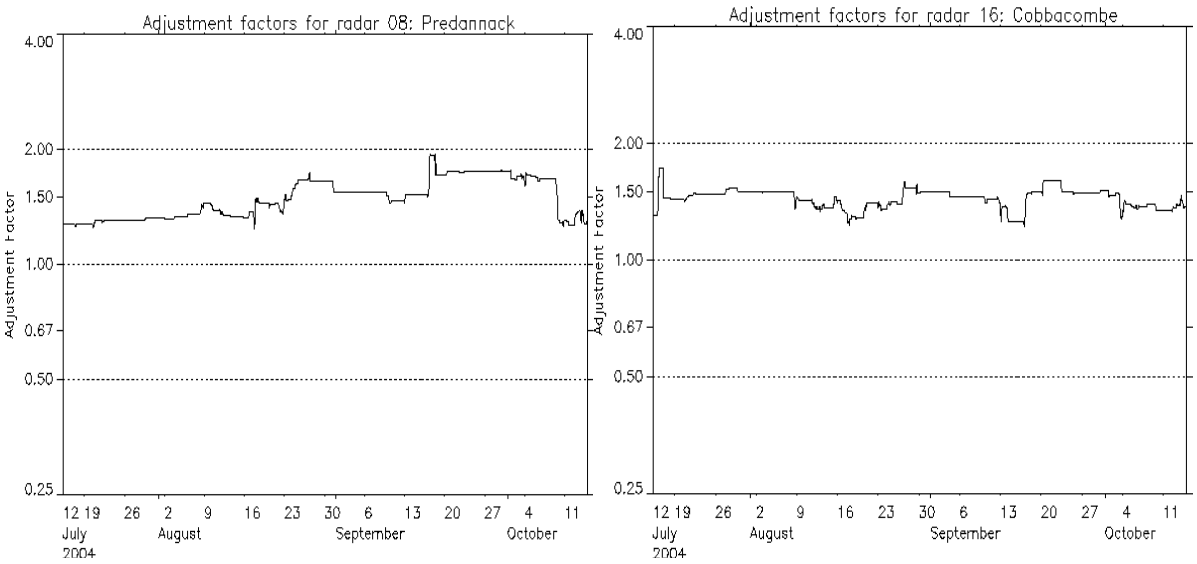

Figure 47 Time series of adjustment factors for the Predannack and Cobbacombe radars

The real-time gauge adjustment applied to radar data will have been based upon hourly radar-gauge comparisons - generally at much lower rates than encountered in the Boscastle storm. For both Cobbacombe and Predannack radars, the gauge adjustment factors in force on Aug 16th were around 1.4. Figure 47 shows the sequence of adjustment factors used through the July to October period, and indicates a high level of stability within about 10% through the relevant part of August. The application of adjustment factors relies on an assumption that the residual errors in surface rainfall estimation vary linearly with rainfall rate. When the adjustment is extrapolated and applied to very high rainfall rates, the assumption is likely to result in greater uncertainty.

4.5. Comparison of rain gauge and radar data

The highest accumulations observed by the raingauges are significantly higher than those recorded by the radars. We must therefore consider whether this indicates a bias in the radar, or is simply a result of sampling differences.

Table 4 Comparison of rain gauge/ radar hourly rainfall totals

Location	12-13UTC	13-14UTC	14-15UTC	15-16UTC	16-17UTC	5hr total
Lesnewth	17/ 10-15	30/ 20-25	28/ 15-20	65/ >50	10/ 0-10	150/ 110-120
Slaughterbridge	10/ 10-15	46/ 30-35	21/ 15-20	1/ 15-20	1/ 0-10	73/ 80-90
Crowford	1/ 0-10	33/ 15-20	13/ 10-15	20/ 10-15	3/ 0-10	74/ 40-60
Woolstone	0/ 0-10	0/ 0-10	2/ 0-10	22/ 0-10	31/ 25-30	54/ 40-60
Tamarstone	0/ 0-10	1/ 0-10	4/ 0-20	8/ 0-10	34/ 15-20	54/ 20-40

It has not been possible within the time available to extract precise comparisons for the gauge locations. Data in Table 4 were extracted by eye from the radar accumulation maps in Figure 49 & Figure 51. They show a considerable variability in the relationship between raingauge and radar, but with a clear tendency for the raingauge to record more in the peaks and less in the troughs. This is consistent with spatial averaging of the rainfall in the radar image, but could also be caused by poor radar calibration at high rates.

Further inspection of the maps in Figure 49 & Figure 51, shows that the gradients of rain accumulation are extremely high: adjacent 2km grid squares in the vicinity of the rain gauges, have 5-hour accumulation differences of up to 50%. Allowing for these trends within pixels is sufficient to explain most of the differences seen in Table 4, while the extremely small and intense features displayed in Figure 37 would indicate even larger variability on scales below the radar resolution.

A much more thorough analysis would be required to reach a definitive conclusion, but the evidence presented cannot rule out the possibility that the differences are purely due to spatial sampling, and that the spatial averages provided by the radar are accurate.

4.6. Summary of rainfall data quality

The daily rain gauge totals are accepted as accurate estimates of the rain that fell at specific locations.

Tipping Bucket Raingauges (TBRs) suffer from known faults in intense rain events. The TBRs around Boscastle are not registered and so have not been formally quality controlled. The general pattern of rainfall amounts is consistent with that observed by radar, but the amounts cannot be relied on, as is shown by the comparison with the daily gauge at Lesnewth. It is noteworthy that the radar estimates a greater accumulation at Slaughterbridge than that observed by the TBR. This may indicate that this measurement is also an underestimate. The best measurement available is to scale the TBR amounts to the daily gauge total where available. At Lesnewth this results in maximum short period accumulations of 82mm in 1 hour, 148mm in 3 hours, and 183mm in 5 hours. The peak instantaneous rain rate at Lesnewth occurred at 1535UTC and was nearly 300mm.hr^{-1}. The precise value depends on interpretation of the times of individual tips, which were only recorded to the nearest 10 seconds.

On 16th August, the conditions were favourable for good quality radar measurements. The radar spatial and temporal distribution is consistent between the two radars and with the available TBRs and there are no known faults in the data. Due to the very high rainfall accumulation gradients, it is not possible to determine whether the differences in accumulations from those observed by gauges are solely due to sampling differences, or whether the radar has a bias at high intensities. However, it is considered that the best estimate of maximum point accumulations can be obtained by scaling the radar to match values from the nearest available daily rain gauges.

Due to the very high spatial variability in the event, it is recommended that the pattern should be taken from the radar. For locations with daily rain gauges, it is recommended that estimates of shorter period point accumulations should be obtained by scaling the nearest radar pixel to agree with the gauge reading over the observed period. This is not a perfect solution, due to the temporal smoothing produced by 2km spatial averaging of the radar. However, it is preferable to using a more distant TBR, which will have sampled a different sequence of storm cells.

5. Rainfall event

5.1. Spatial and temporal characteristics of the extreme rainfall.

In looking at the characteristics of the rainfall, we focus on information provided by radar, bearing in mind the conclusions of the quality control regarding peak rainfall accumulations, and supported by the TBR data where available to give additional information on temporal characteristics.

In this section we will focus on the Valency catchment, shown in Figure 48. Its shape has been transcribed on to the rainfall accumulation maps presented in Figure 49 & Figure 51, where it takes up parts of just six 2km radar pixels.

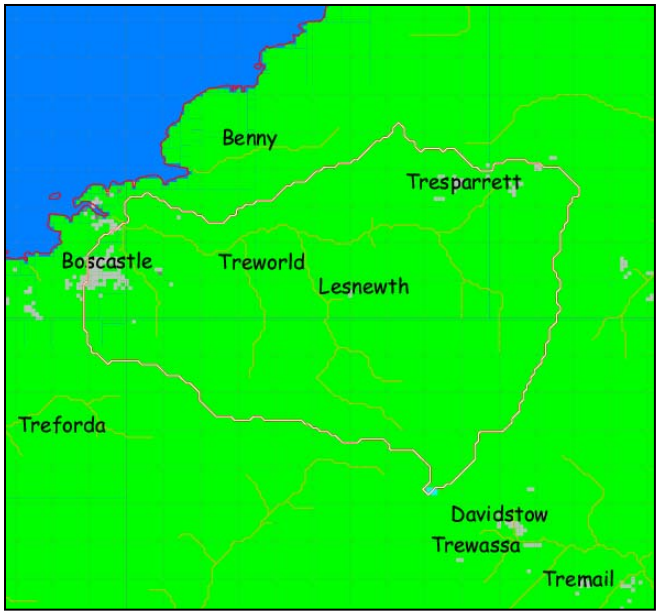

Figure 48 Extent of the Valency and Jordan catchments above Boscastle

The basis for the analysis of rainfall distribution is the sequence of hourly accumulations depicted in Figure 49. These have been obtained by summing 5-minute corrected radar rain rates at 2km resolution from the Cobbacombe Cross radar. The colour scheme has been altered from the usual logarithmic distribution to a linear one, which depicts hourly accumulations of more than 10mm to 5mm precision. The results have been displayed on a map background, with the Valency catchment boundary added, so that features can be geographically located. In the discussion below, the radar pattern is related to the available TBR data, with TBR values given in brackets where available.

During the first hour, 1200-1300UTC, the axis of maximum rainfall lies to the east of the Valency catchment, with three maxima of 15-20mm. Slaughterbridge (10mm) lies between the 1st and 2nd of these and Lesnewth(17mm) lies on the western edge of the 3rd, each having radar accumulations in the 10-15mm range. Otterham lies on the axis of the maximum, with a radar estimate of 15-20mm.

During the period 1300-1400UTC, the rainfall was much heavier, with the axis of maximum rainfall remaining along the east side of the Valency catchment and exceeding 30mm in a single 10km long, 4km wide plume from Slaughterbridge to Otterham. Maximum radar accumulations of 45-50mm occur on the southeast edge of the Valency catchment, between Slaughterbridge (radar: 30-35mm; raingauge:

47mm) and Otterham (radar: 35-40mm). Again Lesnewth (29mm) is off the main axis of the rain with a radar pixel value of 20-25mm.

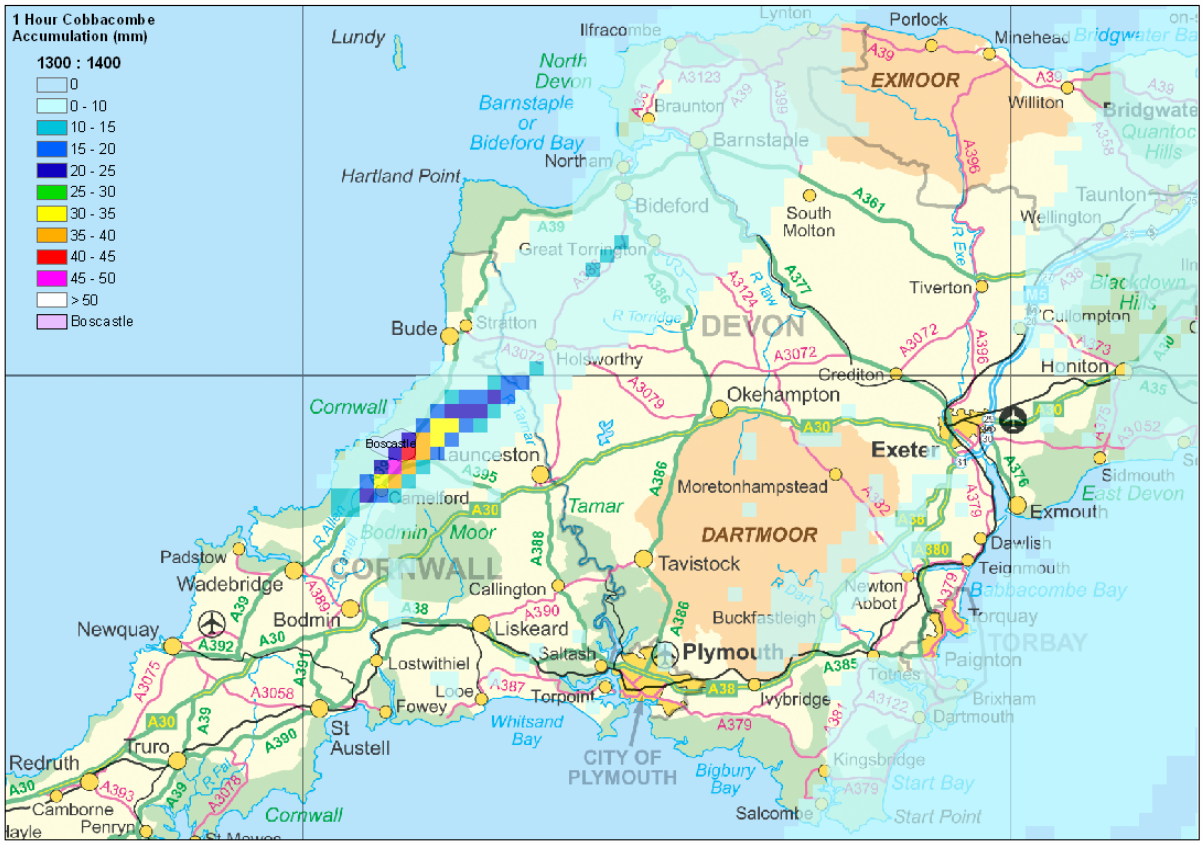

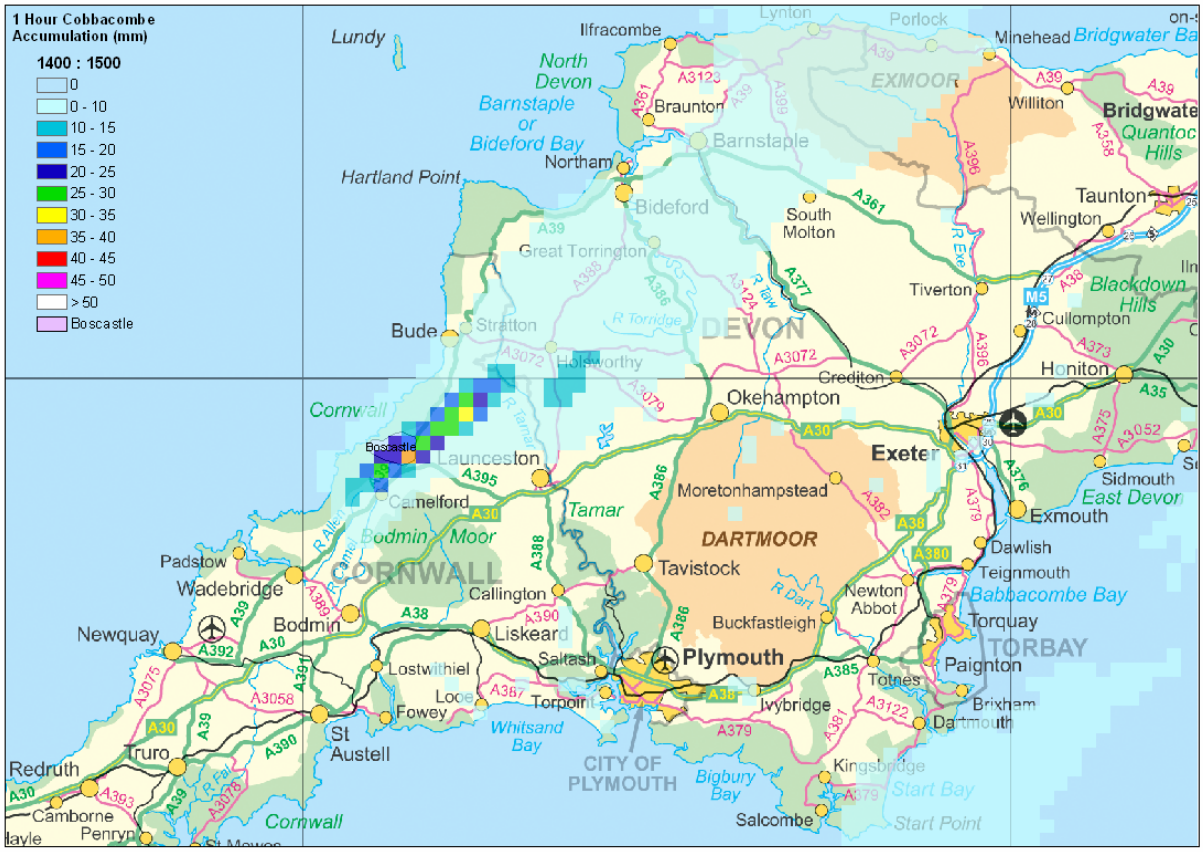

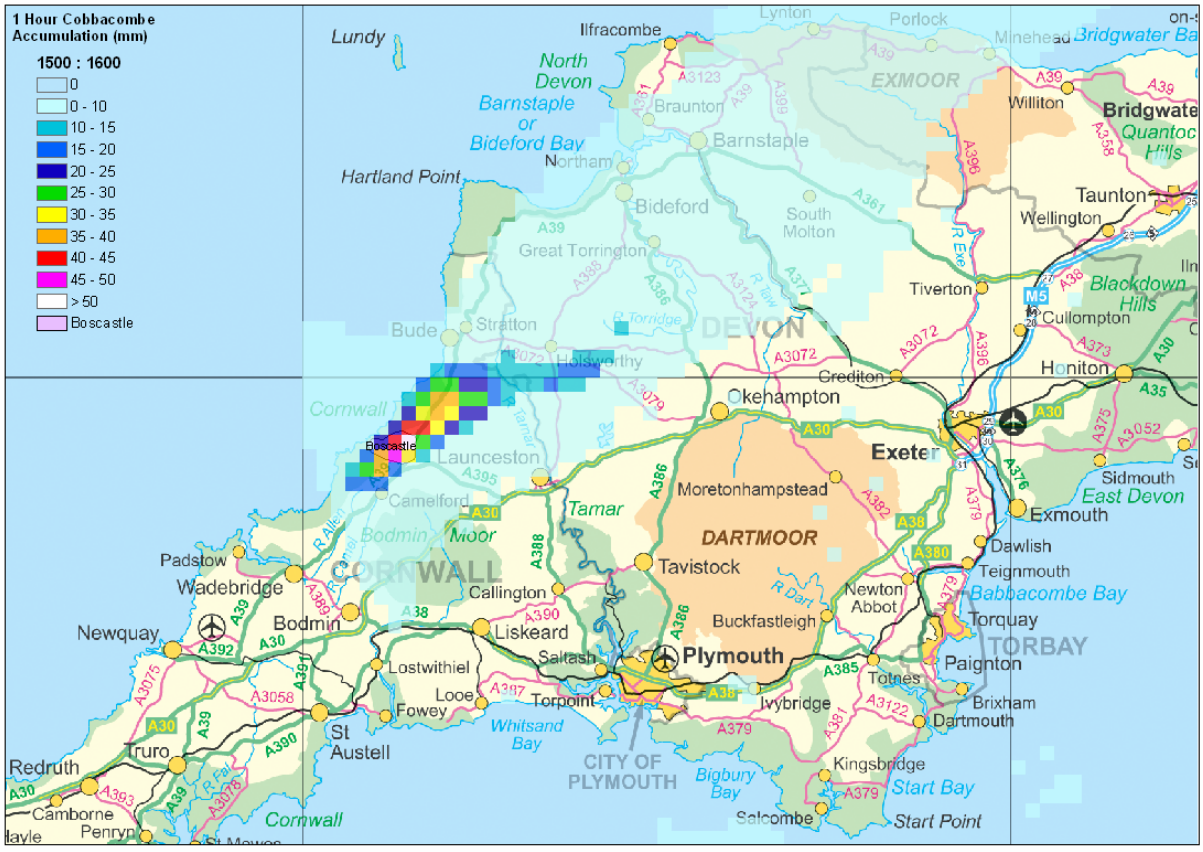

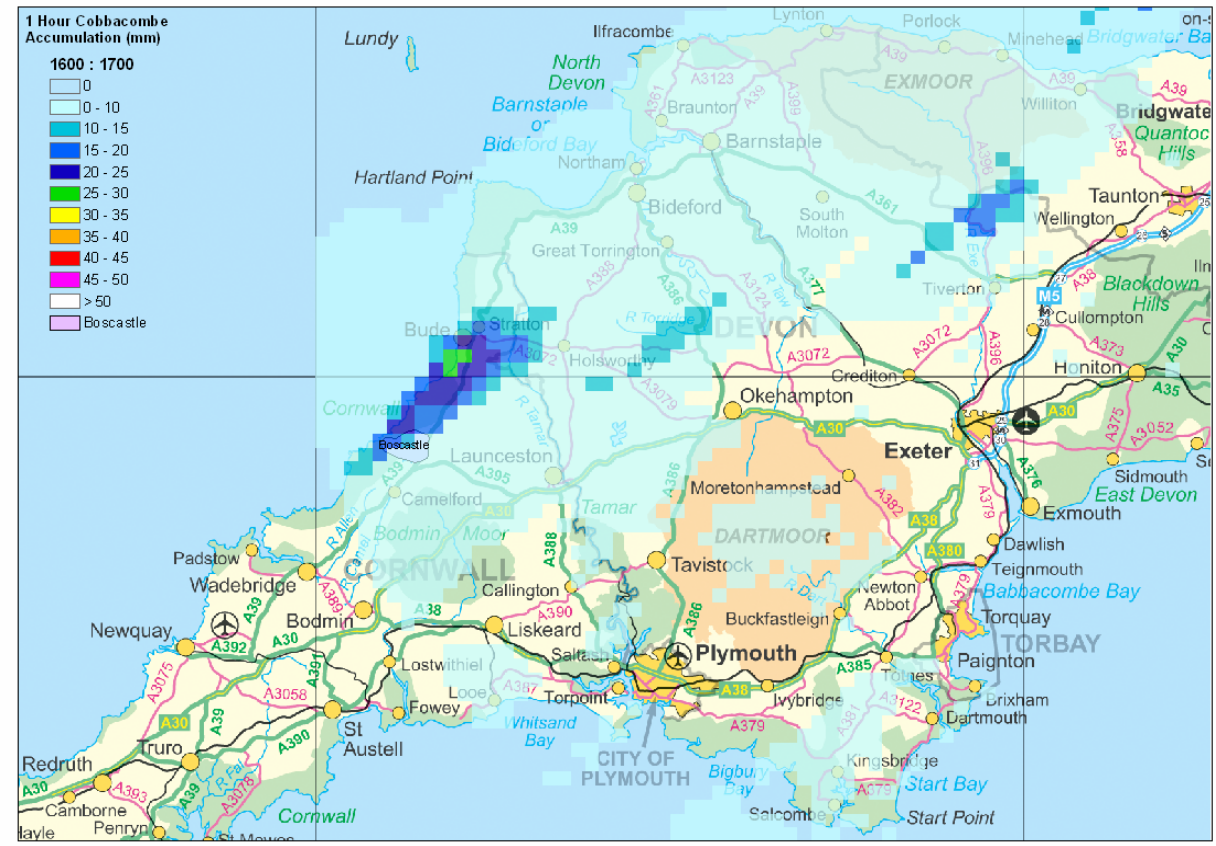

Figure 49 Sequence of hourly accumulations of 2km corrected Cobbacombe radar data, 1200UTC-1700UTC. Note the non-standard colour coding to focus on larger accumulations.

From 1400 to1500UTC, accumulations were lower than in the previous hour, with three local maxima, one of 25-30mm situated between Slaughterbridge and Boscastle, one of 35-40mm over the east part of the Valency catchment, and a more elongated one to the northeast reaching 30-35mm near Credacott. Slaughterbridge (8mm) is upwind of the first maximum, in a 15-20mm pixel; Otterham is downwind of the second maximum in a 25-30mm pixel; and Lesnewth (28mm) is on the western edge of the rain axis in a 15-20mm pixel.

Maximum rainfall is higher again in the hour from 1500-1600UTC, exceeding 35mm in a 12km long, 4km wide plume that runs right through the Valency catchment from near Slaughterbridge to beyond Otterham. The axis has shifted west by about 2km from the earlier position and Lesnewth (54mm) now lies in the heaviest pixel of >50mm. Slaughterbridge (2mm) is upwind of the main maximum in a 15-20mm pixel, while Otterham is on the eastern edge of the maximum in a 40-45mm pixel.

By 1600-1700UTC, the main rain area has moved away north and the remains of the plume have shifted west, putting Boscastle village under the maximum of 15-25mm, while the three local raingauges all lie in pixels of less than 10mm. (Lesnewth TBR: 10mm, Slaughterbridge TBR: 0mm)

The temporal analysis is consistent with the gauge reports, with Slaughterbridge having its highest accumulation in the 1300-1400UTC period and reduced rates thereafter as the maximum shifts downwind, while Lesnewth is off the western axis of the rain maximum until later, receiving its maximum accumulation between 1500-1600UTC. From this analysis, Otterham would be expected to have peaked twice, with 35-40mm from 1300-1400UTC and again with 40-45mm in 1500-1600UTC.

Taking the radar at face value, a location between and to the south of Lesnewth and Otterham, near the A39 road, should have exceeded both gauges with three consecutive hours in excess of 30mm.

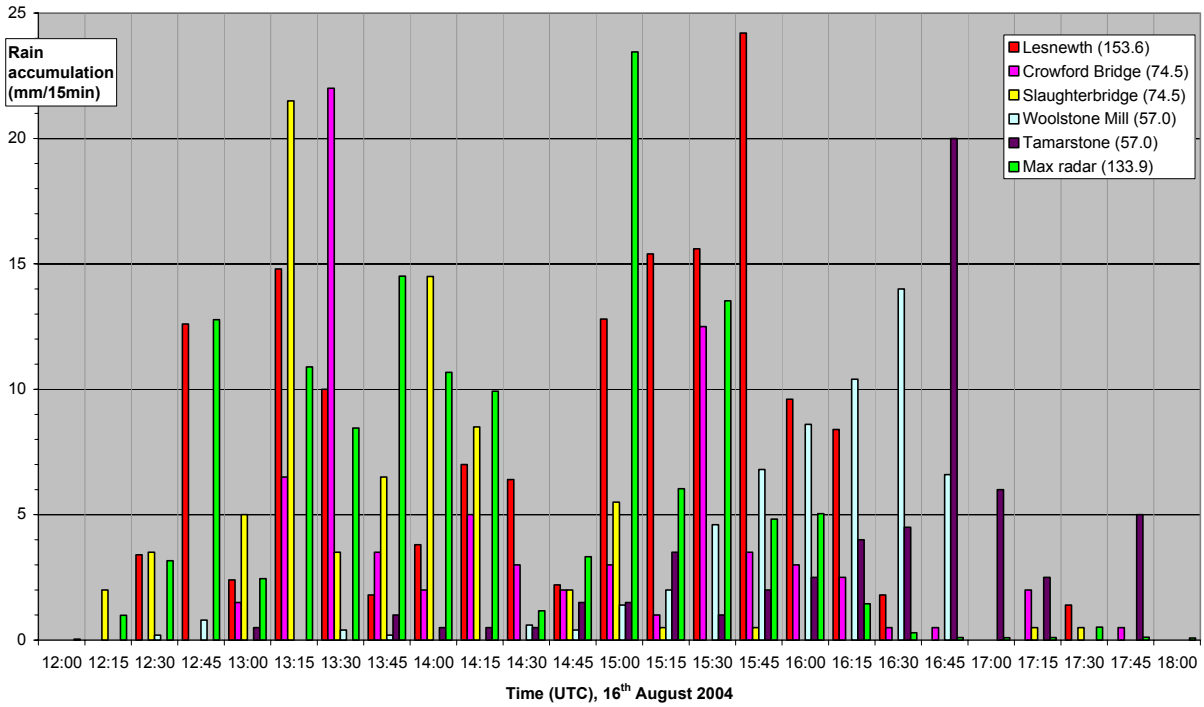

Figure 50 Comparisons between 15min rainfall accumulations at five tipping bucket raingauges (not quality controlled) and the 2km radar pixel having the highest total event accumulation

The spatio-temporal variability of the rain is well displayed in Figure 50, which compares 15-minute totals from five TBRs and from the 2km radar pixel located at the maximum overall accumulation location on the A39. In this diagram, radar values are rates, expressed as 15-minute accumulations. It is noteworthy that the radar values show no systematic bias in this display. The most obvious feature, is the shift of the intense precipitation to later times at Woolstone Mill and Tamarstone, consistent with the general movement northwards after 1600UTC. However, note the earlier peak at Crowford Bridge, also to the north, which occurs at 1315UTC, due to re-invigoration of the second storm cell. By contrast the maxima at Slaughterbridge occur very early. The peak at Lesnewth occurs at 1545UTC, though there are significant falls also in the early period. With accumulations taking such different patterns at different locations, and involving such a large number of peaks, it is surprising that the overall radar accumulation comes out with such a simple spatial pattern.

The fine scale spatio-temporal structure is only available from the Lesnewth time-of-tip data, shown in Figure 37. This re-emphasises the presence of large amplitude variations within the patterns displayed in this section, both from radar and the other rain gauges. Analysis of the radar has indicated that the basic storms were being initiated relatively infrequently, and that the high frequency of the maxima observed further north is due to secondary development following interactions between downdraughts and the coastal convergence. In the early part of Figure 37, we see discreet storms with a detailed substructure which can be related to these mechanisms. However, in the later afternoon, there is an 80 minute period of continuous rain with a clear substructure showing 5-10minute periodicity. Given the speed of movement of these features, we would expect them to have a scale close to the resolution of the radar. Also, we would expect them to have a rather short lifetime.

Without additional data and extensive theoretical and modelling work, these estimates cannot be corroborated, but if true, they would indicate a surface rainfall rate distribution which, if depicted at a resolution of 100m, would show a large amount of apparently random structure, within the overall envelope of the storms. It may be significant that the extreme peak of this profile, reaching over 200mm.hr^{-1} for more than a minute, is one such perturbation. There is no way of knowing how representative this peak is of the sub-2km structure of the storms in general.

To summarise the whole event, Figure 51 shows the total rainfall accumulated on the 2km radar grid for the full period of the event. Note that the apparent width of the rain band is artificially increased over this longer period by the shift in position of the plume after 1500UTC. The pixels recording greater than 80mm can be taken to delineate the main area affected by extreme precipitation. According to the radar, this encompasses just 19 2km pixels, or 76 km^2. If we assume that the difference between the mean 2km pixel at Otterham and the observation by the daily gauge is entirely due to radar calibration, it would be more appropriate to take the area recorded by the radar as receiving over 60mm, which encompasses 29 2km pixels, or 116km^2.

Focussing on the Valency catchment itself, there was a gradient of rainfall accumulation over the five hour period, from modest accumulations of 60-80mm in the lower one-third of the catchment to double this in the upper part near the A39.

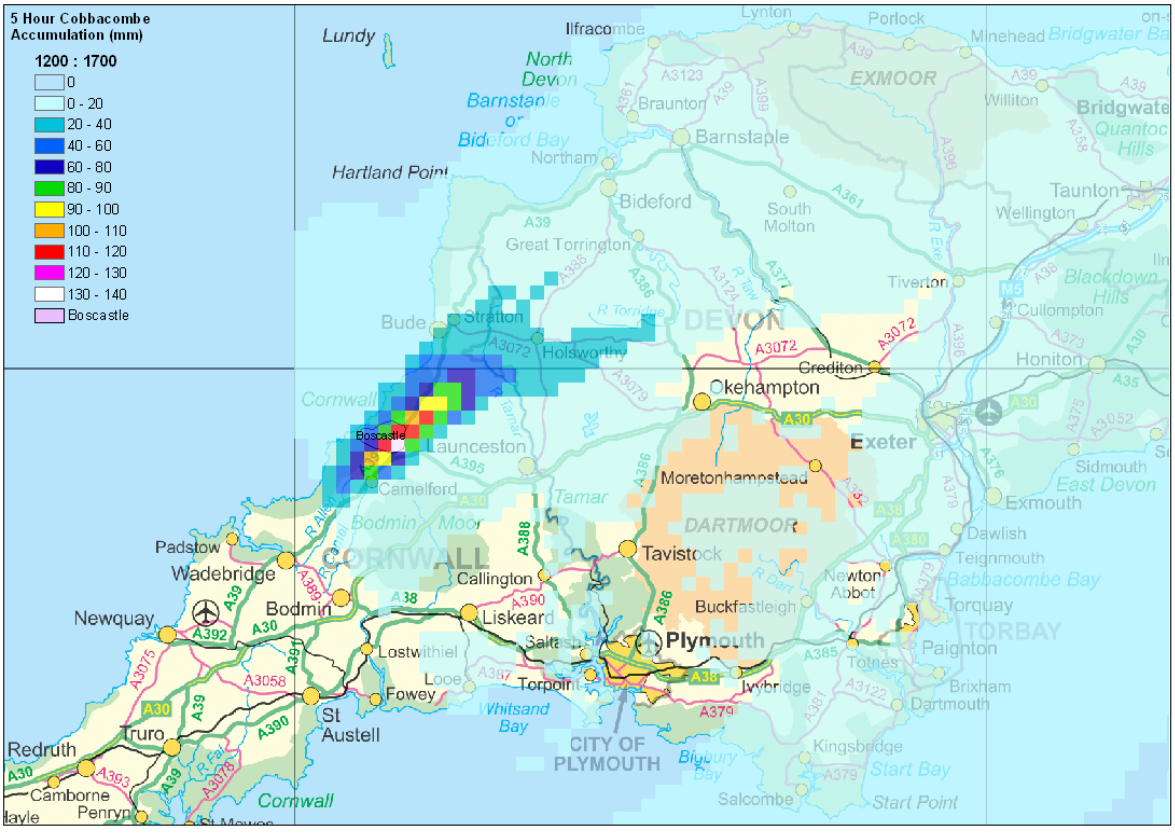

Figure 51 Five hour accumulated rainfall from 2km corrected Cobbacombe radar data, 1200-1700UTC 16th August 2004. Note the non-standard colour coding to focus on larger accumulations

In concluding this analysis, it must be remembered that the radar values are 2km square averages. The gradients of hourly rain accumulation indicated by the radar are extremely large, exceeding 15mm.km^{-1} along the edges of the plume, making the comparison between point and 2km square average rates exceedingly difficult. For events of this type, 1km pixel radar would substantially improve the ability to resolve

local variations in intensity. It is also unfortunate that several of the rain gauge sites that received the heaviest rain have only a TBR, which cannot be relied on to give accurate data in heavy rain. If daily gauges had been available at these locations, it would have been possible to have greater confidence in the point estimates.

6. Probability of the rainfall event

In this section we approach the issue of probability of the event from several viewpoints. First we set the scene by describing the climatology of the area. Then we move on to draw results from the recent study of extreme events of the 20th Century across the UK as a whole. Then we focus in on the south-west as a region and use data on recorded events of the past hundred years, to infer both regional and point probabilities. Finally we focus on the point probabilities using the FEH technique. The section is concluded with a summary which synthesises the results of the different approaches.

6.1. Climatology of rainfall in north-west Cornwall

Rainfall is caused by the condensation of water in air that is being lifted and cooled below its dew point. Rainfall tends to be associated with Atlantic depressions or with convection. The Atlantic depressions are more vigorous in autumn and winter and most of the rain which falls in those seasons in the south-west is from this source. In summer, convection caused by solar surface heating sometimes forms shower clouds and a large proportion of rainfall falls from showers and thunderstorms at this time of year.

The humidity of the air is an important factor determining rainfall, and the sea temperature largely controls this. The sea temperature off southwest England is at its maximum in late summer and autumn, and is coolest in late winter and spring, and as a result rainfall tends to be most in autumn and least in spring.

A final factor which greatly affects the rainfall distribution is altitude. Moist air which is forced to ascend hills may be cooled below the dew point to produce cloud and rain. A map of rainfall looks very like a topographic map.

Most coastal areas of Cornwall and Devon have annual rainfall totals of 900-1000 mm, but up to double this amount falls on uplands such as Dartmoor, Bodmin Moor and Exmoor. These figures can be compared to annual totals around 500 mm typical of the driest parts of eastern England and over 4000 mm in the western Scottish mountains.

Monthly rainfall is also very variable. Most months of the year have recorded totals below 20 mm in coastal districts and many below 10 mm. Even at Princetown one May recorded only 7 mm. The highest monthly totals tend to be in the autumn and winter months. At Plymouth, for example, every month in the year has had more than 100 mm, but totals in excess of 200 mm have only been recorded from December to February.

The numbers of days with rainfall totals of 1 mm or more tend to follow a similar pattern to the monthly rainfall totals. In coastal areas in winter about 15 or 16 days is the norm, but this decreases to nine or 10 in late spring and summer. The numbers of days increase with altitude and at Princetown, for example, there are over 18 days in the winter months and 12 to 13 days in summer.

The southwest peninsula is prone to rare, but very heavy rainfall events lasting from about five to 15 hours. The famous storm which devastated Lynmouth in north Devon on 15 August 1952 was one of these when one place on Exmoor had 228 mm in 12 hours (229.5mm in 24 hours). Other extreme events are the 203.2 mm in 24 hours at Camelford in Cornwall on 8 June 1957, 238.8mm in 24hrs at Cannington in Somerset in August 1924 and 242.8 mm in 13 hours at Bruton in Somerset in June 1917. The heaviest recorded daily rainfall total in UK was at Martinstown in Dorset when 279.4 mm was recorded on 18 July 1955.

A more detailed analysis of the summer climatology of showers in the south-west can be extracted from the work described by Hand (2003). Using a neural network applied to satellite imagery, Hand distinguished areas of convective and stratiform cloud, and then used these to accumulate the hours when convective precipitation was observed by radar over the British Isles, on a 5-km grid. A four year period was used in deriving the climatology. Figure 52 shows sections of the maps produced for south and southwest wind directions in summer. The results are expressed as the probability of convective precipitation occurring, given the specified wind direction. It should be noted that southerly winds are much less common than southwesterly winds. The display does not give the absolute probability of a shower.

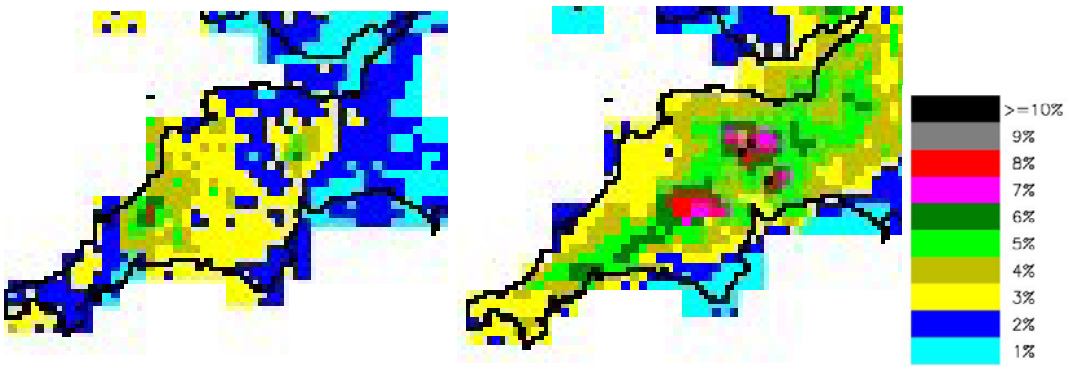

Figure 52 Probability of showers in a South or South-West wind during summer afternoons, determined from radar data in the period 2000-2003.

This analysis shows that the maximum occurrence of showers tends towards the south side of the Cornish peninsula in southwesterly winds, but is focussed over Bodmin Moor in southerly winds. Given a southerly wind on a summer afternoon, on average there will be a shower over Bodmin about 7% of the time. Probabilities of 5-6% extend sufficiently close to the coast to affect the Valency catchment. Note that the Boscastle area has the highest probability of convective rain along the whole coast of the southwest peninsula in this wind direction.

6.2. Frequency of occurrence of the large scale meteorological conditions

The Boscastle event was ascribed in section 3 to intense convective cells, generated in an environment of high low-level moisture content, with significant CAPE and minimal CIN, along a quasi-stationary coastal convergence zone caused by frictional and heating differences between land and sea. The efficiency of the precipitation process may have been enhanced by large scale uplift caused by cyclogenesis in the area, associated with a large scale trough and the left exit region of a propagating jet streak.

The intensity of the individual convective cells was not extreme. Given the large scale atmospheric structure, the likelihood of hourly accumulations, somewhere, of 40mm or more was very high. As shown in Figure 52, climatology shows that Boscastle is more likely than other places to receive such convection when it occurs, if the ambient wind is southerly.

The repeated triggering of convection was not a rare event, and indeed is observed frequently in Cornwall in south-westerly winds. The occurrence of repeated triggering in a southerly wind with the subsequent storms moving up the coastal convergence is more unusual, but not considered rare.

If it was critical for the storms to have sufficient vigour to create heavy precipitation, to be shallow enough to allow close packing of the storms, and to have weak enough

downdraughts to avoid distorting the convergence line, then we may suppose that such conditions occur rarely. It is not possible to quantify how rarely, and neither is it possible to be sure that this combination was critical.

It has been suggested that the prolonged intensity may have been related to mesoscale forcing. The large scale situation with a large quasi-stationary Atlantic depression at all levels of the atmosphere is not a standard summer situation, but it is not rare. The complexity of the upper tropospheric forcing was unusual and, if critical, would certainly indicate a rare event. However, there are no indications that the mesoscale forcing was critical to the storm development.

In summary, the individual conditions that caused the Boscastle storm are not considered to be extreme in themselves. Rather the extreme conditions resulted from the joint occurrence of several conditions. It is not possible, given available data and resources, to judge the joint probability of these events coming together in the way observed at Boscastle. In any case, it is a characteristic of extreme convective events that they each have singular characteristics that are unique to that event. Thus a rigorous approach would require that the joint probability of all possible combinations of events that could lead to extreme rainfall were investigated. There are no tools available to do this.

For this reason, we return, in the remainder of this study, to conventional approaches based on the analysis of historical storms as a whole, or historical point rainfall records.

6.3. Extreme rainfall events of the 20th Century in the UK.

Hand et al (2004) undertook a study of extreme rainfall events in the UK during the 20th Century. He selected the events for study using criteria from the Flood Studies Report Volume II (FSR): "maximum" falls possible for durations less than 1 hour, and the one in one hundred year return period for durations greater than one hour. Values are shown in table 1 below. Note that these values differ from the local Boscastle return periods obtained with the FEH procedure in section 6.5.

Table 5 Maximum falls (mm) possible for durations less than one hour and one hundred year return period falls for durations greater than one hour as a function of average annual rainfall (AAR). Amounts for greater than one hour correspond to the top of the AAR range.

Average Annual Rainfall (AAR) mm	Duration (hours)						
	0.25	0.5	1	24	48	72	96
	Maximum fall (mm) possible			Amount (mm) for 1:100 year return period			
500 – 1400	47	65	83	100	123	135	150
1400 – 2800	**45**	**62**	**79**	**152**	**193**	**219**	**247**
> 2800	43	59	75	228	309	356	410

Since most "extreme" rainfalls occur over lowland Britain, the middle range of AAR in Table 5, highlighted in bold type, was adopted as the lower limit of extreme rainfalls. Event selection was done by searching through a database of "notable rainfall events in the 20th century" held in the Met Office and picking out those that exceeded the criteria. It should be noted that the selection depends both on specification of the threshold, and availability of data, and should not be taken to be comprehensive. Fifty cases were found, of which thirty were predominantly convective, fifteen

predominantly frontal and five orographic. The Boscastle event is convective in this classification, but it should be noted that the Lynmouth event of 1952 was predominantly frontal.

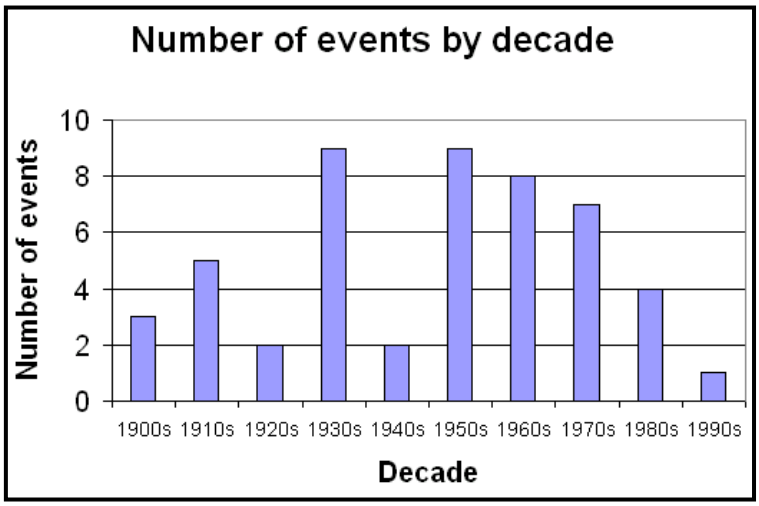

Figure 53 Distribution of extreme rainfall events by decade

The distribution per decade (Figure 53) indicates a high degree of natural variability with no discernible trend. While the overall frequency is one event every second year, the figure indicates that there have been periods when such an event occurred somewhere in the UK almost every year. If we separate out the convective and non-convective events, we have something like a 30% chance of an extreme convective storm event occurring somewhere in the UK each year.

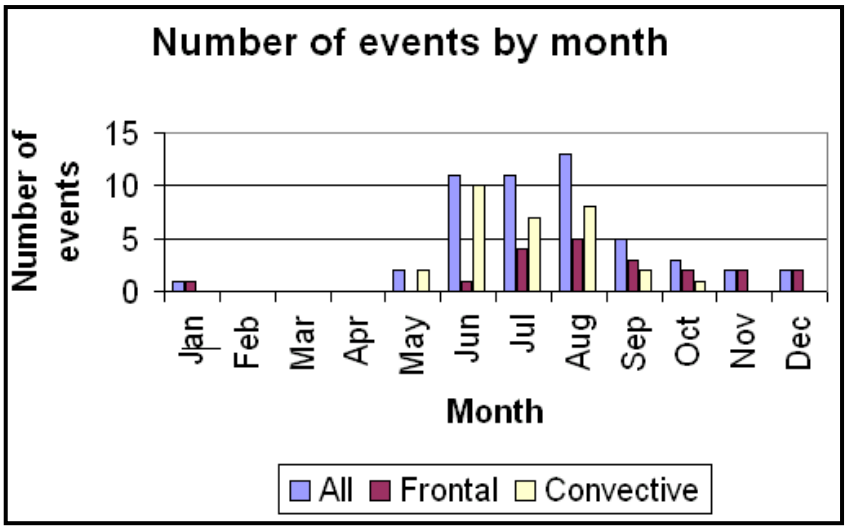

Figure 54 Distribution of extreme rainfall events by month

The monthly distribution (Figure 54) is more discriminating. There were no events in February, March or April. Most events occurred during the summer months with a rapid increase in number in June and a gradual tailing off during the autumn. Convective events tail off more quickly than frontal ones with no convective events in November, December or January since insolation is an important forcing factor for convection. An explanation for this highly skewed distribution is that extreme events only occur when high sea temperatures generate high moisture content air in the vicinity of the UK.

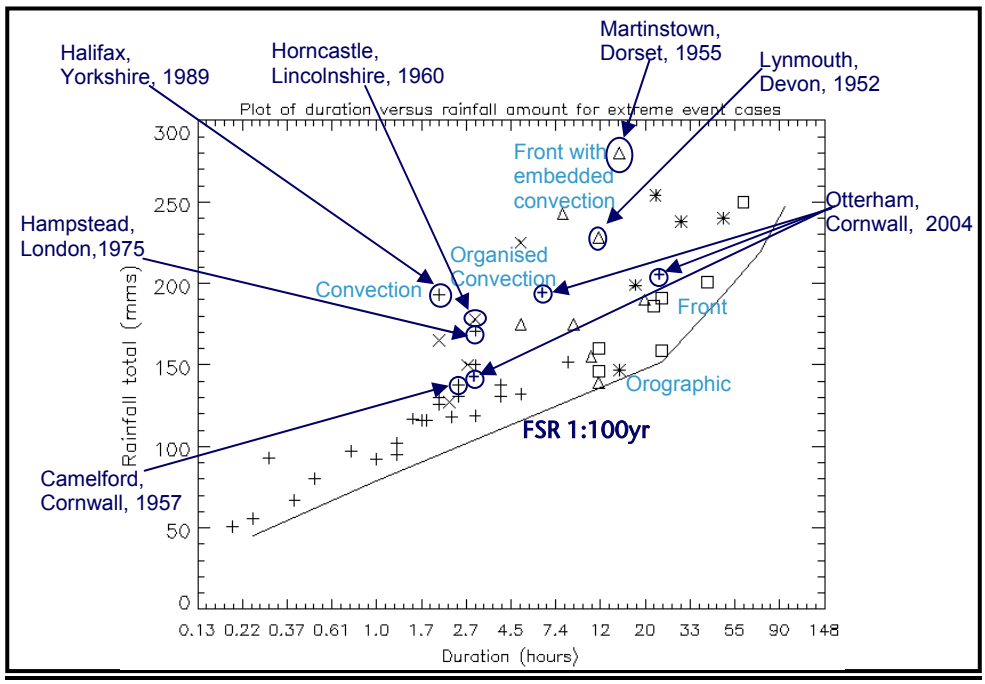

Figure 55 Extreme rainfall events of the 20th century with Boscastle superimposed. The dominant mechanism is convection (+), organised convection (x), frontal (□), frontal with embedded convection (△) or orographic (✱).

Figure 55 summarises the events, in terms of their duration and intensity, and the dominant mechanism. The sub-daily Otterham values have been inferred from the temporal profile of the Lesnewth TBR, and are considered sufficiently accurate for comparison on this scale. The three hour accumulation for this event was very close to that of the 1957 event at Camelford, which also caused floods in Boscastle, but the five hour accumulation is much more extreme. On this timescale it stands out from other purely convective events, except the much shorter duration Halifax storm. Bearing in mind the meteorological analysis in section 3, it might be more appropriate to class Boscastle as an organised convection event, though the mode of organisation is unusual, if not unique, in the UK record.

The convective events broadly fell into two categories:

(a) Forcing was from a synoptic scale feature such as a front, or updraughts and downdraughts in the system were very strong with a high value of convectively available potential energy (CAPE).

(b) Forcing was either from insolation or a meso-scale feature such as a convergence line or sea breeze and smaller values of CAPE.

Events in category (a) were frequently associated with large hail, whereas this was much rarer in category (b). Events that contained large hail and events that did not are plotted in Figure 56. With the exception of one outlier with large hail at the top of the diagram, the remaining large hail cases have durations of 1-3 hours and are associated with intense individual storms, often of multi-cell structure. The Boscastle event was not of this type, the intensity of individual cells being much less extreme than the overall accumulations resulting from the extended duration.

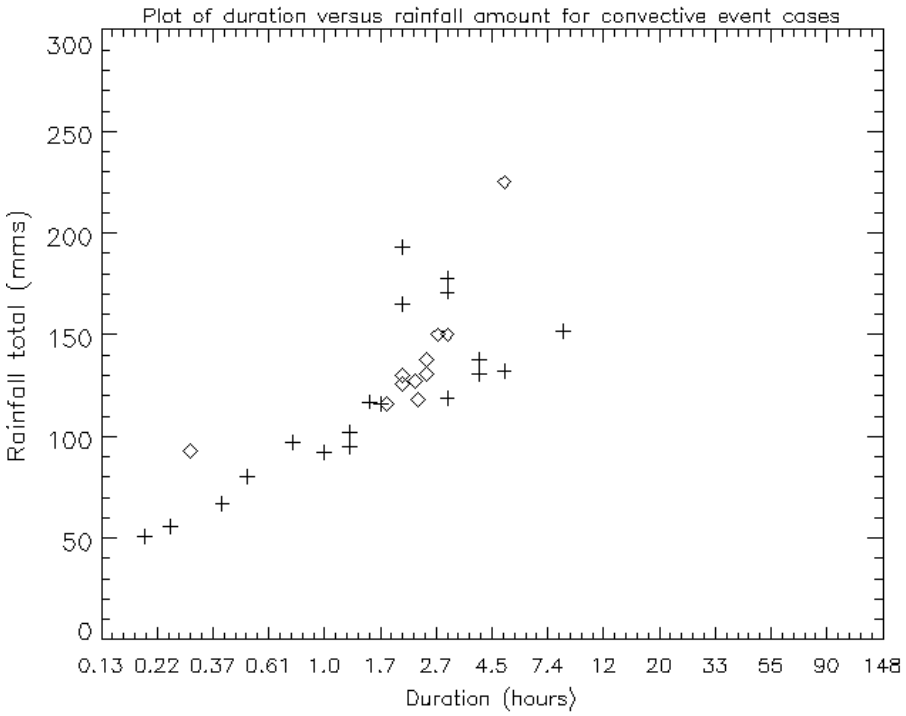

Figure 56 Plot of rainfall amount (mm) versus duration (hr) for the convective events. Crosses indicate events where there was no evidence of large hail and diamonds indicate cases where large hail was reported.

6.4. Extreme events in Boscastle and the south west

Taking the mean frequency of extreme rainfall events across the UK, assuming that the area affected by each is about 100 km^2 and relating this to the area of the UK gives a return period of over 10,000 years for each $1km^2$. However, it is noted that there have been several extreme convective storms in the southwest in the period of the record, and that this may indicate higher frequency of such events in this area. Taking the Cornish storms alone, there were two events in one hundred years, each covering about $100km^2$ which corresponds to a $1km^2$ return period of about 2,000 years. Over the larger area of the south west peninsula, there were six events in one hundred years in an area about three times as large – giving the same point probability. We note in passing that half of these six events over the larger area occurred within just six years in the 1950s. This should emphasise the caution with which short periods and small numbers of events should be treated since had we calculated the probability from just these data we would have estimated just 240 years for the return period at any location. With hindsight, there is no reason to identify a climatic variation that justifies a higher probability estimate for the 1950s, so we conclude that it was a result of natural variability.

6.5. Return period analysis using the FEH technique.

The preliminary analysis conducted at HR Wallingford can be summarised by Figure 57 and Table 6. The sub-daily accumulations used in Figure 57 are based on the Lesnewth TBR, uprated to agree with the Otterham daily total. As discussed earlier, this is not a strictly valid procedure, given the different location of Otterham and Lesnewth relative to the storm tracks. Nevertheless, on the scale of the display, the Lesnewth values themselves are very similar, so the conclusions are not affected.

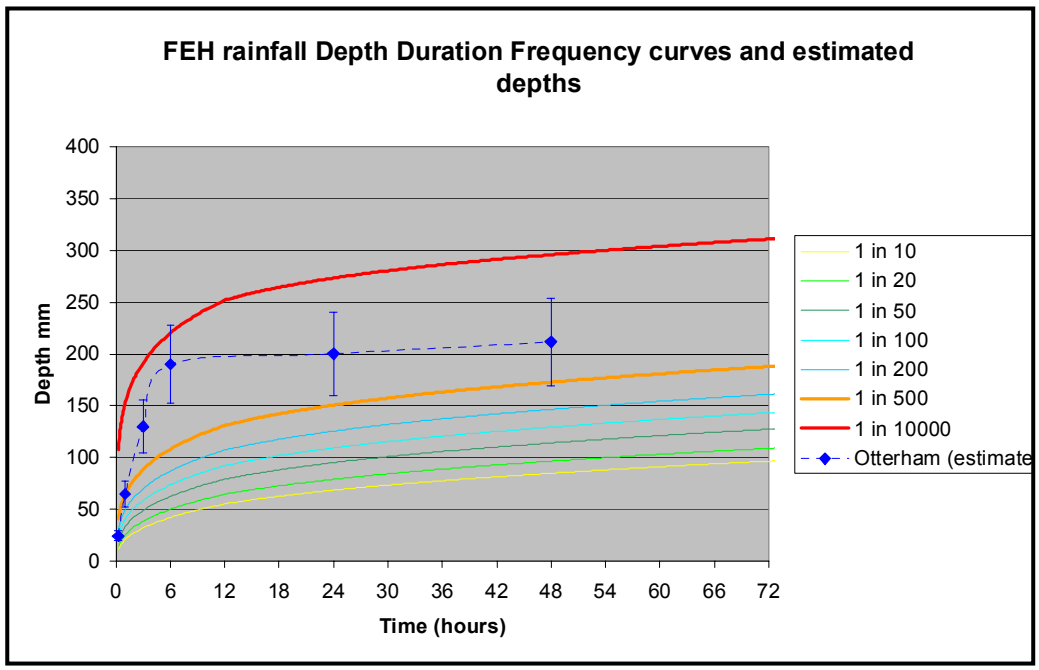

Figure 57 FEH estimates of return period for Otterham

Figure 57 shows curves of rainfall accumulation for a variety of return periods, with data based on the Otterham and Lesnewth observations superimposed. The heaviest accumulations over the shortest time ranges were very high, but the storm was most exceptional when measured over the full afternoon period. This analysis indicates an event with a return period of greater than 2000 years.

Table 6 Rolling peak rainfall accumulations and FEH point rainfall return periods

Duration (hrs)	1	2	3	4	5
Comp. QC 2km Radar (mm)	47	68	99	114	115
Return Period (yrs)	100	200	500	750	5-600
Cobb. QC 2 km Radar (mm)	48	83	117	132	133
Return Period (yrs)	~120	~400	~1000	~1300	~1100
Lesnewth (mm)	68	94	123	150	152
Return Period (yrs)	~400	~700	~1300	~2200	~1900
Slaughterbridge (mm)	46	63	73	74	74
Return Period (yrs)	100	150-200	150-200	100-150	100
Crowford Bridge (mm)	34	47	67	72	72
Return Period (yrs)	20-50	50	100-150	100-150	50-100
Woolstone Mill (mm)	48	70	72	73	74
Return Period (yrs)	100	200	150-200	100-150	100
Tamarstone (mm)	35	44	48	49	50
Return Period (yrs)	20-50	20-50	20-50	20-50	20

Table 6 summarises the numerical values of maximum rainfall accumulation for periods of one to five hours from several TBRs and two radar estimates. These values support a return period of greater than 2000 years for this event. The TBR values in Table 6 are uncorrected. Including the corrections required to match the Lesnewth TBR with the check gauge, as recommended in section 4.6, gives increased maximum accumulations (return periods) of 72mm (~750yr), 100mm (~850yr), 148mm (~2500yr), 181mm (~4500yr) and 183mm (~4000yr) respectively.

6.6. Re-analysis of FEH calculations made by HR Wallingford using supplied raingauge data

The return period estimates quoted in the HR Wallingford data file were checked by computing rainfall depth statistics for two return periods and two durations (100 year and 1000 year; 1-hour and 6-hour) for the point locations of Otterham and Lesnewth, the two gauges which recorded the heaviest totals. The FEH screen shots obtained are shown in Figure 58 and the results are given in Table 7. They compare well with the data supplied by HR Wallingford in their initial assessment and we are satisfied that the values quoted are satisfactory.

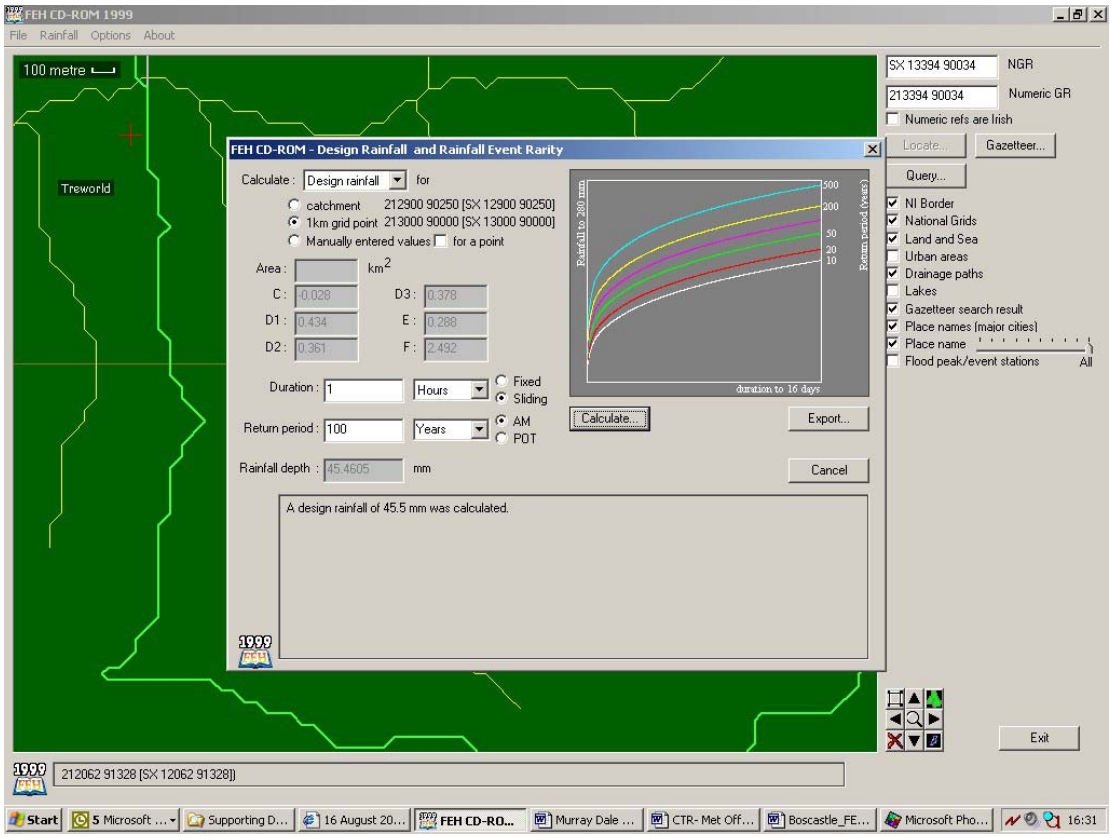

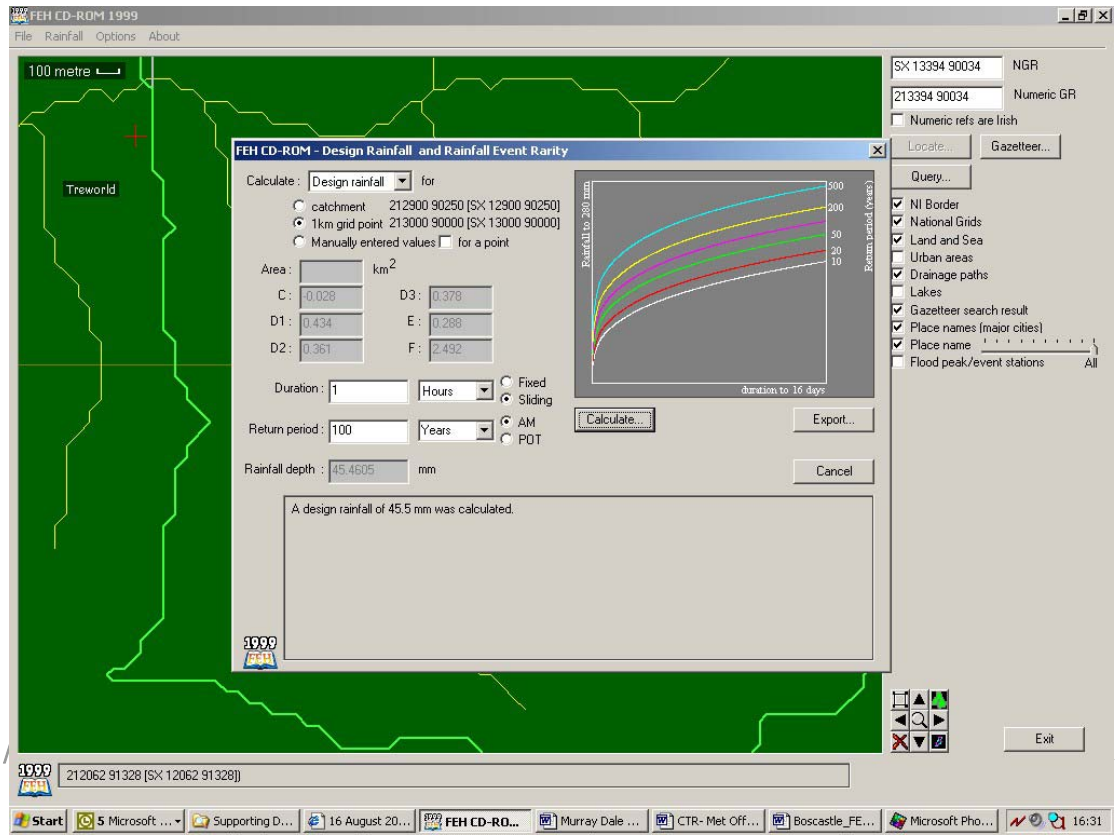

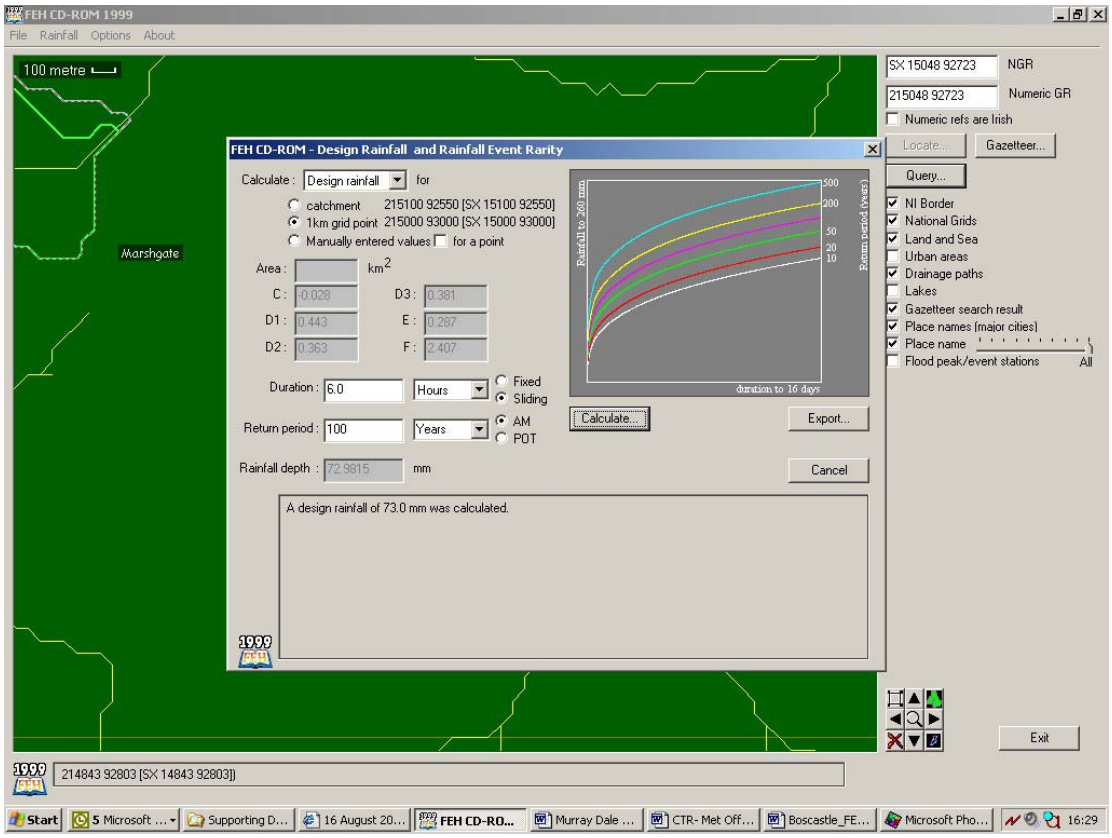

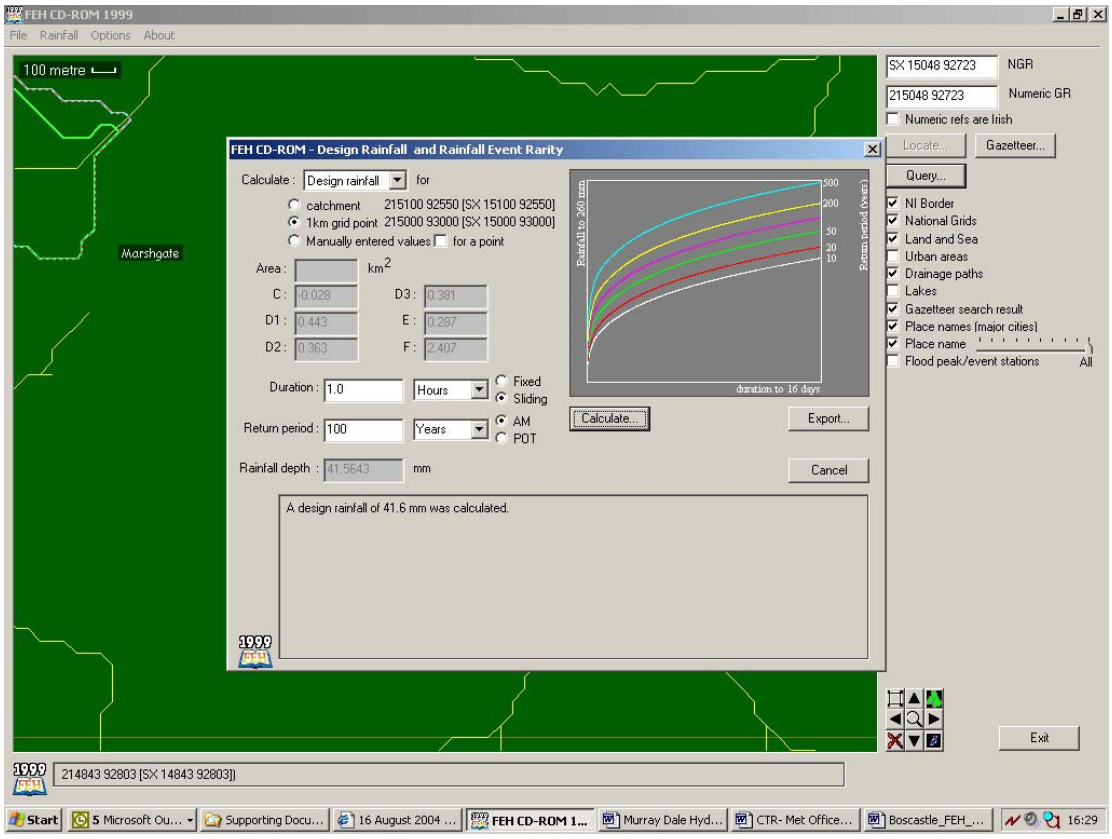

Figure 58 Screen shots of FEH calculations of 100-year RP figures quoted in Table 7

Table 7 Check of return period rainfall depths at two sites for two return periods and 2 durations.

Location	1h, 100y rainfall (FEH) in mm	6h, 100y rainfall (FEH) in mm	1h, 1000y rainfall (FEH) in mm	6h, 1000y rainfall (FEH) in mm
Otterham NGR SX169 916	41.6	73.0	85.6	131.2
Lesnewth NGR SX134 900	45.5	78.5	88.3	136.0

The areal reduction factor (ARF) used in the HR Wallingford analysis is 0.939 which, though not stated, is the value given for a rainfall event of duration 5.0 hours for a catchment of 20.0km^2. This is regarded as reasonable for the August 16th event, bearing in mind the documented limitations of the ARF approach. However, the HR Wallingford file quotes a point rainfall depth of 226.3mm, converted to 212.5mm by the ARF as the total assumed to fall over the catchment during the event. From the raingauge and radar data available this is considered to be an over-estimation of the rainfall during the 5-hour period 1200 to 1700UTC on 16th August 2004. Raingauge totals available for the event indicate 200.4mm in 24 hours at Otterham daily gauge, 155.8mm at Lesnewth tipping bucket gauge (TBR) and 184.9mm at Lesnewth daily check gauge. Radar estimates indicated 132.9mm and their validity is discussed elsewhere in this report.

If return periods based on raingauge data are to be used, it would be more appropriate to use a rainfall profile from the Lesnewth TBR and a total depth from a Thiessen polygon representation of the Valency catchment, based on the Otterham and Lesnewth gauges. In this way, the relative weighting of the Lesnewth and Otterham gauges' totals is incorporated in the catchment estimate. This is likely to result in a rainfall total between 184.9mm and 200.4mm, which could then be reduced slightly by an ARF if deemed appropriate. However, as has been shown earlier, this would only crudely represent the distribution indicated by radar, and the preferred option is to use the radar pattern calibrated with the Lesnewth total. A discussion of the use of radar data in return period analysis is given in the next section.

6.7. Application of the FEH methods to radar estimates

As well as the raingauges at Otterham and Lesnewth, radar data from Cobbacombe Cross radar at 2km resolution are available from the 16th August. The radar data have the benefit of being available at 5 minute intervals and produce good areal estimates of rainfall accumulation at sub-hourly intervals. Of key importance when considering differences between radar data and raingauge data is the point measurement method of a tipping bucket raingauge and the areal estimation of radar across a 2 x 2km (4km^2) cell. In the case of extreme rainfall from convective storms – as was the case in the Boscastle event - rainfall is very spatially variable. For this reason, radar data have the advantage of capturing rainfall that falls over a catchment better than raingauges unless there are many and they are densely located in a catchment.

An assessment of Cobbacombe radar data for the event is made in Table 8. The data are scaled using the inverse of the areal reduction factor (FSR, 1975, FEH vol. 2, 1999) to make a comparison against point raingauge estimates, assuming a 'catchment' of 4km^2. This is consistent with previous approaches (Collier, 1991). This has the effect of increasing the values slightly. Return periods are quoted using FEH DDF tables for the most intense radar cell location shown in Figure 51.

Table 8 Met Office radar data at Cobbacombe for 4km^2 cell over Valency catchment, adjusted to point data using the inverse of the ARF for direct comparison with point gauge data

Duration from 1200UTC	Depth (mm) over 4km^2	Areal Reduction Factor (ARF) applied	Depth at point (using inverse ARF)	FEH return period (years) (1km point)
0 -0.5 hour	4.2	1/0.915	4.59	'commonplace'
0 - 1	19.4	1/0.93	20.86	6.9
0 – 1.5	38.7	1/0.94	41.17	43
0 – 2.0	63.9	1/0.95	67.26	189
0 – 2.5	75	1/0.95	78.95	275
0 – 3.0	101.8	1/0.955	106.60	730
0 – 3.5	121.4	1/0.955	127.12	1264
0 – 4.0	131.2	1/0.96	136.67	1500
0 – 4.5	132.9	1/0.96	138.44	1425

A comparison is made in Table 9 between the radar data for Cobbacombe and the gauge data from Lesnewth TBR and the Lesnewth TBR scaled up to match the Lesnewth check gauge total.

Table 9 Comparison of maximum radar data against raingauge data from two gauges

Duration from 1200UTC	Cobbacombe (ARF-adjusted) rainfall (mm)	Lesnewth TBR raingauge rainfall (mm)	Lesnewth rainfall (mm) scaled to match check gauge total	Lesnewth scaled up rainfall FEH return period (years)
0 -0.5 hour	4.6	3.4	4.1	'commonplace'
0 – 1	20.9	18.4	22.4	8.7
0 – 1.5	41.2	43.2	52.5	103
0 – 2.0	67.3	48.8	59.3	119
0 – 2.5	78.9	62.2	75.6	234
0 – 3.0	106.6	77	93.5	440
0 – 3.5	127.1	108	131.2	1432
0 – 4.0	136.7	141.8	172.3	3786
0 – 4.5	138.4	152.2	184.9	4599

In 1991 Collier reported on problems of estimating rainfall rarity with radar and raingauges when analysing the Walshaw Dean (Halifax) storm of 1989. This event remains the UK record for 2-hour duration with 193mm collected by the Walshaw Dean raingauge. In this event, Collier indicated that the rain gauge just happened to be located on the southern edge of the core area of the storm within which the maximum rainfall fell. In the case of Boscastle it appears that both the Otterham and Lesnewth gauges were particularly well situated to gauge the centres of intense storm cells, though it should be noted that the cells observed were different and much of the additional rain observed over the longer period was from the edges of storm cells.

6.8. FEH rarity estimation

Rarity of raingauge data

FEH (1999) differs in its assessment of rainfall rarity from its predecessor, the Flood Studies Report (1975). FEH uses the FORGEX method to derive growth curves which is capable of estimating rare extreme rainfalls of up to 2000 years (FEH, volume 2). The full method is described in volume 2 of the FEH, pp 33-40, however,

the way in which the growth curves are developed using the 'Focussing, pooling and homogeneity' deserves mention here. The pooling method used in FORGEX allows data from gauges at distances up to 200km from a site to be used in order to make the most of all extreme data available, weighting the data closest to the site with the most importance.

The map of the UK daily raingauges used (figure 13.1 in FEH volume 2) shows a good, relatively dense coverage of data across the UK. However, the map of hourly data used in the analysis (figure 13.3) shows that density of gauges in the south west of England is relatively low. For this reason the pooling method is useful in gathering extreme totals from other hourly data in the UK. Nevertheless, the growth curves derived for the Valency catchment in north Cornwall will inevitably suffer from a dearth of local hourly extreme rainfall data – the chance of extreme sub-daily rainfalls being measured in Cornwall and the south west is low (and certainly lower than in London or Manchester for example) with such a sparse gauge network in this part of the country. This is not a criticism of the FEH methodology, but is an inevitable weakness due to the heterogeneity of the sub-daily data made available during the development of the FEH.

The result of this is that FEH estimates of short-duration (1 – 6 hour) rainfall rarity at Boscastle, and in the south west, may be exaggerated in comparison to other areas of the country. The 4599 year return period estimate of 185 mm of rain gauged at Lesnewth in 4.5 hours may in reality be lower, for example. Secondly, we must bear in mind that that the FORGEX method is not recommended for use above 2000 year return periods.

Therefore, it is recommended that rainfall totals in excess of 2000 year return periods when calculated by FEH, are referred to as having 'return period in excess of 2000 years' and not quoting higher values.

Rarity of radar values

The rarity of radar estimates of rainfall data have come under question, primarily because radar data sample much more rainfall, particularly localised rainfall, than raingauges. The relatively low density of recording raingauges in the UK means that many events captured in the radar record are likely to be 'missed' by the conventional gauge network. As the FEH method is based on fairly sparse data it will produce high return periods for point rainfall events that occur infrequently in data sets derived from raingauge network data, but which occur more frequently in radar data-sets due to better areal coverage. Hence entering radar data sampled values into the FEH DDF (depth duration frequency) tables could derive artificially high return periods. In this case, the raingauges may have recorded higher totals than the radar as they appear to have been fortuitously located under the storm centre. In many flood events, however, particularly those derived from summer convective activity, the radar measures much higher totals than raingauges which are not located under the most intense rainfall cells. This is an issue which is of increasing concern to hydrologists and water engineers.

6.9. Recommendations related to regional estimates

In order to place the Boscastle event of 16th August 2004 in context with severe and/ or extreme rainfalls in the south west region, a more in-depth study would be required than has been possible here. This study has examined the regional pooling method used in FEH by the FORGEX method and highlighted that sub-daily data used in the analysis were limited for the SW region compared to other regions in the country. In order to improve on this, a thorough study of all available hourly and sub-hourly raingauge data for the south west would need to be made, making use of all the more recent data post 1995. The analysis would also benefit from a study of all the major

rainfall events sampled by radar in the last 5 years (since radar data have been of a high quality for quantitative analysis), to make an assessment of how many severe and extreme rainfall events are sampled by available raingauges and whether such events are more common than the raingauge data suggest.

6.10. Summary of probability analysis

The probability of occurrence of the extreme rainfall observed in the vicinity of Boscastle has been studied in the context of climatology, meteorological phenomena, historical occurrence of storms, and historical occurrence of point rainfalls.

As with other extreme storms that have been studied, the conditions do not fit a simple pattern, but are the result of a combination of factors. It is not possible to deduce the likelihood of recurrence from an analysis of the frequency with which each factor occurs.

The observed maximum one hour fall at the Lesnewth TBR, recalibrated to the daily gauge, has a return period of around 400 years. This is associated with the very high efficiency of this part of the storm.

The three hour total, again at Lesnewth, is comparable with the Camelford flood in 1957, and with several other events in other parts of the country, most of which were accompanied by large hail. The return period is about 1300 years.

The overall storm has a return period in excess of 2000 years, but is not as high as the Lynmouth or Martinstown events. All cover very small areas, which contributes to the point rarity.

Given the shortness and sparseness of the instrumental record, the reliability of high return periods such as these must be questioned. It is known that the climate cannot be considered stationary, for natural as well as possibly for human induced reasons, and there is no reason to suppose that the frequency of events such as this one has remained the same through changes like the warm period prior to 1000AD and the little ice age from 1600-1800AD. Nevertheless, it may serve as a convenient representation of the current probability of occurrence.

The south west peninsula has been subjected to six extreme rainfall events in the past century. The point ($1km^2$) probability deduced from a cursory examination of these events indicates a similar return period to that deduced from the instrumental records. While the point probability remains low because of their small spatial extent, it is worth noting that where resources, such as rescue facilities, are allocated regionally, it may be the regional probability that is relevant. Allowing for the sparse observational network, the evidence indicates that an extreme event will occur somewhere in the south west region at least once every 20 years on average.

Ultimately, the intensity of the precipitation in these events depends on the moisture content of the air, and this is the reason that late summer is the time when such storms occur most frequently. If any change in climate were to result in the sea temperature rising to the south west of the UK, it would be expected that the moisture content of air reaching the UK would be higher in suitable circumstances for storm development, and that the intensity of the storm would therefore be greater. This is consistent with the observation that severe rain storms in more southerly latitudes produce significantly heavier rain rates.

7. Conclusions

Weather conditions experienced up to the beginning of August generated a dry soil moisture anomaly for the Valency and neighbouring catchments. Subsequent weather prior to 16th August was significantly wetter than average, but with a highly variable distribution, leading to deficits in the range 40-180mm in North Cornwall and just over 100mm in the Valency catchment itself.

The extreme rainfall that fell on the Valency catchment was produced by a sequence of convective storms that developed along a coastal convergence line caused by the change in friction between the land and sea, reflected in the weak southerly winds over land and the stronger south-westerly jet observed over the sea. This effect was strengthened by heating over land. Updraughts at cloud base were estimated to be 1-2ms^{-1}.

The air mass showed minimal resistance to convective development, and high moisture content at low levels contributed to the intense rain. However, the instability was not extreme, and no hail was observed.

The maximum rainfall in a convective event is strongly determined by the moisture content of the boundary layer air, which increases with increasing temperature. A significantly warmer air mass would produce more precipitation if other conditions were the same. This is confirmed by noting that the observed rain rates were modest compared with those observed in severe rain storms in more southerly latitudes.

The intensity of the rain near Boscastle was associated with development of the storms as they interacted with the coastal convergence. The result was a sequence of closely packed cells about 5km across with cloud tops at about 6.5km. Rain production from these storms may have been assisted by ice falling from previous storms over Brittany.

The efficiency of rainfall production from the convective storms was enhanced by successive storms taking the same track, so that residual cloud from previous storms was incorporated into new ones. It may also have been enhanced by large scale uplift induced by a developing upper tropospheric vortex over south west England. This development was associated with the large scale circulation over the eastern Atlantic Ocean which was manifested in a complex structure of upper tropospheric disturbances.

The daily raingauge observations are confirmed, including a maximum accumulation at Otterham of 200.4mm.

Accumulations from the Tipping Bucket Raingauge at Lesnewth should be scaled to match the daily raingauge from the same site to give maximum short period accumulations of 82mm in 1 hour, 148mm in 3 hours, and 183mm in 5 hours. The peak instantaneous rain rate at Lesnewth was nearly 300mm.hr^{-1} at 1535UTC.

Observations of the spatial pattern of precipitation were well captured by the Cobbacombe and Predannack radars. Maximum values over 4km^2 pixels differed from those observed by the raingauges due to sampling differences, but the overall pattern was consistent. Maximum values were also somewhat lower in the radar estimates, but information was insufficient to rule out the possibility that this was purely due to sampling. The radar spatial pattern indicates that the heaviest total rainfall accumulation probably occurred a few kilometres to the southwest of Otterham near the A39.

Point return periods in excess of 2000 years were confirmed for the storm. A storm of this intensity occurs somewhere in southwest England every 20 years. It was noted that natural variability has resulted in several such storms occurring in some decades.

References

Bader, M.J., Forbes, G.S., Frant, J.R., Lilley, R.B.E. & Waters, A.J., 1995: Images in Weather Forecasting, Cambridge University Press.

Collier, C. G., 1989: Applications of Weather Radar Systems: A guide to uses of radar data in meteorology and hydrology, Ellis Horwood.

Collier, C. G., 1991: Problems of estimating extreme rainfall from radar and raingauge data illustrated by the Halifax storm of 19 May 1989, *Weather*, **46**

Gibson, M., 2000: Comparative study of several gauge adjustment schemes. Phys Chem Earth (B) 25, 921-926.

Gibson, M., 2000: NEXRAD and modified NEXRAD gauge adjustment schemes. Observation Based Products Technical Report No. 31. Met Office internal report available from the National Meteorological Library, Exeter.

Golding, B., 1998: Nimrod: A system for generating automatic very-short-range forecasts. *Meteor. Appl.*, **5**, 1–16.

Hand, W., 2002: The Met Office Convection Diagnosis Scheme. *Meteor. Appl*., **9**, 69–83.

Hand, W. H., 1996: A technique for nowcasting heavy showers and thunderstorms. *Meteor. Appl*., **3**, 31–41.

——, 2002: The Met Office Convection Diagnosis Scheme. *Meteor. Appl*., **9**, 69–83.

Hand, W.H., Fox, N.I., Collier C.G., 2004: A study of twentieth century extreme rainfall events in the United Kingdom with implications for forecasting. *Meteor. Appl*., **11**, 15–31

Harrison,D.L., Driscoll,S.J. & Kitchen,M., 2000: Improving precipitation estimates from weather radar using quality control and correction techniques. Meteorol. Appl. **6**, 135-144.

Hough M.N. & Jones, R.J.A., 1997: The United Kingdom Meteorological Office rainfall and evaporation calculation system: MORECS version 2.0 – an overview. Hydrol and Earth System Sciences, **1**, 227-239

Hunt, J.C.R., Orr, A., Rottman, J.W. & Capon, R., 2004: Coriolis effects in mesoscale flows with sharp changes in surface conditions. Quart. J. Roy. Meteorol. S., **130**, 2703-2731.

Kitchen,M. & Blackall, R.M., 1992: Representativeness errors in comparisons between radar and gauge measurements of rainfall. J. Hydrol., **134**, 13-33

Kitchen,M., Brown, R. & Davies,A.G., 1994: Real time correction of weather radar data for the effects of bright band, range and orographic growth in widespread precipitation. Quart. J. Roy. Meteorol. Soc., **120**, 1231-1254.

Lee, A.C.L., 1986: An operational system for the remote location of lightning flashes using a VLF arrival time difference technique. J. Atmos. Ocean. Tech., **3**, 630-642

Met Office, 1982: Observers Handbook, HMSO, London.

Moore, R.J., 1985: The probability distributed principle and runoff prodiction at point and basin scales. Hydrol. Sci. J., **30**, 263-297

NERC, 1975: Flood Studies Report

NERC, 1999: Flood Estimation Handbook

Pamment,J.A. & Conway,B.J., 1997: Objective identification of echoes due to anomalous propagation in weather radar data. J. Atmos. Ocean. Tech., **15**, 98-113.

Roberts, N.M., 2000, A guide to aspects of water vapour imagery interpretation: the significance of dry regions. Met Office NWP Tech Rep No. 294, copy available from National Meteorological Library, FitzRoy Road, Exeter EX1 3PB.

Robinson A.C. & J.C. Rodda, 1969: Rain, wind and the aerodynamic characteristics of rain gauges. Meteorol. Mag, **98**, 113-120.

Smith, J. A., and M. Kitchen, 1998: A review of the quality control and quality evaluation of radar rainfall measurements carried out at the UK Met. Office. *Proc. of the COST 75 Final International Seminar on Advanced Weather Radar Systems*, Locarno, Switzerland.

Smith, R.N.B., Blyth, E.M., Finch, J.W., Goodchild, S., Hall, R.L. & Madry, S., 2004, Soil state and surface hydrology diagnosis based on MOSES in the Met Office Nimrod nowcasting system. Submitted to Meteorol. Appl.

Sumner, G., 1988, "Precipitation: Process and Analysis", Wiley.

